Few Quantum Particles on One Dimensional Lattices

Scattering, binding and transport

D I S S E R T A T I O N

zur Erlangung des akademischen Grades

doctor rerum naturalium
(Dr. rer. nat.)
im Fach Physik

eingereicht an der
Mathematisch-Naturwissenschaftlichen Fakultät I
Humboldt-Universität zu Berlin

von
Herr Ldo. Manuel Valiente Cifuentes
geboren am 05.11.1983 in Jaén, Spanien

Abstract

There is currently a great interest in the physics of degenerate quantum gases and low-energy few-body scattering due to the recent experimental advances in manipulation of ultracold atoms by light. In particular, almost perfect periodic potentials, called optical lattices, can be generated. The lattice spacing is fixed by the wavelength of the laser field employed and the angle betwen the pair of laser beams; the lattice depth, defining the magnitude of the different band gaps, is tunable within a large interval of values. This flexibility permits the exploration of different regimes, ranging from the "free-electron" picture, modified by the effective mass for shallow optical lattices, to the tight-binding regime of a very deep periodic potential. In the latter case, effective single-band theories, widely used in condensed matter physics, can be implemented with unprecedent accuracy. The tunability of the lattice depth is nowadays complemented by the use of magnetic Feshbach resonances which, at very low temperatures, can vary the relevant atom-atom scattering properties at will. Moreover, optical lattices loaded with gases of effectively reduced dimensionality are experimentally accessible. This is especially important for one spatial dimension, since most of the exactly solvable models in many-body quantum mechanics deal with particles on a line; therefore, experiments with one-dimensional gases serve as a testing ground for many old and new theories which were regarded as purely academic not so long ago. The physics of few quantum particles on a one-dimensional lattice is the topic of this thesis. Most of the results are obtained in the tight-binding approximation, which is amenable to exact numerical or analytical treatment.

For the two-body problem, theoretical methods for calculating the stationary scattering and bound states are developed. These are used to obtain, in closed form, the two-particle solutions of both the Hubbard and extended Hubbard models; it is found that the latter can show resonant scattering behavior. A new theorem, which characterizes all two-body bound states on a one-dimensional lattice with arbitrary finite range interactions, is proven here. The methods used for the simplest Hubbard models are then generalized to obtain exact results for arbitrary interactions and particle statistics.

The problem of binding and scattering of three identical bosons is studied in detail, finding new types of bound states with no continuous space counterparts. The physics of these trimers is revealed by an effective model which is then applied to "dimer"-"monomer" scattering on the lattice.

Stationary states of other lattice systems are also considered. First, the problems of binding and scattering of a single particle on a superlattice off a static impurity are analytically solved. Among the results obtained, the presence of a second bound state for any lattice and interaction strengths is highlighted. Second, a model of the harmonic oscillator on the lattice, preserving most of the properties of its continuous space analog, is presented and analytically solved. Two different models, being formally equivalent to the aforementioned lattice oscillator, are then constructed and solved exactly.

Quantum transport of a a single particle and a bound particle pair on a one-dimensional lattice superimposed with a weak trap is investigated. Based on the knowledge of the results obtained for stationary states, coherent, non-dispersive transport of one and two particles can be achieved. A surprising fact – repulsively bound pairs are tighter bound than those with attractive interaction – is found and physically explained in a simple way.

Zusammenfassung

Der aktuelle experimentelle Fortschritt bei der Manipulation ultrakalter Atome mit Licht löst gegenwärtig ein großes Interesse an der Physik entarteter Quantengase und der niederenergetischen Streuung weniger Teilchen aus. Insbesondere ist es möglich, nahezu perfekte periodische Potenziale, sogenannte optische Gitter, zu generieren. Der Gitterabstand wird durch die Wellenlänge und den Winkel zwischen den Strahlen des verwendeten Laserfeldes festgelegt, während die Gittertiefe, welche die Größenordnung der verschiedenen Bandlücken definiert, über eine weite Bandbreite variiert werden kann. Diese Flexibilität erlaubt die Untersuchung verschiedenster Regime, vom Bild des "freien Elektrons", welches im Falle flacher optischer Gitter durch die effektive Masse modifiziert wird, bis zum tight-binding-Regime (Regime der festen Bindung), das mit einem sehr tiefen periodischen Potenzial simuliert werden kann. Liegt das letztere Regime vor, so lassen sich die effektiven Einzelbandtheorien, die weitgehend in der Physik der kondensierten Materie Verwendung finden, mit hervorragender Genauigkeit implementieren. Die Durchstimmbarkeit der Gittertiefe wird heutzutage durch das Ausnutzen magnetischer Feshbachresonanzen komplementiert, welche bei sehr niedrigen Temperaturen die atomaren Streueigenschaften nach Belieben variieren können. Darüber hinaus sind mit Gasen gefüllte optische Gitter, deren Dimensionalität effektiv reduziert ist, experimentell zugänglich. Dies ist speziell für eine einzige räumliche Dimension sehr von Bedeutung, da die meisten der exakt lösbaren Modelle der quantenmechanischen Vielteilchentheorie das Verhalten von Teilchenketten beschreiben. Somit stellen Experimente mit eindimensionalen Gasen für viele alte und neue Theorien, die noch vor nicht allzu langer Zeit nur als rein akademisch angesehen wurden, eine praktische Versuchsplattform dar. Die Untersuchung des Verhaltens weniger Quantenteilchen in einem eindimensionalen Gitter ist Thema dieser Arbeit. Der Großteil der Ergebnisse ist im Rahmen der tight-binding-Näherung erhalten worden, welche eine exakt numerische oder analytische Behandlung ermöglicht.

Für das Zweikörper-Problem konnten theoretische Methoden zur Berechnung der stationären Streu- und Bindungszustände entwickelt werden. Mit deren Hilfe ist es gelungen, sowohl für das Hubbard-Modell, als auch für das erweiterte Hubbard-Modell die Zweiteilchen-Lösungen in kompakter Form zu erhalten; es ist gezeigt worden, dass letzteres ein resonantes Streuverhalten aufweisen kann. Ferner konnte ein neues Theorem, das alle Zweikörper-Bindungszustände in einem eindimensionalen Gitter mit beliebiger endlich reichweitiger Wechselwirkung charakterisiert, bewiesen werden. Die Methoden für die einfachsten Hubbard-Modelle sind verallgemeinert worden, um exakte Ergebnisse für beliebige Wechselwirkungen und Teilchenstatistiken herzuleiten.

Bei der genauen Untersuchung der Streuung und Bindung dreier identischer Bosonen sind neue Typen von Bindungszuständen gefunden worden, denen im kontinuierlichen Raum kein Pendant zugeordnet werden kann. Die Physik dieser Trimere wird durch ein effektives Modell beschrieben, welches auch auf die Streuung von Dimeren mit Monomeren in Gittern angewandt wurde.

Es wurden zudem die stationären Zustände anderer Gittersysteme betrachtet. Zuerst konnten die Streu- und Bindungszustände eines Teilchens in einem Supergitter mit einer statischen Störung analytisch bestimmt werden. Aus den erhaltenen Resultaten ist das Auftreten eines zweiten gebundenen Zustandes, unabhängig von den Gitterparametern und der Wechselwirkungsstärke, hervorzuheben. Des weiteren wurde ein Modell des harmonischen Oszillators auf dem Gitter eingeführt, das die Eigenschaften wie im kontinuierlichen Raum weitgehend erhält, und analytisch

gelöst. Anschließend konnten zwei unterschiedliche, zum besagten harmonischen Gitteroszillator formal äquivalente Modelle konstruiert und gelöst werden.

Schließlich wurde der Quantentransport eines einzelnen Teilchens und eines gebundenen Teilchenpaars in einem eindimensionalen Gitter, überlagert mit einer schwachen Falle, untersucht. Ausgehend von den erhaltenen Ergebnissen für die stationären Zustände kann ein kohärenter, nicht-dispersiver Transport eines oder zweier Teilchen erreicht werden. Es wurde der überraschende Effekt gefunden und in einfacher physikalischer Weise erklärt, dass repulsiv gebundene Paare stärker gebunden sind als solche mit einer attraktiven Wechselwirkung.

List of publications

Manuel Valiente and David Petrosyan.
Quantum dynamics of one and two bosonic atoms in a combined tight-binding periodic and weak parabolic potential.
Europhys. Lett., **83**:30007, 2008.

Manuel Valiente and David Petrosyan.
Two-particle states in the Hubbard model.
J. Phys. B, **41**:161002, 2008.

Manuel Valiente and David Petrosyan.
Scattering resonances and two-particle bound states of the extended Hubbard model.
J. Phys. B, **42**:121001, 2009.

Manuel Valiente, David Petrosyan and Alejandro Saenz.
Three-body bound states in a lattice.
Phys. Rev. A, **81**:011601(R), 2010.

Manuel Valiente.
Lattice two-body problem with arbitrary finite range interactions.
Phys. Rev. A, **81**:042102, 2010.

Contents

Contents

1. Introduction

Advances in cooling and trapping of atoms had lead to the experimental observation of Bose-Einstein condensation in a dilute, ultracold gas [AEM+95] some fifteen years ago. This progress awakened renewed interest in the study of degenerate quantum gases.

With the high controllability of ultracold atoms by means of laser fields it is now possible to create artificial periodic potentials – optical lattices. Such systems may serve as "quantum simulators" of the fundamental models of condensed matter physics. By combining two or more optical lattices, it is even possible to create superlattices having different subperiods, in which the induced splitting of the original bands into the so-called mini-bands can emulate, for instance, more complicated crystals formed by heteronuclear ions.

In 2002, a quantum phase transition from the Mott insulator phase (an incompressible, gapped phase with a number of bosons commensurate with the number of lattice sites) to the superfluid phase (a compressible phase in which the many-body system, when subject to an external velocity field, remains at rest) was realized [GME+02] with ultracold bosonic atoms loaded in an optical lattice. More recently, repulsively-bound pairs of atoms in an optical lattice were produced and characterized [WTL+06] experimentally. These exotic, metastable bound pairs have energies lying in a band gap, and, in optical lattices free of phonons and defects, they cannot decay into the scattering continuum. This effect, unobserved in traditional solid state materials due to fast energy dissipation, has triggered the investigation of novel few-body lattice effects [WB09, Wei10, JCS09, PM07, PNM08] and were also the subject of this thesis [VP08a, VP08b, VP09, Val10, VPS10], which can be probed when the cold gas is sufficiently dilute. Furthermore, many researchers have since studied the implications of the few-body bound states on the many-body physics in a lattice [PSAF07, WHC08, SBE+09, SJ09, SJS10, RRBV08, SGJ+08].

Ultracold atoms loaded in optical lattices are robust systems to explore few-body phenomena. Using magnetic Feshbach resonances [Fes58, BLV+09] to modify the low-energy properties of atom-atom interactions, the scattering length can be very precisely tuned in a wide interval. A particularly interesting implication is the Efimov effect [Efi70], originally predicted in the context of nuclear physics four decades ago, which results in a sequence of weakly bound trimers with universal properties appearing near the two-body threshold. Since the first evidence of the existence of such trimers in a single well of an optical lattice [KMW+06], the Efimov physics has become an important topic of theoretical [vSDG09, DGE09, MRDG08, TFJ+09, WE09] and experimental [KFM+09, FKB+09] research.

The extreme experimental control over ultracold atoms in optical lattices makes it possible to set the number of particles per unit cell to one [GME+02] or few. Single-site addressability (emptying lattice wells at will), recently achieved in [WLG+09], complemented by the control over the lattice filling, opens up new possibilities for exploring few-body effects on a lattice, which may allow the observation of phenomena associated

with translational invariance, which are those considered in this thesis.

The physics of few particles on a lattice (or in systems with a non-trivial band structure) is, on the other hand, relevant in condensed matter as well. The most traditional condensed matter systems where few-body physics play a role are, without any doubts, semiconductors. The study of fundamental problems on the binding of the exciton, an electron-hole pair, was an active area of research two decades ago. Among these, the long standing question "what is the mass of the exciton?" was then answered [MG84]. It was shown, theoretically, that the effective mass of the exciton depends on its center of mass energy, shortly confirmed experimentally by Cafolla and co-authors in [CST85]. A closely related effect appears in most of the models considered in this thesis, however in a different context. More recently, there is also growing interest in the physics of excitons due to the experimental advances in the search for the Aharonov-Bohm effect [AB59] with a single exciton in quantum dot nanorings [FVCPR09, TVCLR$^+$10].

The few-body problem is also relevant to the physics of magnetism. Certain elementary excitations of magnetic materials, called magnons, can be regarded as a collection of few interacting (quasi-) particles on a lattice. A benchmark example is the two-magnon spectrum of the spin-half one-dimensional Heisenberg model, already solved by Bethe almost 70 years ago [Bet31] by means of his celebrated ansatz. Direct experimental observation of two-magnon bound states in a spin-1 chain was recently reported in [ZWB$^+$07], while evidence of Bose-Einstein condensation of quasi-particles, in this case spin triplets, was unambiguously obtained in a seminal experiment by Zapf and collaborators [ZZH$^+$06]. These recent achievements highlight the importance of few-particle effects in realistic many-body systems.

The work presented in this thesis is focused on the transport, scattering and binding of few particles on a deep one-dimensional lattice. This research is mainly motivated by the recent experimental advances in few-body physics in optical lattices. But the findings are expressed in a general form so that they are independent of the particular physical realization of the models. This work aims at filling the gap between the widely studied one- and many-body (finite density) problems on a lattice. Its relevance lies mostly, but not only, on the methodology, which simplifies and generalizes previous works [WTL$^+$06, PM07, Mat86], and is extendable to the physics of magnetic materials. The exact solutions presented in this thesis yield clear physical interpretation of the results; while for systems with no analytic solution, effective theories are constructed to clarify their physics.

In this thesis, I discuss the quantum dynamics of a single particle and a bound particle pair in a deep lattice superimposed by a weak harmonic potential, which is a realistic experimental situation for cold atoms in optical lattices. It is found that coherent, non-dispersive transport of wavepackets can be achieved from one side of the trap to the other [VP08a]. Moreover, it is shown that carefully "engineered" initial wave packets, being localized at essentially one lattice well, can also exhibit periodic oscillations between the two sides of the shallow trap. It is also demonstrated that, in a weak harmonic trap, repulsively interacting pairs can be tighter bound than those subject to attractive interaction. The interpretation of this effect turns out to be a simple consequence of the solutions obtained for the homogeneous lattice in [VP08b].

By using a methodology introduced by the author in [VP08b], the two-body problem on a one-dimensional lattice with nearest-neighbor interactions is also studied. It is shown that, contrary to what happens in the pointlike interacting case [WTL$^+$06, PM07,

VP08b], finite- and low-energy resonances can exist [VP09] in such system. We derive exact solutions for both bound and scattering states and find that, in general, two different bound states can exist. These findings are relevant in view of the recent interest in dipolar atoms or molecules in optical lattices [GWH+05].

Next, by generalizing the methods introduced in [VP08b] and [VP09], it is shown that any two-body problem on a one-dimensional lattice with arbitrary but finite range interactions is exactly solvable [Val10]. As an important mathematical result, it is proven that all bound states are fully characterized by roots of polynomials of a well defined degree, which depends on the range of the interactions.

The results for the two-body problem are extended to investigate the binding [VPS10] and scattering of three bosonic particles on a one-dimensional lattice. A complete, exact numerical solution of the integral equation [Mat86] for three-body bound states is given, and it is found that, apart from the trivial bound states consisting of three bosons co-localized at the same site, there exist two hitherto unknown weakly bound states. These states correspond to a strongly-bound boson pair and a third particle at a neighboring site, interacting via an effective particle-exchange interaction. Within this effective theory, the pair-particle scattering is analytically solved, using the methods derived for the two-body problem.

The problem of collision and binding of a mobile particle and a heavy (static impurity) one on a superlattice is here addressed. It is shown that a simple modification of the methods introduced for the two-body problem on a homogeneous lattice, to account for Bloch's theorem, suffices to obtain the exact solutions. By solving either an integral equation in quasi-momentum space or a transcendental equation obtained from direct lattice representation, it is found that, independently of the strength of the particle-impurity interaction, there are always two bound states of the mobile particle being trapped by the immobile impurity. This is then formalized by finding that the scattering length can have no poles.

The fundamental question of constructing a lattice harmonic oscillator which, in its ground state, preserves all the "good" properties of its analog in continuous space, such as supersymmetric algebraic structure and minimal uncertainty relation, is also addressed here. The formalism is then applied to two different but related problems: low-energy scattering off a static impurity in a periodic potential, and a many-body interacting system on a finite ring. This topic and the particle-impurity collisions on the superlattice represent work in progress.

Outline

In chapter 2, we introduce most of the theoretical and mathematical tools needed for the understanding of the rest of the thesis. In particular, we present the physics of optical lattices and the tight-binding approximation. The experts in the field may skip this chapter.

In chapter 3, after introducing two kinds of boundary conditions for particles on a finite, one-dimensional lattice, we give the exact solution of some well-known one-body problems, which illustrate the usefulness of the quasi-momentum representation. We then explain our results on coherent transport of a single particle in a lattice superimposed by a harmonic potential.

The scattering, binding and transport of two lattice particles are studied in chapter 4.

A detailed treatment of the three-body problem is given in chapter 5. The scattering of a single particle off an impurity on a superlattice is the topic of chapter 6. Finally, our model of the harmonic oscillator on the lattice, with some applications to other physical systems, is discussed in chapter 7.

2. Formalism of Quantum Lattice Physics

Quantum Mechanics on a tight-binding, single band lattice, which we call "Quantum Lattice Physics", requires the use of a formalism which differs in some aspects from the "usual" Quantum theory due to the discrete nature of the underlying physical space.

In this chapter we introduce how optical lattices can be experimentally created by means of laser-atom interaction. We then briefly explain the single-particle band structure in a periodic potential, and the tight-binding approximation.

Next, we will show how to construct a discrete kinetic energy operator assuming that we only know an approximate functional form of the energy dispersion in terms of the single-particle (quasi-) momentum. Though we can take any functional form, with a certain periodicity in quasi-momentum space, we will restrict ourselves to the one we will derive in subsect. 2.2, which is the simplest possible approximation. We apply what is known as Peierls' substitution [Pei33], which maps the single-particle problem to direct lattice space. This is the basic idea behind any discrete quantum-mechanical theory.

After Peierls' substitution, we are left with a self-adjoint kinetic energy operator which links a function at a given point only with its nearest neighbors[1] on the lattice [Mat86]. Since the functions involved must be only defined at lattice points, we have to choose a Hilbert space $\mathcal{H}$ in accordance with the discretization. It is natural therefore to choose $\mathcal{H}$ as the space of square summable functions – ℓ^2 – in direct lattice representation; otherwise, if we would choose spaces of square integrable functions – $\mathcal{L}^2$ –, the solutions to the problems we are interested in would not be uniquely defined! In reciprocal (quasi-momentum) representation, we use an $\mathcal{L}^2$ space of periodic functions. Changing from one representation to the other is made possible thanks to the discrete version of the Fourier transform [Bri88].

Since most of the results below are special topics in scattering theory on the one-dimensional lattice, we briefly introduce in this chapter the lattice version of collision theory which is, in fact, very similar to scattering theory in free space [Joa75]. In particular, we will discuss the Green's function approach [Eco90] to the problem and obtain the free particle Green's functions for the one-dimensional case.

2.1. Optical lattices

The interaction of atoms with light has a broad range of applications. Among the most relevant ones are laser cooling and trapping of atoms [PS08]. We briefly introduce here near-resonant laser-atom interaction, and use it to describe the generation of laser-induced periodic potentials – optical lattices.

In the dipole approximation, the interaction between the laser electric field and the

---

[1]The models used throughout this thesis are mostly coupling only nearest-neighbors.

atom is given by

$$\hat{V}_d = -\mathbf{d} \cdot \mathbf{E}, \tag{2.1}$$

where $\mathbf{d}$ is the dipole moment of the atom and $\mathbf{E}$ is the (classical) electric field. If the field is static, $\mathbf{E} \neq \mathbf{E}(t)$, the perturbative correction to the ground state energy of an atom is given by

$$\Delta = -\sum_e \frac{|\langle e| \hat{V}_d |g\rangle|^2}{\xi_e - \xi_g}, \tag{2.2}$$

where e runs over all excited states of the atom, g labels its ground state, and $\xi_{e(g)}$ is the excited (ground) state energy of the unperturbed atom. By writing the electric field as $\mathbf{E} = E\mathbf{u}$, where $\mathbf{u}$ is the unit vector in the direction of the electric field, the perturbative correction (dc Stark shift) becomes

$$\Delta = -\frac{1}{2}\alpha|\mathbf{E}|^2, \tag{2.3}$$

where we have defined the static polarizability of the atom as

$$\alpha = 2\sum_e \frac{|\langle e| \mathbf{d} \cdot \mathbf{u} |g\rangle|^2}{\xi_e - \xi_g}. \tag{2.4}$$

We now assume that the electric field of the laser is, to a good approximation, monochromatic with a frequency ω. The time-dependent electric field acquires the form

$$\mathbf{E}(\mathbf{r}, t) = \mathbf{E}^{(+)}(\mathbf{r})e^{-i\omega t} + \mathbf{E}^{(-)}(\mathbf{r})e^{i\omega t}, \tag{2.5}$$

where we have used the standard notation $\mathbf{E}^{(\pm)}$ for the positive and negative frequency parts of the electric field [LP07]. Since the electric field is real, we have $[\mathbf{E}^{(+)}]^* = [\mathbf{E}^{(-)}]$.[2] The time averaged ground state energy (or ac-Stark) shift is given in this case by

$$\Delta = -\frac{1}{2}\alpha(\omega)\langle|\mathbf{E}(\mathbf{r}, t)|^2\rangle, \tag{2.6}$$

with

$$\langle|\mathbf{E}(\mathbf{r}, t)|^2\rangle = \frac{1}{T}\int_0^T |\mathbf{E}(\mathbf{r}, t)|^2 dt \tag{2.7}$$

the time averaged squared electric field over a period $T = 2\pi/\omega$, and the dynamic polarizability given by

$$\alpha(\omega) = 2\sum_e (\xi_e - \xi_g)\frac{|\langle e| \mathbf{d} \cdot \mathbf{u} |g\rangle|^2}{(\xi_e - \xi_g)^2 - (\hbar\omega)^2}. \tag{2.8}$$

If the frequency is close to a single, isolated atomic resonance $g \to e$, we can approximate the polarizability as

$$\alpha(\omega) \approx \frac{|\langle e| \mathbf{d} \cdot \mathbf{u} |g\rangle|^2}{\xi_e - \xi_g - \hbar\omega}. \tag{2.9}$$

Since we only want to briefly introduce all these concepts, we avoid further complications by not considering the finite lifetime of the excited state here.

---

[2]If the electric field would be quantized, this corresponds to the hermiticity of the E-field operator.

We can now interpret the energy shift Δ in the ground state of the atom due to the external laser field as a potential felt by the atom. In this way, we find that the external potential has the form

$$V(\mathbf{r}) = -\frac{1}{2}\alpha(\omega)\langle|\mathbf{E}(\mathbf{r}, t)|^2\rangle. \tag{2.10}$$

For a one-dimensional lattice, it suffices to consider a standing wave laser field, which is a superposition of two linearly polarized counterpropagating laser fields of the form $E_0\cos(\pm kx - \omega t)$, so that

$$E(x, t) = E_0[\cos(kx - \omega t) + \cos(kx + \omega t)] = 2E_0\cos(kx)\cos(\omega t), \tag{2.11}$$

and therefore the time averaged intensity has the form

$$\langle|E(x, t)|^2\rangle = 2E_0^2\cos^2(kx). \tag{2.12}$$

The optical lattice potential then becomes

$$V(x) = -\alpha(\omega)E_0^2\cos^2(kx), \tag{2.13}$$

which is a periodic potential with lattice spacing $d = \pi/k$. Note that for $\alpha(\omega) > 0$ ($\alpha(\omega) < 0$), the periodic potential is attractive (repulsive) at the local maxima of the intensity (2.12). In the following section we study the general band structure of a periodic potential and the tight-binding approximation.

2.2. The band structure

Periodic potentials have general properties which are independent of their particular form. The single-particle energy spectrum consists of different bands which are usually separated by gaps – forbidden energy regions. Each of the energies in the bands can be labeled by an integer band index s and a continuous vector "index" called quasi-momentum $\mathbf{k}$, as we will discuss in this section.

We start with the single-particle stationary Schrödinger equation for a particle with mass m

$$H\psi = \left(-\frac{\hbar^2}{2m}\nabla^2 + V(\mathbf{r})\right)\psi = E\psi, \tag{2.14}$$

with $V(\mathbf{r} + \mathbf{R}) = V(\mathbf{r})$, that is, V is periodic – invariant under a translation $\mathbf{r} \to \mathbf{r} + \mathbf{R}$, where $\mathbf{R}$ is a lattice vector. We state a simple, yet extremely important result, known as Bloch's theorem [AM76]:

Theorem. The eigenstates of H, Eq. (2.14), can be written as

$$\psi(\mathbf{r}) \equiv \psi_{s,\mathbf{k}}(\mathbf{r}) = e^{i\mathbf{k}\cdot\mathbf{r}}\phi_{s,\mathbf{k}}(\mathbf{r}), \tag{2.15}$$

where $\phi_{s,\mathbf{k}}(\mathbf{r} + \mathbf{R}) = \phi_{s,\mathbf{k}}(\mathbf{r})$.

To illustrate the concept of band structure, we solve here a famous exactly solvable model in one dimension, the so-called Kronig-Penney (KP) model. The periodic poten-
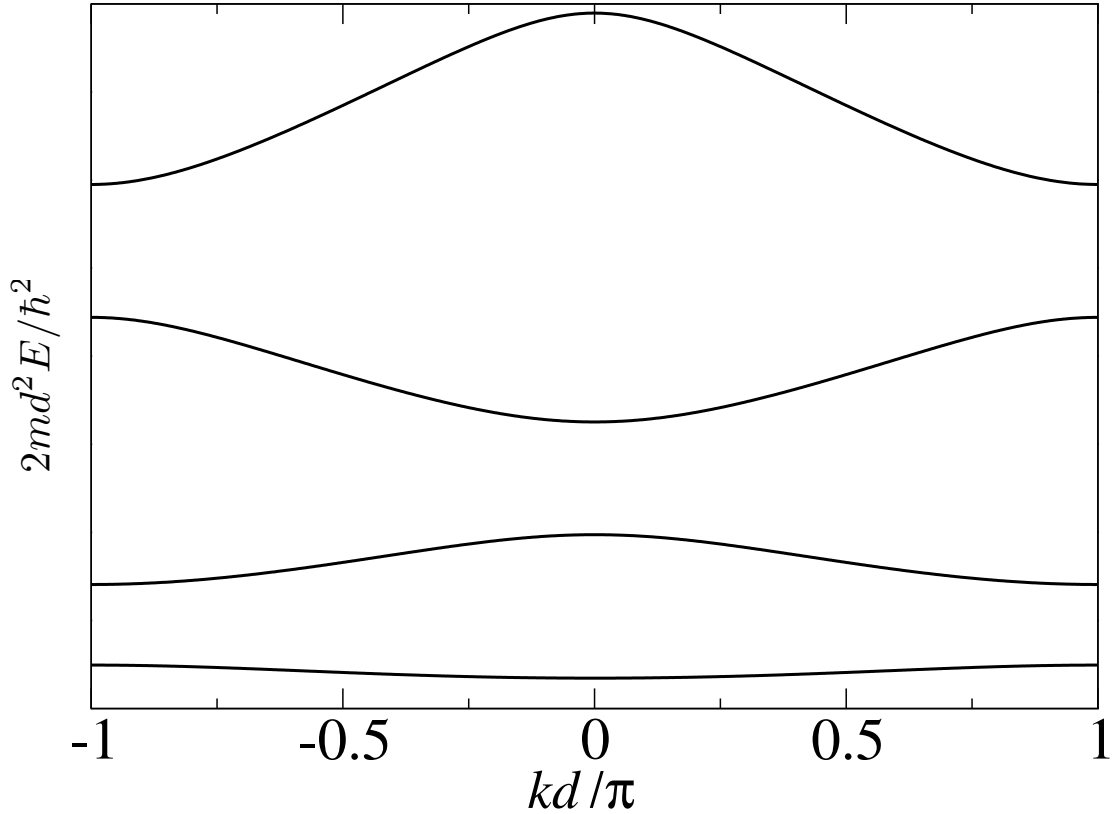
Figure 2.1.: Band structure of the Kronig-Penney model, calculated from Eq. (2.17) for $2md^2g/\hbar^2 = 10$.

tial of the KP model has the form

$$V(x) = g \sum_{n=-\infty}^{+\infty} \delta(x - nd), \tag{2.16}$$

where d is the lattice spacing and δ is a Dirac delta. The problem is trivially shown to have its energy spectrum obtained by solving the following transcendental equation for each value of the Bloch quasi-momentum k

$$\frac{2mg}{\hbar^2\alpha} \sin(\alpha d) + \cos(\alpha d) = \cos(kd), \tag{2.17}$$

where $\alpha^2 = 2mE/\hbar^2$ and E is the energy eigenvalue. In Fig. 2.1 we show the first four bands for $2md^2g/\hbar^2 = 10$ in the reduced band scheme [AM76], that is, we show the energies only in the first Brillouin zone (1BZ). The band gaps are clearly identified there. The value of g chosen for Fig. 2.1 is quite large, since it is comparable to the energy of a free particle at the edges of the 1BZ, $E_0 = \hbar^2\pi^2/2md^2 \approx g$. Therefore, the gaps are rather big: we say that in this case we are in the tight-binding regime. If $g \ll E_0$ the band gaps would become very small, and the energies, in the extended zone scheme, would resemble a free particle parabola: we say we are in the quasi-free regime.

2.2.1. Tight-binding approximation

Throughout this thesis, most of the results are obtained in the tight-binding regime, where we use extensively the so called single-band approximation: if the gaps between bands $s - 1$, s and $s + 1$ are large compared to the typical strength of the pairwise interactions, and if there is no inelastic transition between the bands due to such interactions, phonons or external fields, we can basically assume that, once the particles occupy the s-th band, they will remain there. In order to illustrate the tight-binding method, we have to introduce first an orthonormal basis – the Wannier basis [AM76] – such that the exact Bloch functions are expanded in terms of the Wannier functions w_s as

$$\psi_{s,k}(x) = \sum_R e^{ikR} w_s(x - R) \equiv \sum_n e^{ikx_n} w_s(x - x_n), \tag{2.18}$$

where, for simplicity, we have assumed a one-dimensional lattice. If the periodic potential is deep, the Wannier functions of the lowest Bloch band are actually localized around the local minima of the periodic potential (which we assume to be at $x_n = nd$, with $n \in \mathbb{Z}$). We will assume from now on that the particles are ocupying the lowest Bloch band only.

Let us consider a many-body system with pairwise interactions $U(x - x')$ in the presence of periodic confinement $V(x + x_n) = V(x)$. The action is given by [SGD09]

$$S[\Psi^*, \Psi] = \int_0^{\hbar\beta} d\tau \int dx \, \Psi^*(x, \tau) \left(\hbar \frac{\partial}{\partial \tau} - \frac{\hbar^2}{2m} \frac{\partial^2}{\partial x^2} + V(x) \right) \Psi(x, \tau)$$

$$+ \frac{1}{2} \int_0^{\hbar\beta} d\tau \int dx \int dx' \Psi^*(x, \tau) \Psi^*(x', \tau) U(x - x') \Psi(x', \tau) \Psi(x, \tau), \tag{2.19}$$

where Ψ and $\Psi^* = [\Psi]^*$ are the complex fields, $\beta = 1/k_B T$, and τ is the imaginary time. We now expand the fields in terms of Wannier functions as

$$\Psi(x, \tau) = \sum_{s,n} b_{s,n}(\tau) w_s(x - x_n). \tag{2.20}$$

Since we assume that only the lowest Bloch band is occupied, we only retain terms with $s = 0$ in the above sum. The final result reads in this case

$$S[b^*, b] = S_0[b^*, b] + S_U[b^*, b], \tag{2.21}$$

with the free action given by

$$S_0[b^*, b] = \int_0^{\hbar\beta} \left[\sum_n b_n^*(\tau) \left(\hbar \frac{\partial}{\partial \tau} + \epsilon_n \right) b_n(\tau) - \sum_{n \neq m} b_n^*(\tau) J_{nm} b_m(\tau) \right], \tag{2.22}$$

where the on-site energies are defined as

$$\epsilon_n = \int dx \, w_0^*(x - x_n) \left[-\frac{\hbar^2}{2m} \frac{\partial^2}{\partial x^2} + V(x) \right] w_0(x - x_n), \tag{2.23}$$

and the tunneling rates between sites n and m are given by

$$J_{nm} = -\int dx w_0(x - x_n) \left[-\frac{\hbar^2}{2m} \frac{\partial^2}{\partial x^2} + V(x) \right] w_0(x - x_m). \qquad (2.24)$$

If the periodic potential is very deep, the Wannier functions are strongly localized around the center of the given lattice site. We can then assume that, to a good approximation, the tunneling rate is practically zero if $|n - m| > 1$. We then have $J_{n,m\pm1} \equiv J \neq 0$ and $J_{nm} = 0$ otherwise. For the interacting part of the action we also simplify the problem by assuming that the interaction potential U is very weak when the particles do not lie on the same site, and therefore we have

$$S_U[b^*, b] = \int_0^{\hbar\beta} d\tau \frac{U}{2} \sum_n b_n^*(\tau) b_n^*(\tau) b_n(\tau) b_n(\tau), \qquad (2.25)$$

where we have defined

$$U \equiv \int dx \int dx' w_0^*(x - x_n) w_0^*(x' - x_n) U(x - x') w_0(x' - x_n) w_0(x - x_n). \qquad (2.26)$$

Again, for simplicity, we consider only bosons, and the action (2.21) corresponds to the second quantized Hamiltonian

$$H = -J \sum_n (\hat{b}_n^\dagger \hat{b}_{n+1} + \hat{b}_{n+1}^\dagger \hat{b}_n) + \sum_n \epsilon_n \hat{N}_n + \frac{U}{2} \sum_n \hat{N}_n(\hat{N}_n - 1), \qquad (2.27)$$

where $\hat{b}_n^\dagger$ ($\hat{b}_n$) is the bosonic creation (annihilation) operator at site n, and where we have defined the number operator $\hat{N}_n = \hat{b}_n^\dagger \hat{b}_n$. The immediate consequence of the tight-binding Hamiltonian (2.27) is that the single particle energy band, for $\epsilon_n \equiv \gamma = $ constant has the form

$$\epsilon(k) = -2J \cos(kd) + \gamma, \qquad (2.28)$$

which is the well-known tight-binding dispersion relation [AM76]. In the following sections we will derive the first-quantized form of Eq. (2.27), i.e. valid for bosons, fermions, mixtures or distinguishable particles in general, by means of the so-called Peierls' substitution.

A more sophisticated approach to obtaining an interacting Bose-Hubbard Hamiltonian was given by Schneider and collaborators in [SGS09].

2.3. Peierls' substitution

In order to construct a quantum theory of an interacting N-body system of particles allowed to have only discrete lattice positions at $\ldots, -nd, -(n-1)d, \ldots, (n-1)d, nd, \ldots$, it is necessary to introduce Hermitian operators which are only defined at such discrete positions. Here we introduce what is called Peierls' substitution, which makes it possible to define a discrete kinetic energy operator.

The lowest energy band of a single particle in a tight-binding periodic potential has the form (see Eq. (2.28))

$$\epsilon(k) = -2J \cos(kd), \qquad (2.29)$$

where J is the so-called tunneling rate, $k \in (-\pi/d, \pi/d]$ is the quasi-momentum of the particle and d is the lattice spacing. Peierls' substitution consists of replacing the quasi-momentum by an operator, namely

$$k \to -\mathrm{i}\partial_x. \tag{2.30}$$

Therefore, the energy is no longer a scalar, but it becomes a function of an operator,

$$\epsilon \to \hat{T} = -2J\cos(-\mathrm{i}d\partial_x) = -J(e^{d\partial_x} + e^{-d\partial_x}). \tag{2.31}$$

We take a function $\psi(x)$, which is assumed to be analytic $\forall x$. The action of any analytic function of an operator on $\psi(x)$ is defined via its Taylor expansion [Con94, Kat95]. For the operator $\hat{T}$, we have

$$(\hat{T}\psi)(x) = -J\sum_{n=0}^{\infty}\left(\frac{d^n}{n!}\partial_x^n\psi(x) + \frac{(-d)^n}{n!}\partial_x^n\psi(x)\right). \tag{2.32}$$

Since $\psi(x)$ is an analytic function, its Taylor series exists at every point, so we have the following expression

$$\psi(x \pm d) = \sum_{n=0}^{\infty}\frac{(\pm d^n)}{n!}\partial_x^n\psi(x). \tag{2.33}$$

We therefore conclude that

$$(\hat{T}\psi)(x) = -J\left(\psi(x+d) + \psi(x-d)\right), \tag{2.34}$$

where, of course, x should be points of the discrete lattice, that is, $x/d \in \mathbb{Z}$.

The action of the kinetic energy operator $\hat{T}$ on a wave function ψ can be regarded as "hopping" of a particle from one lattice site $n = x/d$ to its neighboring sites $n+1$ and $n-1$, with a certain hopping (tunneling) rate J. Unless otherwise stated, lattice sites will be labeled by integer numbers n instead of their lattice positions x which are less convenient, contrarily to finite difference discretization where the continuum limit is the final goal. Note that the continuum limit of the discrete kinetic energy is indeed the second derivative

$$\lim_{d\to 0} -\frac{\hat{T} + 2J\hat{\mathbb{1}}}{Jd^2} = \partial_x^2. \tag{2.35}$$

Mathematically, the discrete kinetic energy operator $\hat{T}$ is called a second-order finite-difference operator.

2.4. Hilbert spaces for a lattice and the discrete Fourier transform

In this section we define the relevant Hilbert spaces, and the discrete Fourier transform between quasi-momentum and direct lattice representations.

2.4.1. Direct lattice space

Usually, in Quantum Mechanics, a system of N particles is assumed to move in a D-dimensional Euclidean space $\mathbb{R}^D$. The Hilbert space associated with the system is the Lebesgue $\mathcal{H}' = \bigotimes_{i=1}^N \mathcal{L}^2(\mathbb{R}^D)$ space, that is, the N-body wave function $|\psi\rangle$ must be square integrable,

$$\langle\psi|\psi\rangle = \int_{\mathbb{R}^{ND}} |\psi(\mathbf{r}_1, \mathbf{r}_2, \ldots, \mathbf{r}_N)|^2 d\mathbf{r}_1 d\mathbf{r}_2 \ldots \mathbf{r}_N < \infty, \tag{2.36}$$

with $\mathbf{r}_i \in \mathbb{R}^D$.

If the physical system is not defined in a continuous space, but on a lattice, the situation changes drastically, since we can no longer define the Hilbert space as $\mathcal{H}'$. In a D-dimensional hypercubic lattice, the lattice points must satisfy $\mathbf{n} \in \mathbb{Z}^D$ (with $\mathbf{n} = \mathbf{r}/d$). Since it is not possible to integrate in a discrete space, we substitute integrals in $\mathcal{L}^2$ by sums in ℓ^2 spaces. Therefore, the natural Hilbert space of the system is $\mathcal{H} = \bigotimes_{i=1}^N \ell^2(\mathbb{Z}^D)$. If $|\psi\rangle \in \mathcal{H}$, then

$$\langle\psi|\psi\rangle = \sum |\psi(\mathbf{n}_1, \mathbf{n}_2, \ldots, \mathbf{n}_N)|^2 < \infty. \tag{2.37}$$

The scalar products in ℓ^2 are defined as usual: if $|\psi\rangle$, $|\phi\rangle \in \mathcal{H}$ then

$$\langle\phi|\psi\rangle = \sum \phi^*(\mathbf{n}_1, \ldots, \mathbf{n}_N)\psi(\mathbf{n}_1, \ldots, \mathbf{n}_N). \tag{2.38}$$

2.4.2. Reciprocal space. The discrete Fourier transform

In order to construct an interacting theory capable of describing scattering and binding of microscopic particles, the lattice analog of the momentum representation – the quasi-momentum representation – can be very useful.

In the continuum, the Fourier-Plancherel transform maps wave functions from real to momentum space. There is a discrete version of the Fourier transform on a lattice, namely the discrete Fourier transform (DFT). To define it, assume, for simplicity, that we have a single-particle wave function in one dimension and in direct lattice representation. Furthermore, assume that the lattice has a finite number of points consisting of the elements of the subset $\{-L, \ldots, L\} \subset \mathbb{Z}$, and we are interested in the limit $L \to \infty$. Then,

$$|\psi\rangle = (\psi(-L), \psi(-L+1), \ldots, \psi(0), \ldots, \psi(L-1), \psi(L)). \tag{2.39}$$

The DFT of $|\psi\rangle$ is defined as follows

$$\tilde{\psi}(q) \equiv (\mathcal{F}\psi(x))(q) = \sum_{n=-L}^{L} \psi(n)e^{-\frac{2\pi}{2L+1}iqn}, \tag{2.40}$$

where $q = -L, \ldots, L$ is an integer number. The DFT above is not a unitary transformation, so the norms are not preserved. However, this definition is more convenient in order to properly take the limit $L \to \infty$. The norms are related as $\langle\tilde{\psi}|\tilde{\psi}\rangle = (2L+1)\langle\psi|\psi\rangle$, so

the normalization condition implies

$$\frac{1}{2L+1}\langle\tilde{\psi}|\tilde{\psi}\rangle = \frac{1}{2L+1}\sum_{q=-L}^{L}|\tilde{\psi}(q)|^2 = \frac{1}{2\pi}\sum_{q=-L}^{L}|\tilde{\psi}(q)|^2\Delta_L < \infty, \qquad (2.41)$$

where $\Delta_L \equiv 2\pi/(2L+1)$. In the limit of $L \to \infty$, the sum turns into an integral, and the normalization condition reads

$$\frac{1}{2\pi}\int_{-\pi}^{\pi}dk|\tilde{\psi}(k)|^2 < \infty. \qquad (2.42)$$

The normalization condition stated above is evidently equivalent[3] to $|\tilde{\psi}\rangle \in \mathcal{L}^2((-\pi,\pi])$. Therefore, the natural generalization of the Hilbert space to N particles and D dimensions is $\tilde{\mathcal{H}} = \bigotimes_{i=1}^{N}\mathcal{L}^2(\Omega)$, where Ω is the Brillouin zone hypervolume $\Omega = (-\pi,\pi]^D$.

2.5. Discrete Schrödinger equation

We consider here the Schrödinger equation for, first, a single particle with and without an external potential, in one dimension; and, second, for an arbitrary number of interacting particles, possibly in an external potential, in any dimension.

2.5.1. Single-particle equation

Let us consider a free particle moving on a one-dimensional lattice. The Hamiltonian of the system is then simply the discrete kinetic energy, that is,

$$H = \hat{T} = -J(e^{d\partial_x} + e^{-d\partial_x}). \qquad (2.43)$$

The stationary Schrödinger equation $H|\psi\rangle = E|\psi\rangle$ reads in this case

$$-J(\psi(n+1) + \psi(n-1)) = E\psi(n), \qquad (2.44)$$

where $n = x/d$. The Schrödinger equation is equivalent to a three-term recurrence relation with the condition $|\psi(n)| \leq C \in \mathbb{R}$ for all $n \in \mathbb{Z}$. Applying the plane-wave ansatz

$$\psi(n) = e^{iknd}, \qquad (2.45)$$

which is bound by 1 $\forall n$, we obtain

$$-2J\cos(kd)e^{iknd} = Ee^{iknd} \Rightarrow E = \epsilon(k) = -2J\cos(kd). \qquad (2.46)$$

The energy of a free lattice particle could have also been obtained by means of the spectral mapping theorem (SMT) [Con94]. Since the discrete kinetic energy, Eq. (2.43), was obtained with Peierls' substitution, and the spectrum of $-i\partial_x$ is the whole real line, the SMT implies that the spectrum of $H = \hat{T}$ is $E = -2J\cos(kd)$, where $k \in \mathbb{R}$ are the eigenvalues of $-i\partial_x$. Since the cosine is a periodic function of kd, we restrict k to $(-\pi/d, \pi/d]$, hence recovering the whole spectrum of the free Hamiltonian.

---

[3]We have avoided further complications by considering only the Riemann integral. Rigorously speaking, we should have used the Lebesgue construction.

We consider now a single particle subject to an external potential $v(n)$, which can be a trap ($\lim_{n\to\pm\infty} v(n) = \infty$), a finite-range potential ($v(n) = 0$ if $n > n^+ \in \mathbb{Z}_+$ or $n < n^- \in \mathbb{Z}_-$), a commensurate periodic potential ($v(n + n_0) = v(n)$ for some $n_0 \in \mathbb{Z}$), an incommensurate periodic potential ($v(n + z_0) = v(n)$ for some $z_0 \in \mathbb{R} - \mathbb{Z}$), a random potential ($v(n)$ is a random sequence), or some combination thereof.

The Hamiltonian of the system is the sum of kinetic and potential energies, $H = \hat{T} + v$, and the stationary Schrödinger equation reads

$$(H\psi)(n) = -J(\psi(n + 1) + \psi(n - 1)) + v(n)\psi(n) = E\psi(n). \tag{2.47}$$

Depending on the shape and properties of the external potential, the eigenenergies and eigenfunctions of H may be calculated analytically but, in general, a numerical solution of Eq. (2.47) will be required. Some of the exactly solvable single-particle Schrödinger equations are discussed in chapter 3.

2.5.2. Many-body systems of interacting particles

Most of the physically interesting lattice effects are associated with several interacting particles. Furthermore, the combined effects of the lattice, the interactions and an external potential yield even richer physics. Assuming that only two-body interactions are present, the Hamiltonian for $N > 1$ particles reads

$$H = \sum_{i=1}^{N} (\hat{T}_i + v_i) + \sum_{i<j=1}^{N} V_{i,j}, \tag{2.48}$$

where $\hat{T}_i$ and v_i are, respectively, the kinetic and potential energy of particle i, and $V_{i,j}$ represents the two-body interaction between particles i and j. Unless otherwise stated, V will be assumed to be symmetric, that is, $V_{i,j} = V_{j,i}$. The stationary Schrödinger equation $H\,|\psi\rangle = E\,|\psi\rangle$ is

$$-J\sum_{i=1}^{N}\left(\sum_{s=1}^{D}\psi(\mathbf{n}_1,\ldots,\mathbf{n}_i+\mathbf{e}_s,\ldots,\mathbf{n}_N) + \sum_{s=1}^{D}\psi(\mathbf{n}_1,\ldots,\mathbf{n}_i-\mathbf{e}_s,\ldots,\mathbf{n}_N)\right)$$

$$+\left(\sum_{i=1}^{N}v_i(\mathbf{n}_i) + \sum_{i<j=1}^{N}V_{i,j}(\mathbf{n}_i,\mathbf{n}_j)\right)\psi(\mathbf{n}_1,\ldots,\mathbf{n}_N) = E\psi(\mathbf{n}_1,\ldots,\mathbf{n}_N), \tag{2.49}$$

where the translation vectors are defined as

$$\mathbf{e}_s \equiv (0,\ldots,1,\ldots,0), \tag{2.50}$$

that is, $\mathbf{e}_s$ is a normalized D-dimensional vector.

Important note: From now and in the rest of the thesis we will implicitly assume that $d \equiv 1$, unless otherwise stated. In chapter 7, the lattice spacing will not be set to 1, since we will need it for the continuum limit.

2.6. Collision theory on the lattice

In analogy with the usual quantum mechanics in continuous space, the collision of particles moving on a discrete lattice can be described in terms of a modified version of the integral equation of scattering (the Lippmann-Schwinger equation). Our starting point is the discrete Schrödinger equation for a particle scattered off a finite range potential v

$$[(\hat{T} - \epsilon(k))\psi_k](n) = -v(n)\psi_k(n), \tag{2.51}$$

where $\hat{T}$ is the discrete kinetic energy operator and $\epsilon(k)$ is the single-particle energy band. The general solution of this equation can be written as

$$\psi_k(n) = \phi_k(n) - \sum_m G_k^{(0)}(n, m)v(m)\psi_k(m), \tag{2.52}$$

where ϕ_k is the solution of the homogeneous difference equation

$$[(\hat{T} - \epsilon(k))\phi_k](n) = 0, \tag{2.53}$$

and the free particle Green's function $G_k^{(0)}$ satisfies

$$[(\hat{T}_n - \epsilon(k))G_k^{(0)}](n, m) = \delta_{n,m}. \tag{2.54}$$

The subscript n in $\hat{T}_n$ signifies that it only acts on coordinate n, and $\delta_{n,m}$ is the Kronecker delta.

If we are interested in bound states with eigenenergies E lying outside the continuum, $|E| > \max|\epsilon(k)| = 2J$, then the Schrödinger equation reads

$$[(\hat{T} - E)\psi_E](n) = -v(n)\psi_E(n), \tag{2.55}$$

and the eigenfunctions ψ_E satisfy the homogeneous equation

$$\psi_E(n) = -\sum_m G_E^{(0)}(n, m)v(m)\psi_E(m), \tag{2.56}$$

where the Green's function $G_E^{(0)}$ for energies outside the continuum satisfies the equation

$$[(\hat{T}_n - E)G_E^{(0)}](n, m) = \delta_{n,m}. \tag{2.57}$$

As seen, the lattice version of the integral equation of scattering is analogous to its continuum counterpart [Joa75], and the only difference is that we have to replace the integral by a sum.

2.6.1. Lattice Green's functions I: scattering states

We have already introduced the free particle Green's function on the lattice. Lattice Green's functions (LGF) have a wide range of applications, arising in general problems involving partial differential equations when dealing with finite difference methods. In our case, the free LGFs are important not only for potential and two-body scattering, but also for the three-body problem in chapter 5. It is therefore convenient to introduce

them and, at least in one dimension, outline some of their properties.

In 1D, the recurrence relation satisfied by the free LGF is

$$-J[G_k^{(0)}(n+1,m) + G_k^{(0)}(n-1,m)] + 2J\cos(k)G_k^{(0)}(n,m) = \delta_{n,m}, \tag{2.58}$$

and since this equation depends only on $z = n - m$, we can rewrite it as

$$-J[G_k^{(0)}(z+1) + G_k^{(0)}(z-1)] + 2J\cos(k)G_k^{(0)}(z) = \delta_{z,0}, \tag{2.59}$$

where $G_k^{(0)}(z) = G_k^{(0)}(n-m) = G_k^{(0)}(n,m)$. We will be mainly dealing with bosons, and their respective problems after separation of the center of mass and relative coordinates. Therefore, we will calculate here the free symmetric LGF, while in one dimension the "antisymmetric" – fermionic – LGF[4] can be built from the solutions for hard-core bosons [Gir60]. For the symmetric LGF we use the most general solution at $z \neq 0$,

$$G_k^{(0)}(z) = C\cos(kz) + D\sin(k|z|), \tag{2.60}$$

which upon insertion in Eq. (2.59), yields $C \equiv 0$ and[5]

$$D = -\frac{\csc(k)}{2J}, \tag{2.61}$$

and therefore the symmetric LGF has the form

$$G_k^{(0)}(n,m) = -\frac{\csc(k)}{2J}\sin(k|n-m|). \tag{2.62}$$

2.6.2. Lattice Green's functions II: bound states

We calculate now the one-dimensional free LGFs $G_E^{(0)}$ for energies outside the continuous spectrum $\epsilon(k)$ of the discrete Hamiltonian. We have to solve Eq. (2.57) which, expressed in "relative coordinate" $z = n - m$ reads

$$-J[G_E^{(0)}(z+1) + G_E^{(0)}(z-1)] - EG_E^{(0)}(z) = \delta_{z,0}. \tag{2.63}$$

Since $|E| > 2J$, we perform a conformal mapping for the energy

$$E = -J\frac{1+\alpha^2}{\alpha}, \tag{2.64}$$

with $\alpha \in \mathbb{R}$ and $|\alpha| < 1$. Substituting this expression, Eq. (2.64), into Eq. (2.63) for $z \neq 0$, we obtain the symmetric LGF

$$G_E^{(0)}(z) = C\alpha^{|z|}, \tag{2.65}$$

---

[4]Properly speaking, the LGF implying an antisymmetric eigenstate of the Schrödinger equation is not antisymmetric.

[5]Below, $\csc(x)$ denotes the cosecant of x.

with C a constant. We now use this result in Eq. (2.63) for $z = 0$, to obtain

$$C = \frac{\alpha}{J(1 - \alpha^2)}. \tag{2.66}$$

In order to get $G_E^{(0)}$ as a function of the energy, we invert the conformal mapping (2.64), so that

$$\alpha = \frac{-E \pm \sqrt{E^2 - (2J)^2}}{2J}. \tag{2.67}$$

Since the LGF $G_E^{(0)}(z) \propto \alpha^{|z|}$, and $G_E^{(0)}$ must be normalizable, the final expression for α must be

$$\alpha = \frac{-E - \text{sgn}(E)\sqrt{E^2 - (2J)^2}}{2J}, \tag{2.68}$$

and therefore the LGF for bound-state energies becomes

$$G_E^{(0)}(n, m) = \frac{\text{sgn}(E)}{\sqrt{E^2 - (2J)^2}} \left[\frac{-E - \text{sgn}(E)\sqrt{E^2 - (2J)^2}}{2J} \right]^{|n-m|}. \tag{2.69}$$

In a similar way, we can obtain the "antisymmetric" (fermionic) Green's function; however, we will omit it and use fermionization [Gir60] instead, when needed.

2.7. Equivalence between repulsive and attractive potentials

We state here a general result for an N-body system on a hypercubic lattice in any dimension which, although being usually implicitly assumed, is useful and important to keep in mind, especially when dealing with purely attractive or repulsive two-body interactions. We will need it throughout this thesis.

Let H be the following second-quantized Hamiltonian

$$H = -J \sum_{\langle \mathbf{m}, \mathbf{n} \rangle} \hat{b}_{\mathbf{m}}^\dagger \hat{b}_{\mathbf{n}} + \hat{F}(\{\hat{N}\}), \tag{2.70}$$

where J is the single-particle tunneling rate, $\langle \mathbf{m}, \mathbf{n} \rangle$ denotes that the sum runs over nearest neighbors, $\hat{b}_{\mathbf{n}}^\dagger$ ($\hat{b}_{\mathbf{n}}$) is the creation (annihilation) operator of a single particle (boson or fermion) at site $\mathbf{n}$ and $\hat{F}$ is an arbitrary analytic function of the number operators at each site $\mathbf{n}$, $\hat{N}_{\mathbf{n}} \equiv \hat{b}_{\mathbf{n}}^\dagger \hat{b}_{\mathbf{n}}$.
If $\mathbf{n} \equiv (n_1, n_2, \dots, n_D)$ is a point of a D-dimensional hypercubic lattice, we define the unitary operation $\hat{G}$, so that $\hat{G} = \hat{G}^\dagger = \hat{G}^{-1}$, with the actions

$$\hat{G}\hat{a}_{\mathbf{n}} = (-1)^{\sum_{s=1}^{D} n_s} \hat{a}_{\mathbf{n}},$$
$$\hat{G}\hat{a}_{\mathbf{n}}^\dagger = (-1)^{\sum_{s=1}^{D} n_s} \hat{a}_{\mathbf{n}}^\dagger. \tag{2.71}$$

We easily see that $H - 2\hat{F} = -\hat{G}H\hat{G}^{-1}$ is unitarily equivalent to $-H$. This implies that the spectrum of a Hamiltonian containing the potentials included in $\hat{F}$ is obtained by changing the sign of every point in the spectrum of the corresponding Hamiltonian having $\hat{F}$ replaced by $-\hat{F}$. In the case of $\hat{F}$ containing purely repulsive (or attrac-

tive) two-body interactions, this result implies a formal equivalence of the solutions for attractive and repulsive potentials.

2.8. Low-energy collisions. Scattering lengths

In free space, when two particles, in one dimension for simplicity, collide with low relative momentum $k \to 0$, much of the physics can be extracted from a single quantity called scattering length. This is defined rigorously as the number a appearing in the zero-energy solution of the stationary Schrödinger equation at larger distances than the finite range (R) of the interaction potential [LSSY05]

$$\phi(x) = \frac{|x| - a}{R - a}. \tag{2.72}$$

By knowing the scattering length of a system, one has many immediate consequences. First of all, a pole in the scattering length denotes the entry (from $a \to -\infty$ to $a \to +\infty$) or exit (from $a \to +\infty$ to $a \to -\infty$) of a bound state. If the scattering length is large and positive, then the least bound state has a binding energy $E \propto -1/a^2$, and its size depends linearly on it, $\langle |x| \rangle \propto a$.

On a one-dimensional lattice, the scattering continuum is bound from below, as well as from above. This has important consequences, one of them being that the limits of low-energy $(E \to -2J)$ and high-energy $(E \to +2J)$ collisions are essentially equivalent (see sect. 2.7). Therefore, there are two different scattering lengths; the first, at energy $E \to -2J$, is defined exactly as in free space, Eq. (2.72), but with x being a discrete coordinate, while the second can be defined in the same way after applying the transformation $\hat{G}$ of the previous section. The consequences one draws from the scattering lengths on the lattice remain unchanged from those in free space discussed above.

3. The one-body problem

The most fascinating aspect of lattice systems, as we have already remarked, is the presence of several particles that interact with each other. However, a deep understanding of any few- or many-particle system requires an even deeper knowledge of the single-particle problem. Not only is the one-body problem the basis for many approximate theories – especially mean-field theories – and necessary ingredient in few-body scattering theory and perturbative calculations, but it also represents an interesting topic by itself. One can, in fact, build a large number of exactly solvable *many-body* problems by simply realizing that a certain one-body problem is solvable via supersymmetric Quantum Mechanics [CKS95]. This is the case of, for example, Sutherland's model [Sut71] and the attractive Lieb-Liniger gas [Mat93]; in chapter 7 we introduce another example which, in fact, can be applied to several different situations.

In this chapter we first introduce two different kinds of boundary conditions for a particle on a finite lattice. Then, we proceed to show, briefly, the solution of two well-known single-particle problems on the lattice. Finally we will show our results [VP08a] on coherent quantum transport of wave packets in a combined lattice and parabolic potential pertinent to the recent experimental progress with ultracold atoms in optical lattices.

3.1. Boundary conditions

We deal here with the problem of one free particle on the lattice which, although being trivial, will be needed in many discussions throughout the text. We define two types of finite lattices, namely, with open and periodic boundary conditions.

3.1.1. Open boundary conditions

Assume a lattice consisting of L sites denoted by $n = 1, \ldots, L$. The open boundary conditions require that the solutions $|\psi\rangle$ of the stationary Schrödinger equation $H |\psi\rangle = E |\psi\rangle$, with $H = \hat{T}$ given by Eq. (2.34), vanish outside a one-dimensional box, that is, $\psi(0) = \psi(L+1) = 0$. The only possible solutions are obviously of the form

$$\psi(n) = \sin(kn), \tag{3.1}$$

while the boundary conditions imply the discretization of the quasi-momenta $k = k_N = N\pi/(L+1)$, with $N = 1, \ldots, L$, and the eigenenergies are given by the usual expression

$$E_N = -2J \cos(k_N). \tag{3.2}$$

Note that the solutions for open boundary conditions, when the lattice space is extended to $\mathbb{Z}$, are also (excited) eigenstates.

3.1.2. Periodic boundary conditions

We now solve the problem with periodic boundary conditions, by setting $\psi(1) = \psi(L + 1) \neq 0$. The eigenstates of H take the form

$$\psi(n) = e^{ikn}, \tag{3.3}$$

and the boundary condition implies $k = k_N = 2\pi N/L$, with $N = 0, \dots, L - 1$, and of course the eigenvalues have the form $E_N = -2J\cos(k_N)$.

3.2. Solution of the Schrödinger equation with some external potentials

We consider here two well-known examples of single-particle discrete Schrödinger equations under external potentials: the discrete harmonic oscillator and linear potentials. In order to study them more easily, we first prove an important result. If an extension of the potential in space representation from $\mathbb{Z}$ to $\mathbb{R}$, $V(x) = \langle x|\hat{V}\rangle$ is an analytic function of $x \in \mathbb{R}$ in the neighborhoods of all integers n, that is, if

$$V(n) = \sum_{j=0}^{\infty} c_j n^j, \tag{3.4}$$

for small open balls (in $\mathbb{R}$) around each $n \in \mathbb{Z}$, then

$$\tilde{V}(k) \equiv \langle k|\hat{V}\rangle = \sum_{j=0}^{\infty} c_j \mathrm{i}^j \frac{\partial^j}{\partial k^j}. \tag{3.5}$$

To show this, it suffices to consider the particular case $V(n) = n^j$, $j \in \mathbb{Z}$. Then by applying the DFT on a wave function ψ, we get

$$(\tilde{V}\psi)(k) = \sum_n n^j \psi(n) e^{-ikn} = \sum_n \psi(n)\mathrm{i}^j \frac{\partial^j e^{-ikn}}{\partial k^j} = \mathrm{i}^j \frac{\partial^j}{\partial k^j}\Big[\sum_n \psi(n) e^{-ikn}\Big] = \mathrm{i}^j \frac{\partial^j}{\partial k^j}\psi(k). \tag{3.6}$$

Note that this fact corresponds to a transformation dual to the Peierls' substitution. We will call the correspondence

$$n \to \mathrm{i}\frac{\partial}{\partial k} \tag{3.7}$$

the inverse Peierls' substitution. We proceed now to solve the Schrödinger equations we have mentioned.

3.2.1. The linear potential

It is well-known [Wan60] that the spectrum of the discrete Hamiltonian

$$H = \hat{T} + \alpha \sum_n n \,|n\rangle\langle n|, \tag{3.8}$$

with $\hat{T}$ given by Eq. (2.34), is linearly spaced, that is, its eigenenergies satisfy $E_{s+1} - E_s = $ constant. This structure of the spectrum is called the Wannier-Stark ladder, and it plays an important role in the physics of semiconductors, exhibiting interesting phenomena such as Bloch oscillations and is the basis for interband transitions [SLS$^+$08].

An exact solution of the eigenvalue problem for H, Eq. (3.8), is possible, in position space, involving Bessel functions [AS64]. Instead, we study the problem in quasi-momentum space, which is even simpler than the direct lattice approach. After using the inverse Peierls' substitution, Eq. (3.7), in the Schrödinger equation $H |\psi\rangle = E |\psi\rangle$, we get

$$i\alpha \frac{\partial \psi}{\partial k}(k) = (E + 2J\cos(k))\psi(k), \tag{3.9}$$

with the periodic boundary condition $\psi(k + 2\pi) = \psi(k)$. The general unnormalized solution of the above equation has the form

$$\psi(k) = \exp\big[-\mathrm{i}(Ek + 2J\sin(k))/\alpha\big]. \tag{3.10}$$

By using now the periodic boundary condition, we obtain the spectrum

$$E = E_s = \alpha s, \tag{3.11}$$

with $s \in \mathbb{Z}$. Therefore we have shown, by simple means, that the energy spectrum is given by the Wannier-Stark ladder, Eq. (3.11).

3.2.2. The discrete harmonic oscillator

We deal now with the potential

$$v(n) = \tilde{\Omega} n^2. \tag{3.12}$$

The Schrödinger equation in quasi-momentum space reads in this case

$$-\tilde{\Omega} \frac{\partial^2 \psi(k)}{\partial k^2} - 2J\cos(k)\psi(k) = E\psi(k), \tag{3.13}$$

subject to the boundary condition $\psi(k + 2\pi) = \psi(k)$, of course. The above equation is nothing but the Mathieu equation [AS64]. We transform Eq. (3.13) into its canonical form [AS64],

$$\frac{\partial^2 y(v)}{\partial v^2} + (a - 2s\cos(2v))y(v) = 0, \tag{3.14}$$

by identifying $v = (k + \pi)/2$, $\psi(k) = y(v)$, $a = 4E/\tilde{\Omega}$ and $s = 4J/\tilde{\Omega}$. Therefore the functions $y(v)$ we have introduced are π-periodic Mathieu functions ($\psi(k + 2\pi) = \psi(k) \Rightarrow y(v + \pi) = y(v)$). The properties of these functions are well-known [AS64], and we will derive some of them in the next section where they will be needed.

3.3. Dynamics of a single-particle in a combined lattice and parabolic potential

Many experiments concerning ultracold atoms in periodic potentials – optical lattices – aim at simulating fundamental models of condensed matter physics [BDZ08]. However,

a fundamental difference with respect to traditional solid state physics is the unavoidable presence of an external harmonic trap. One can expect that, if the trap is weak enough, the physics in the center of the trap will not differ much from that for the flat lattice situation; however, there are additional effects associated with the presence of the weak harmonic trap.

In this section we investigate the single-particle problem on a lattice with an additional superimposed weak parabolic potential. We present a detailed discussion of the author's results in [VP08a]. We give a comprehensive explanation of the single-particle energy spectrum based on which we study the coherent dynamics of wave packets. We find that using discretized Gaussian wave packets as initial states can lead to non-dispersive dynamics. Moreover, motivated by the recent interest in optical lattice-based quantum transport, we show how coherent transport of a carefully engineered localized initial wave packet can be achieved in the system under consideration.

3.3.1. The model

We consider in general many non-interacting particles moving on a one-dimensional tight-binding periodic and weak parabolic potentials. The Hamiltonian in second quantization has the form

$$H = \sum_n \left[\tilde{\Omega} n^2 \hat{N}_n - J(\hat{b}_n^\dagger \hat{b}_{n+1} + \hat{b}_{n+1}^\dagger \hat{b}_n) \right], \tag{3.15}$$

where $\hat{b}_n^\dagger$ $(\hat{b}_n)$ is the bosonic creation (annihilation) operator[1] at site $n \in \mathbb{Z}$, $\hat{N}_n = \hat{b}_n^\dagger \hat{b}_n$ is the number operator, $\tilde{\Omega}(>0)$ quantifies the strength of the external harmonic potential and $J(>0)$ is the tunnel coupling between adjacent sites n and $n \pm 1$. The basis we use for Hamiltonian (3.15) is the Fock basis $\{ |N_n\rangle \}$, whose elements are defined as

$$|N_n\rangle \equiv \frac{1}{\sqrt{N!}} (\hat{b}_n^\dagger)^N |0\rangle, \tag{3.16}$$

with $|0\rangle$ being the vacuum state corresponding to an empty lattice. We will refer to the Hamiltonian (3.15) as the trapped non-interacting Bose-Hubbard Hamiltonian.

3.3.2. Single particle stationary states and eigenenergies

We restrict now the domain of Hamiltonian (3.15) to a single particle, that is, we seek eigenstates $|\psi\rangle$ of (3.15) satisfying $\hat{N}_{\text{tot}} |\psi\rangle = 1 |\psi\rangle$, with $\hat{N}_{\text{tot}} = \sum_n \hat{N}_n$ the total number operator. The wave function has the form

$$|\psi\rangle = \sum_n \psi(n) |1_n\rangle, \tag{3.17}$$

with the normalization condition $\sum_n |\psi(n)|^2 < \infty$, that is, $|\psi\rangle$ is an $\ell^2(\mathbb{Z})$ function. Indeed, from second quantization, we identify $|1_n\rangle \equiv |n\rangle$; then, from the stationary

---

[1]It is here not relevant to make a distinction between CCR or CAR algebras for the creation and annihilation operators, since here we will restrict ourselves to the single-particle subspace.

Schrödinger equation $H \ket{\psi} = E \ket{\psi}$ we get the difference relation

$$[(\hat{T} + v)\psi](n) = E\psi(n), \tag{3.18}$$

where $\hat{T}$ is the discrete kinetic energy operator, Eq. (2.34), and $v(n) = \tilde{\Omega}n^2$ is the harmonic potential (3.12). The single particle problem is sketched in Fig. (3.1).
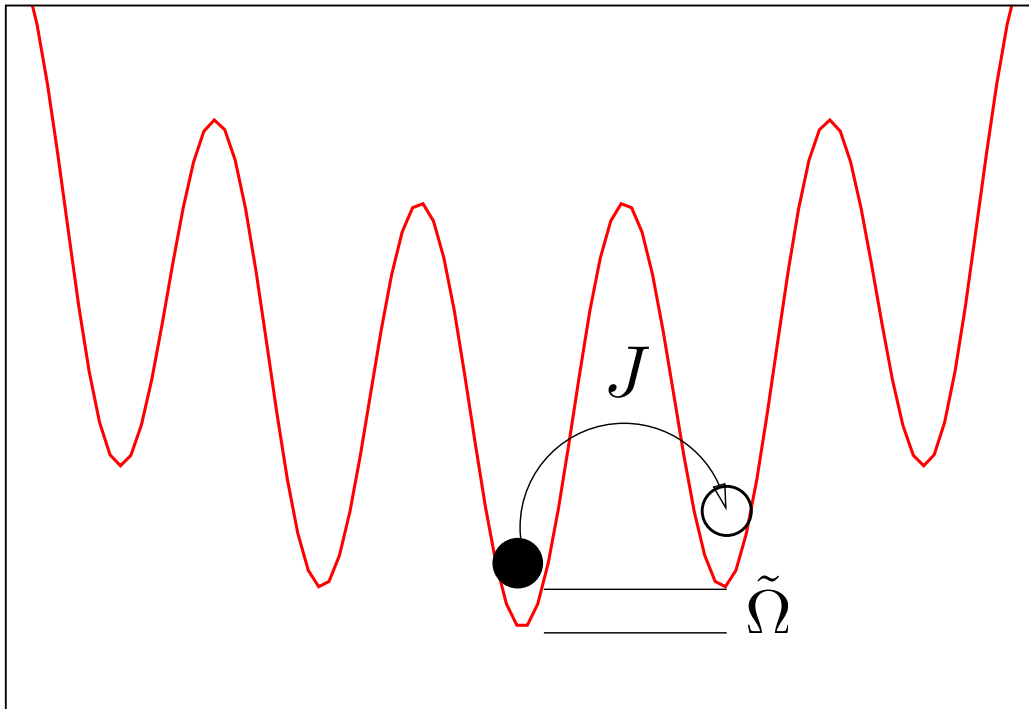
Figure 3.1.: Sketch of single particle tunneling and harmonic potential for Hamiltonian (3.15).

The difference equation (3.18) above is just the discrete harmonic oscillator studied in subsect. 3.2.2. Therefore its eigenstates, in quasi-momentum representation, are given by Mathieu functions, and its eigenenergies are characteristic values of the Mathieu equation. In Fig. 3.2 we plot the single-particle spectrum calculated via exact diagonalization in a (large enough) finite box for $J/\tilde{\Omega} = 140$. There we see that the spectrum is separated in three parts, namely (i) linear, (ii) Bloch-like and (iii) parabolic regions. We consider here the most relevant case of a weak parabolic potential, with $J/\tilde{\Omega} \gg 1$.

(i) The linear spectrum. If $J/\tilde{\Omega}$ is a large number, we can expect the lattice harmonic oscillator to have, to a good approximation, an evenly spaced low-energy spectrum. The reason is quite simple, and follows from re-incorporating the lattice spacing d into the problem. To this end, consider the finite-difference discretization of the harmonic oscillator in continuous space, by making use of the discrete Laplacian, Eq. (2.35), before taking the continuum limit, that is, before making the lattice spacing d go to
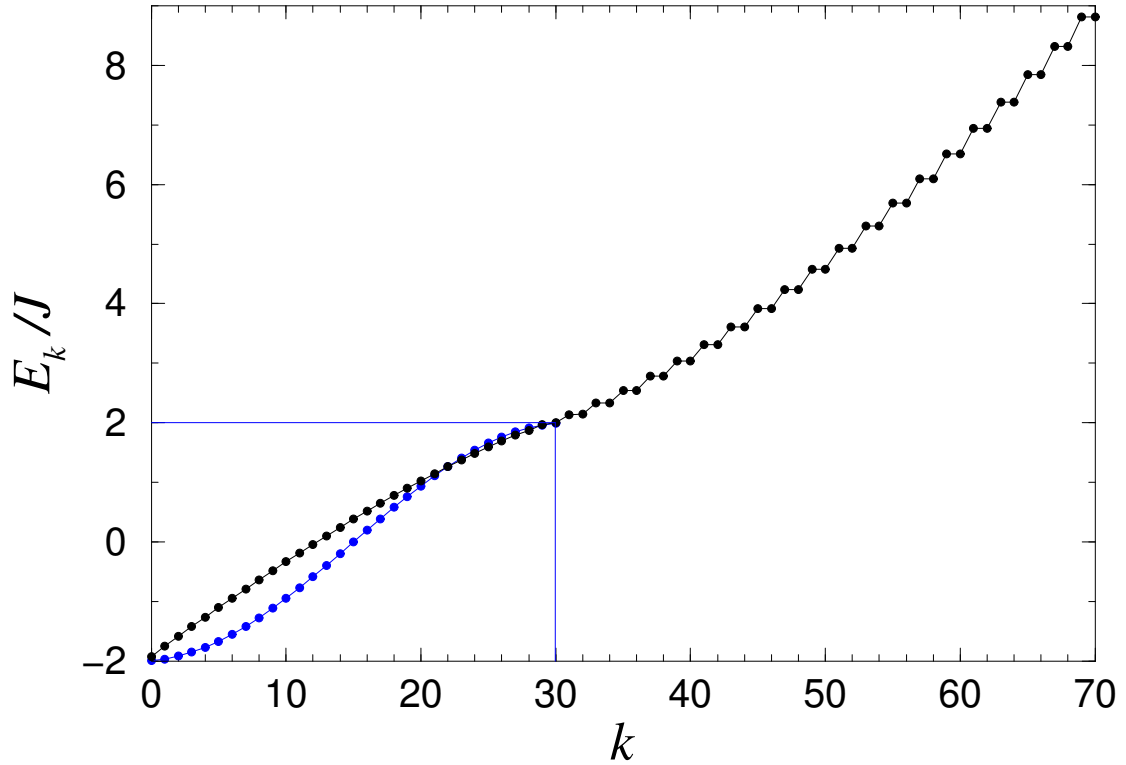
Figure 3.2.: Single-particle energy eigenvalues E_k in a combined periodic and parabolic potential obtained by numerical diagonalization of Hamiltonian (3.15) with $J/\tilde{\Omega} = 140$. For comparison, the eigenvalues $\bar{E}_k$ within the Bloch mini-band for a flat lattice ($\Omega = 0$) of length $L = 31$ with open boundary conditions are also plotted with dots (below E_k at $k = 0$).

zero. The continuum harmonic potential is then discretized as

$$\frac{1}{2}m\omega^2 x^2 \rightarrow \frac{1}{2}m\omega^2 d^2 n^2, \tag{3.19}$$

from which we identify $\tilde{\Omega} = m\omega^2 d^2/2$. The continuum limit is then properly taken as $d \rightarrow 0$,[2]

$$\lim_{d \rightarrow 0} J/\tilde{\Omega} = \lim_{d \rightarrow 0} \frac{\hbar^2}{m^2\omega^2}\frac{1}{d^4} = \infty, \tag{3.20}$$

which is equivalent to $J/\tilde{\Omega} \rightarrow \infty$. Therefore, for large $J/\tilde{\Omega}$, the low-energy excitation spectrum should be approximately linear.

We can now estimate the lowest energies and their respective eigenfunctions. Identi-

---

[2]Here, nd becomes the continuous variable x in the continuum limit.

fying

$$J \to \frac{\hbar^2}{2md^2}, \tag{3.21}$$

$$\tilde{\Omega} \to \frac{1}{2}m\omega^2 d^2, \tag{3.22}$$

the effective frequency describing the linear part of the spectrum is $\hbar\omega = 2\sqrt{J\tilde{\Omega}}$. Therefore for small k the energies E_k and associated eigenstates $|\chi_k\rangle$ of (3.15) are

$$E_k \approx -2J + 2\sqrt{J\tilde{\Omega}}(k+1/2), \tag{3.23}$$

$$|\chi_k\rangle \approx \mathcal{N}\sum_n (2^k k!)^{-1/2} e^{-\zeta_n^2/2} H_k(\zeta_n)|1_n\rangle, \tag{3.24}$$

where $\mathcal{N}$ is a normalization constant, $\zeta_n = n\sqrt[4]{\tilde{\Omega}/J}$ is the discretized coordinate, and $H_k(\zeta)$ is the k-th Hermite polynomial. In fact, these approximations for E_k and $|\chi_k\rangle$ are quantitatively correct, since they represent the lowest order approximation to the small-k solutions of the Mathieu equation [AS64].

(ii) The Bloch-like spectrum. The low-energy excitations studied in the previous paragraph can be described in such way because their corresponding states essentially occupy only the central region of the trap, and hence their approximate Gaussian tails prevent the largest portion of their density to be affected by the "hard wall" generated by the lattice harmonic potential.

We now explain this concept of hard wall: tunneling has to be dramatically suppressed once the potential energy due to the trap is of the order of, or larger than, the maximal kinetic energy on the lattice, that is, when $\tilde{\Omega}n^2 \geq 2J$. This means that the maximum number of non-localized states is approximately given by $N_{\max} = 2\lfloor n_{\max}\rfloor + 1$, with

$$n_{\max} \equiv \sqrt{\frac{2J}{\tilde{\Omega}}}, \tag{3.25}$$

where $\lfloor n_{\max}\rfloor$ is an estimate of the largest value of $|n|$ occupied by the non-localized states. This means that if some excited states have a non-negligible population close to $\pm n_{\max}$, they feel hard walls at $\pm n_{\max}$, since it is not possible to tunnel to $\pm(n_{\max}+1)$ or further. Therefore, the highest-energy excited states for which $E_k < 2J$ must have an energy spectrum similar to that corresponding to the spectrum of a particle on a finite lattice with open boundary conditions, Eq. (3.2). This fact is shown in Fig. 3.2, where the Bloch mini-band with $L = N_{\max}$ sites is compared to the actual spectrum of Hamiltonian (3.15).

(iii) The parabolic spectrum. After the discussions concerning the linear and Bloch-like spectra, it is now clear where the parabolic spectrum comes from. Evidently, when the state number k is larger than $N_{\max}$, there should be two quasi-degenerate states with energies $E_{2|n|+1} \approx E_{2|n|+2} \approx \tilde{\Omega}n^2$ and with associated eigenstates of the form $(|1_n\rangle \pm |1_{-n}\rangle)/\sqrt{2}$. The states of these kinds are therefore tightly localized and, once

the particle is initially high enough in the trap, $|n| > n_{\max}$, it will stay there forever.[3]

3.3.3. Coherent dynamics of a single-particle wave packet
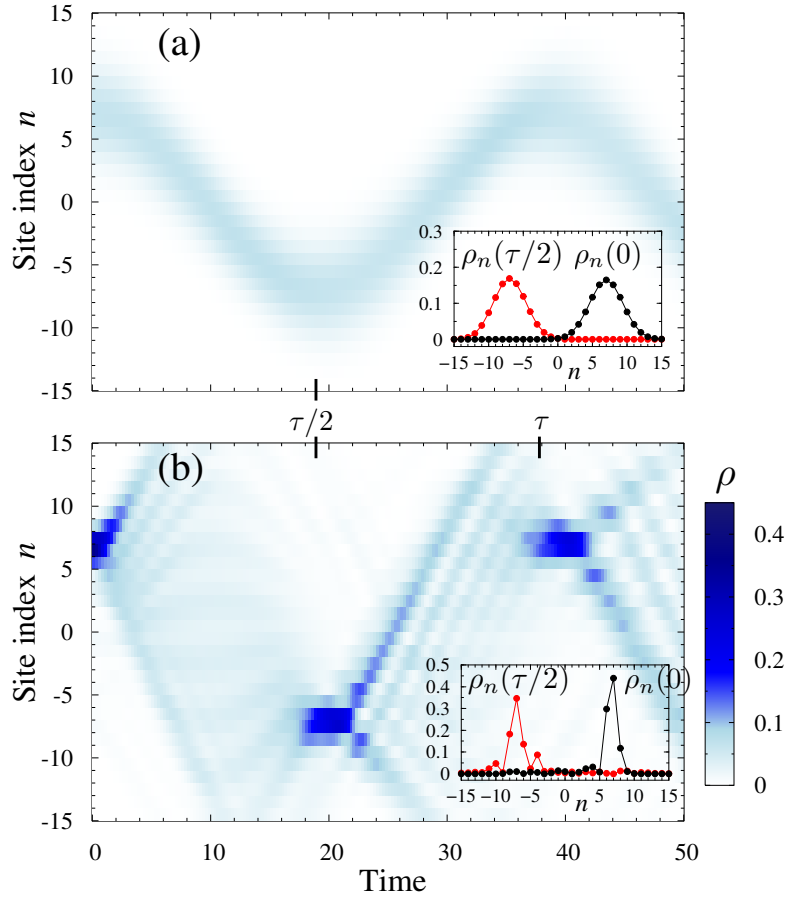
Figure 3.3.: Time evolution of density $\rho_n \equiv \langle \hat{N}_n \rangle$ for a single-particle wave packet $|\psi\rangle$ in a combined periodic and parabolic potential with $J/\tilde{\Omega} = 140$. (a) Initial state $|\psi(0)\rangle$ corresponds to the ground state $|\chi_0\rangle$ (discrete Gaussian) shifted by 7 sites from the trap center. (b) Initial state $|\psi^{(n')}(0)\rangle$ is a localized around $n' = 7$ wave packet constructed from the $k = 0, 1, \ldots 20$ eigenstates $|\chi_k\rangle$. Insets in (a) and (b) show the density distribution ρ_n at $t = 0$ and $t \simeq \tau/2$. Time is measured in units of $\hbar J^{-1}$.

From the previous analysis, it is clear that if we restrict ourselves to the harmonic oscillator–like states belonging to the lowest part of the energy spectrum, we can expect a quasi-periodic dynamics in the system. Non-dispersive transport of a single-particle wave packet from one side of the shallow parabolic potential to the other can then be achieved. In Fig. 3.3(a) we show the dynamics of a single particle wave packet $|\psi\rangle$, represented by the ground state of the system $|\chi_0\rangle$, Eq. (3.24), initially shifted by 7 sites

---

[3]Note that when there is more than one particle and these particles interact, this statement might no longer be true.

from the trap center. Numerical solution of the Schrödinger equation using Hamiltonian (3.15) reveals almost perfect periodic oscillations of the discrete Gaussian wave packet between the two sides of the parabolic potential with period $\tau \simeq 2\pi/\omega = (\pi\hbar/J)\sqrt{J/\tilde{\Omega}}$.

From the set of harmonic oscillator–like states $|\chi_k\rangle$ of Eq. (3.24), we can construct a well-localized wave packet $|\psi^{(n')}\rangle$ centered at a prescribed site n' ($|n'| < n_{\max}$). If we write the initial state as

$$|\psi(0)\rangle = \sum_k A_k |\chi_k\rangle,\qquad(3.26)$$

the probability amplitude a_n for a particle to be at site n is given by

$$a_n = \langle 1_n|\psi(0)\rangle \propto \sum_k A_k \left(2^k k!\right)^{-1/2} e^{-\zeta_n^2/2} H_k(\zeta_n).\qquad(3.27)$$

To obtain a localized around site n' state $|\psi^{(n')}\rangle$, we maximize $|a_{n'}|^2$, which determines the set of coefficients $\{A_k\}$ in Eq. (3.26). In Fig. 3.3(b) we show the time evolution of such a localized state, which exhibits periodic collapses and partial revivals at sites $-n'$ and n' with time steps $\tau/2$. The revivals are not complete since, as noticed above, the energy spectrum E_k for small k is only approximately linear in k. Nevertheless, our results suggest that coherent non-dispersive transport of carefully engineered atomic wave packets can be achieved in optical lattices in the presence of a shallow parabolic potential.

3.4. Conclusions

In this chapter we have considered some specific single-particle problems which can be solved exactly or, at least, recast in terms of known functions. We have then applied the theory outlined for stationary states to study coherent transport of a single-particle wave packet from one side to the opposite side of a trapped lattice. Our results may be relevant for physical implementation of optical lattice-based quantum transport and quantum information transfer.

On the purely theoretical side, we would like to remark that the model used for the lattice harmonic oscillator in this chapter is not unique, in the sense that it is not the only model on the lattice that tends, in the continuum limit, to the usual harmonic oscillator. In fact, we will see in chapter 7 that the model used here – which is the most common in the literature – is, by far, not the best discrete oscillator model one can build.

4. The two-body problem

In free space, with no external potentials, the collision and binding of two particles interacting via short range potentials is simple [Mes99, Joa75, Tay06]. The continuous spectrum of two-body collisions corresponds to the sum of the kinetic energies of the two unbound particles, and is therefore bound from below and unbound from above. On the other hand, the energy of a bound particle pair should lie below the scattering continuum. This is the reason why the particles in free space need to interact attractively,[1] at least in part, in order to be able to get bound. In one and two dimensions, any attractive potential, no matter how weak or strong, can bind two particles [Kla77, Sim76, LL58]. This is not the case in three dimensions, and the deepest bound state of a potential will be present only after the first zero-energy resonance [Cwi77, Lie76]. Aparently, this has major consequences in many-body problems, already showing up for three interacting bosons [Efi70, KMW+06, KFM+09, FKB+09, NFJG01]. An overview of the quantum mechanical three-body problem will be given in the beginning of chapter 5.

As we noted in chapter 2, discretized theories naturally arise as single band approximations to the physics of interacting particles in periodic potentials. These models are also used as a finite-difference discretization of underlying theories in continuous space [MM05]; a remarkable example is that of Lattice Gauge Theories [Rot05], where the finite-difference discretization appears to be the only way of obtaining non-perturbative results in Quantum Chromodynamics. Of course, discrete theories share certain common features with their continuous space counterparts, especially at low (quasi-) momenta, but there are also major differences. The fact that the continuous spectrum of a single lattice particle is not only bound from below, but also from above[2], is responsible for many (though not all) of the differences between the properties of interacting particles on and off the lattice. In a more realistic model – continuous space with a periodic potential – these effects are associated with the existence of band gaps.

One of the most celebrated predictions of the discretized tight-binding theory is the existence of two-body bound states due to purely repulsive interactions [WTL+06]. Since the continuous spectrum of the two-body problem has an upper bound, there can be stable states lying above the continuum; in reality, these states lie in a band gap [WO06]. Another consequence of the lattice discretization is the non-trivial dependence of the two-body wave functions on the center of mass quasi-momentum. Indeed, the original two-body problem before the tight-binding approximation is not separable, and this fact remains, though in a weaker sense, in the tight-binding theory. The resulting effect is that if the total quasi-momentum is close to the edge of the first Brillouin Zone, the bound states become totally co-localized [WTL+06] or, in more realistic energy bands, they become almost but not completely co-localized [PM07]. This is similar to the

---

[1]A short range attractive potential, in Quantum Mechanics, is defined as any negative potential, and repulsive any non-negative potential. In Classical Mechanics, a positive potential not monotonically decreasing is not called repulsive [LSSY05].

[2]In this case, we say that the Hamiltonian of the theory is a continuous or bound operator [Con94].

Mattis-Gallinar (MG) effect [MG84], which states that the effective mass of the exciton – a bound particle-hole pair – is appreciably larger than the sum of the two effective masses of its constituents, if the interactions are strong, and that it depends on the center of mass energy of the bound composite. In a tight-binding theory, the MG effect is a direct consequence of the non-Galilean nature of the lattice kinematics. The effect was observed in semiconductors by Cafolla and collaborators in [CST85]. When the total quasi-momentum approaches the edge of the Brillouin zone, the effective strength of the two-body interactions increases dramatically. This seemingly unimportant remark, at least for the case of a flat lattice and low temperatures, has however a major consequence in a harmonic trap, present in all experiments with ultracold atoms: the repulsively bound pairs are bound tighter than their attractive counterparts, as the author and his collaborator demonstrated in [VP08a]. Very recently, some qualitative features of photon-assisted tunneling in an optical lattice [SLS+08] were proven to be a consequence of the energy dispersion of a boson pair [WB09], which is yet another demonstration of the effects of the absence of Galilean invariance on the lattice.

In this chapter we focus on the two-body problem on a one dimensional lattice described by a discrete – tight-binding – Hamiltonian. We first discuss the simplest two-body problem, with zero range interaction on a flat lattice. A derivation of the two-particle states was given by the author and his collaborator in [VP08b], which accounts for a much simpler – even pedagogic – approach to the solution as compared to earlier treatments, and is the topic of sect. 4.1. A complicated derivation was given by Scott *et al.* in [SEG94], where the authors, on the way to the exact solution of the two-body problem, "separated" the coordinates in an inconvenient fashion, employing the matrix form of the eigenvalue problem. The two-body problem was solved in quasi-momentum space by Winkler *et al.* [WTL+06], though their conclusions about the three-dimensional case were innacurate;[3] later on Piil and Mølmer [PM07] solved the single band problem using more realistic energy dispersions. One of the conclusions is that for zero range interacting pairs there is no resonance in the system for any value of the total quasi-momentum. This is a consequence of the dimensionality: as in free space, there is always a bound state in one dimension [DHKS03]. Therefore, simulating resonant phenomena with such model is not possible and, moreover, it is the limiting case of a short range interaction.

The author gave an exact, analytic treatment of the problem with on-site as well as nearest-neighbor interactions in [VP09]; a more detailed solution and discussion of this problem is given in sect. 4.2. There we prove that two-body resonances can emerge in the presence of extended range interactions, and we study all the scattering and bound state properties of the system. We have to note that for the particular case of spin-polarized fermions (or hardcore bosons), the problem was already studied by Scott *et al.* in [SEG94], however with the cumbersome methods we have referred to above.

After the completion of [VP09], the author of this thesis derived, in a systematic way, the equations satisfied by the bound state solutions of the two-body problem with arbitrary finite range interactions. It was then proved by the author, mathematically, that the corresponding solutions are always described by roots of polynomials [Val10]. The bound states can then be simply calculated, toghether with the full spectrum and

---

[3]The authors gave a wrong estimation of the two-body resonance by a factor of around 16. The original, exact result was given more than 70 years ago by Watson [Wat39].

eigenstates of any two-body Hamiltonian on a homogeneous lattice in one dimension, provided the interactions have a finite range. A detailed discussion is presented in sect. 4.3.

In the last section of this chapter, based upon part of our results in [VP08a], we describe the dynamics of two bosons in a combined lattice and parabolic potential, which is relevant for physical implementation schemes of quantum information and quantum transport. It is the generalization of sect. 3.3 to two particle dynamics and transport of bound pairs. We show that, if the external trapping potential is weak, the bound "dimers" can exhibit coherent dynamics, behaving effectively as single particles. We also explain, with the help of the physics described throughout this chapter, why a repulsively bound pair in its ground state is tighter bound than its attractive counterpart, if the lattice is superimposed with a weak trap.

4.1. Two-particle states with on-site interaction

We begin by considering two identical bosons in a one dimensional lattice interacting via an attractive or a repulsive on-site interaction of strength U.[4] The problem is relevant to ultracold atoms in optical lattices, and most of the physics of the repulsively-bound atom pairs [WTL$^+$06] is captured by the model. Here we present a simple and exact analytical solution of the two-body problem in position (direct lattice) space, which is important for understanding most of the rest of this thesis.

Instead of using the method described in [VP08b] we will employ the exact lattice Green's functions (2.62) and (2.69). These LGFs were actually calculated by using a more general analog of the method in [VP08b] in subsects. 2.6.1 and 2.6.2. The LGFs, and correspondingly the solution to this problem, were also obtained by Piil and Mølmer in [PM07], in quasi-momentum space.

In second quantized form, the Hamiltonian of the problem is that of the Bose-Hubbard model

$$H = -J \sum_n (\hat{b}_n^\dagger \hat{b}_{n+1} + \hat{b}_{n+1}^\dagger \hat{b}_n) + \frac{U}{2} \sum_n \hat{N}_n(\hat{N}_n - 1). \tag{4.1}$$

We restrict ourselves here to the two particle sector, considering solutions $|\psi\rangle$ of the stationary Schrödinger equation which satisfy $\hat{N}_{\text{tot}} |\psi\rangle = 2 |\psi\rangle$, where $\hat{N}_{\text{tot}} \equiv \sum_n \hat{N}_n$ is the total number operator. A sketch of the tunneling and interaction processes is represented in Fig. 4.1.

We rewrite Hamiltonian (4.1) in first quantized form and consider its eigenstates which are symmetric under the exchange of the two particles (the polarized fermionic case is trivial, since the zero-range interaction has no effect). The correspondence between first and second quantized forms follows by the definitions $|2_n\rangle = |n, n\rangle$ and $|1_n, 1_m\rangle = \frac{1}{\sqrt{2}}(|n, m\rangle + |m, n\rangle)$ ($n < m$). The single-particle Hamiltonian for particle i is given by the usual tight-binding expression

$$H^{(i)} = -J \sum_{n_i} (|n_i\rangle\langle n_i + 1| + |n_i + 1\rangle\langle n_i|), \tag{4.2}$$

---

[4]As usual, $U > 0$ ($U < 0$) is said to be repulsive (attractive).
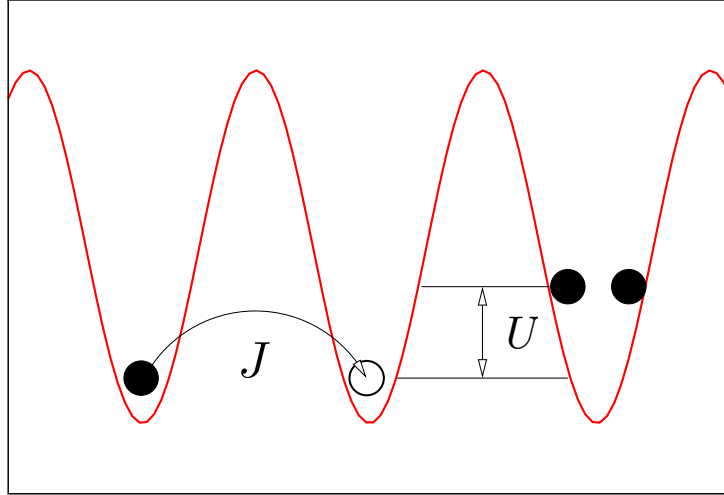
4. The two-body problem

Figure 4.1.: Sketch of single particle tunneling and two-body interaction for Hamiltonian (4.1).

and consequently the two-body Hamiltonian is

$$H = H^{(1)} \otimes I^{(2)} + I^{(1)} \otimes H^{(2)} + U \sum_{n_1} |n_1, n_1\rangle\langle n_1, n_1|, \tag{4.3}$$

where $I^{(i)} = \sum_{n_i} |n_i\rangle\langle n_i|$ is the identity operator acting on the degrees of freedom of particle i, and $|n_1, n_2\rangle \equiv |n_1\rangle \otimes |n_2\rangle$.

We solve the Schrödinger equation by first expanding the eigenstates as

$$|\psi\rangle = \sum_{n_1, n_2} \psi(n_1, n_2) |n_1, n_2\rangle, \tag{4.4}$$

so that the eigenvalue problem $H |\psi\rangle = E |\psi\rangle$ is equivalent to the following recurrence relation,

$$\begin{aligned} -J\big[\psi(n_1 + 1, n_2) + \psi(n_1 - 1, n_2) \\ + \psi(n_1, n_2 + 1) + \psi(n_1, n_2 - 1)\big] \\ + U\delta_{n_1,n_2}\psi(n_1, n_2) = E\,\psi(n_1, n_2). \end{aligned} \tag{4.5}$$

We separate the equation in center of mass ($R = (n_1 + n_2)/2$) and relative ($z = n_1 - n_2$) coordinates by using the ansatz

$$\psi(R, z) = e^{iKR}\phi_K(z), \tag{4.6}$$

where remarkably the relative wave function ϕ_K depends parametrically on the center of mass quasi-momentum $K \in (-\pi, \pi]$ since, after substituting Eq. (4.6) in Eq. (4.5), we see that ϕ_K satisfies

$$-J_K[\phi_K(z + 1) + \phi_K(z - 1)] + U\delta_{z,0}\phi_K(z) = E\phi_K(z), \tag{4.7}$$

where $J_K = 2J\cos(K/2)$. Note that the energy is not additive in the sense that it is not the sum of a center of mass and a relative energies, but depends on K as a parameter. This is a consequence of the breakdown of Galilean invariance on the lattice, since $\epsilon(k) \neq \hbar^2 k^2/2m$. In Mathematics, operators which, after conservation of total quasi-momentum, still depend non-trivially on K are called fiber operators.

4.1.1. Scattering states

We first seek the symmetric scattering states of Eq. (4.7). The resulting tight-binding Hamiltonian

$$H_K \equiv -J_K \sum_z (\,|z+1\rangle\langle z| \,+\, |z\rangle\langle z+1|\,) + U \sum_z \delta_{z,0}\,|z\rangle\langle z|\,, \tag{4.8}$$

is equivalent to the problem of a single particle with tunneling rate J_K scattering off one impurity located at the center of the lattice. Since the potential has short range, the eigenenergies of H_K in the continuum are given by

$$E \equiv E_{K,k} = -2J_K\cos(k) = -4J\cos(K/2)\cos(k). \tag{4.9}$$

We solve for the scattering states by making use of the lattice Green's function (LGF) formalism of chapter 2. Recall that the symmetric scattering states satisfy Eq. (2.52) which, in our specific problem, reads

$$\phi_{K,k}(z) = \cos(kz) - \sum_m G_k^{(0)}(z,m)U\delta_{m,0}\phi_{K,k}(m). \tag{4.10}$$

The symmetric non-interacting LGF has in this case the form (2.62)

$$G_k^{(0)}(z,m) = -\frac{\csc(k)}{2J_K}\sin(k|z-m|), \tag{4.11}$$

which, introduced in (4.10), yields the scattering wave functions

$$\phi_{K,k}(z) = \cos(kz) + \frac{U}{2J_K}\csc(k)\sin(k|z|). \tag{4.12}$$

Clearly, $\phi_{K,k}$ is a superposition of a free bosonic state and a fermionized state[5] [Gir60]. For weak interactions, $U \to 0$, $\phi_{K,k}$ reduces to the free bosonic solution while for very strong interactions, $U \to \infty$, it becomes fermionized, that is, the wave functions of scattering states are equal to the absolute value of the free fermionic wave function with the same relative quasi-momentum k.

The scattering states (4.12) are valid only for $\sin(k) \neq 0$. On the lattice, due to the symmetry of the continuous spectrum, i.e. $E_{K,k} = -E_{K,k\pm\pi}$, we have to generalize the limit of "low-energy" scattering. To understand this, note that the group velocity

$$\hbar v_g = \frac{\partial E_{K,k}}{\partial k} = 2J_K\sin(k), \tag{4.13}$$

---

[5]Note that these two states are not orthogonal in any sense.

vanishes in the limit of $k \to 0$ and $k \to \pi$. We can then define two different limits of "low-energy" scattering. As a consequence, there are two distinct scattering lengths of the system (see sect. 2.8). By taking the corresponding limits, we see that

$$\lim_{k \to 0} \phi_{K,k}(z) \propto |z| - \left(\frac{-2J_K}{U}\right), \tag{4.14}$$

and

$$\lim_{k \to \pi} \phi_{K,k}(z) \propto \left(|z| - \frac{2J_K}{U}\right)(-1)^z, \tag{4.15}$$

from which we deduce that the two scattering lengths are

$$a_K^\pm = \mp \frac{2J_K}{U}. \tag{4.16}$$

This result for the scattering length already gives us some important information: in this model there is only one bound state, since none of the scattering lengths has a pole for $U \neq 0$, that is, there is no "zero-energy" resonance. Another relevant quantity we can calculate is the phase shift $\delta_{K,k}$. We rewrite the wave function $\phi_{K,k}$ as

$$\phi_{K,k}(z) \propto \cos(k|z| + \delta_{K,k}), \tag{4.17}$$

where the phase shift is given by

$$\tan(\delta_{K,k}) = -\frac{U}{2J_K} \csc(k), \tag{4.18}$$

which, in the limit of non-interacting particles reduces to $\delta_{K,k} = 0$, while for infinitely strong interactions it becomes $\delta_{K,k} = -\mathrm{sgn}(U)\pi/2$. The scattering length can also be calculated in the standard way using the phase shift as

$$a_K^\pm = -\lim_{k \to 0,\pi} \frac{\partial \delta_{K,k}}{\partial k} = \mp \frac{2J_K}{U}. \tag{4.19}$$

In Fig. 4.2 we plot the continuous spectrum $E_{K,k}$ of H as a function of the total quasi-momentum K, with a shading proportional to the density of states (DOS)

$$\rho(E,K) \propto \left(\frac{\partial E}{\partial k}\right)^{-1} = \frac{1}{\sqrt{(2J_K)^2 - E^2}}, \tag{4.20}$$

which is divergent when the energy approaches the top ($E = 2J_K$) or bottom ($E = -2J_K$) of the scattering continuum.

4.1.2. Bound states

The on-site interaction $U \neq 0$ can bind the two bosons together into a close dimer [WTL$^+$06, VP08b, PM07, PSAF07] whose energy is above ($U > 0$) or below ($U < 0$) the continuum (4.9) of scattering states. We now derive simple analytic solutions for the bound dimer states. For $|K| = \pi$ ($J_K = 0$), Eq. (4.7) immediately yields $E_{K=\pi} \equiv E_\pi = U$ and

$$\phi_\pi(0) = 1, \qquad \phi_\pi(z \neq 0) = 0. \tag{4.21}$$
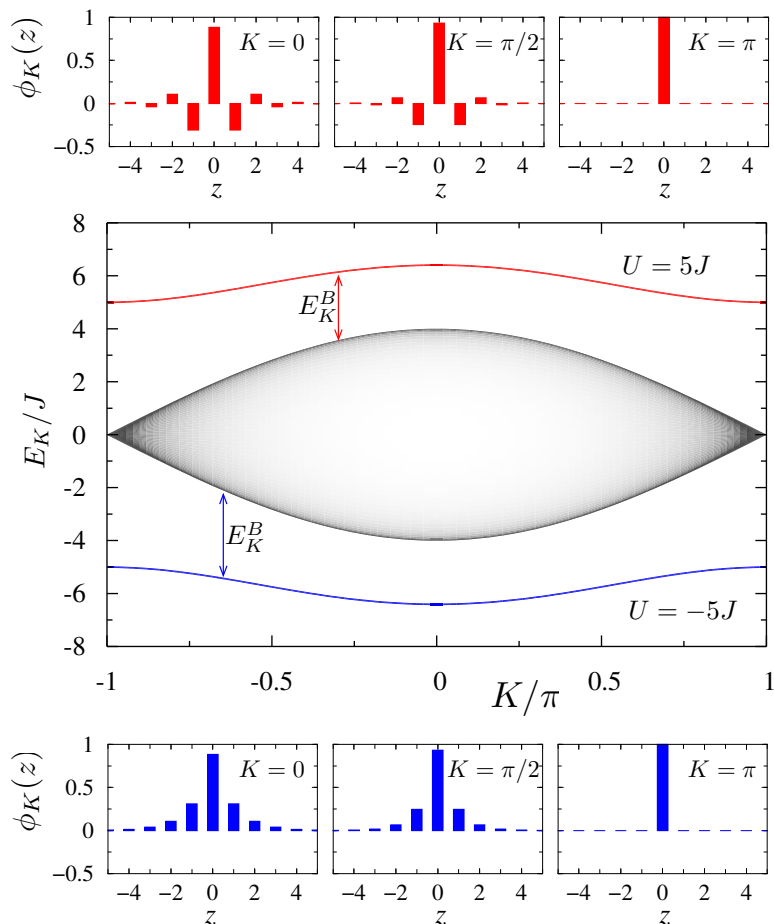
Figure 4.2.: Energies E_K versus the center-of-mass momentum K for a pair of bosons in a 1D lattice described by the Hubbard model. The continuum spectrum corresponds to energies (4.9) of the scattering states, with the shading proportional to the density of states (4.20). The line below and the line above the scattering band are, respectively, the energies of the attractively-bound dimer with $U = -5J$ and the repulsively-bound dimer with $U = 5J$. Their relative coordinate wave functions (4.28) at $|K| = 0, \pi/2, \pi$ are shown on the bottom and the top panels.

For energies outside the continuum $|E_K| > 2J_K$ and $|K| \neq \pi$, we use the LGF from Eq. (2.69)

$$G_E^{(0)}(n, m) = \frac{\text{sgn}(E_K)}{\sqrt{E_K^2 - (2J_K)^2}} \left[\frac{-E_K - \text{sgn}(E_K)\sqrt{E_K^2 - (2J_K)^2}}{2J_K} \right]^{|n-m|}. \qquad (4.22)$$

We perform the conformal mapping (2.64), so that the energy is written as $E_K = -J_K(\alpha_K + 1/\alpha_K)$, where α_K is real with $|\alpha_K| < 1$, and the LGF is recast as

$$G_\alpha^{(0)}(n, m) = \frac{\alpha_K}{J_K(1 - \alpha_K^2)} (\alpha_K)^{|n-m|}. \qquad (4.23)$$

4. The two-body problem

We can now calculate the bound state wave functions with the help of equation (2.56), which becomes

$$\phi_K(z) = -G_\alpha^{(0)}(z, 0) U \phi_K(0).$$ (4.24)

The equation for the energies of the bound states is obtained by setting $z = 0$ in the above equation, leading to

$$G_\alpha^{(0)}(0, 0) = -\frac{1}{U},$$ (4.25)

which is equivalent to a polynomial equation in α_K with the solution

$$\alpha_K = \frac{U \pm \sqrt{U^2 + (2J_K)^2}}{2J_K}.$$ (4.26)

Using Eq. (4.24) for $z \neq 0$, we see that the eigenenergies and the (normalized) eigenstates have the form

$$E_K = \text{sgn}(U)\sqrt{U^2 + 4J_K^2},$$ (4.27)

$$\phi_K(z) = \frac{\sqrt{\text{sgn}(U)\mathcal{U}_K}}{\sqrt[4]{\mathcal{U}_K^2 + 1}} \left(\mathcal{U}_K - \text{sgn}(U)\sqrt{\mathcal{U}_K^2 + 1}\right)^{|z|},$$ (4.28)

with $\mathcal{U}_K \equiv \frac{U}{2J_K}$. In Fig. 4.2 we plot the bound state energy band (4.27) and the associated eigenfunctions (4.28) at different quasi-momenta for repulsive ($U/J = 5$) and attractive ($U/J = -5$) interactions. Increasing the total quasi-momentum leads to tighter localization of the relative coordinate wave function at $z = 0$, which in the limit of $|K| \to \pi$, becomes completely localized, as we have seen from Eq. (4.21).

Note that, in this model, a bound state exists for any non-zero value of the on-site interaction U, independently of its sign. If $U > 0$, then the relative wave function changes sign from one site to the next, which is a signature of repulsive binding (the bound state has an energy above and not below the continuum). The bound pair has an effective mass

$$M^* = \hbar^2 \left[\frac{\partial^2 E_K}{\partial K^2}\right]_{K=0}^{-1} = \text{sgn}(U)\frac{\hbar^2\sqrt{U^2 + (4J)^2}}{4J^2}.$$ (4.29)

The effective mass is positive for an attractively bound pair, and is negative if the pair is repulsively bound. For weak interaction $|U| \ll J$, we have $M^* \simeq \pm\hbar^2/J = \pm 2m$, i.e., twice the single particle effective mass $m = \hbar^2/(2J)$ of Eq. (3.21). On the other hand, for strong interaction $|U| \gg J$, we obtain $M^* \simeq \hbar^2/(2J^{(2)})$, where $J^{(2)} \equiv -2J^2/U$ is the effective tunneling rate of the dimer between the neighboring lattice sites [WTL+06, PM07, PSAF07, VP08b, VP09]. Now the dimer effective mass is large due to its slow tunneling $|J^{(2)}| \ll J$, with the sign of $J^{(2)}$ determining the sign of M^*. In this limit the bound state energy can be approximated as

$$E_K \simeq (U - 2J^{(2)}) - 2J^{(2)}\cos(K),$$ (4.30)

where the first term on the right-hand side represents the dimer "internal energy", while the second term is the kinetic energy of a dimer with quasi-momentum K. Equation (4.30) can be used to derive a single-dimer effective Hamiltonian. After Peierls' substi-

tution, the Hamiltonian for a dimer under an external potential v has the form

$$H = -J^{(2)} \sum_n \left(|n+1\rangle\langle n| + |n\rangle\langle n+1| \right) + \sum_n v(n)\, |n\rangle\langle n| + (U - 2J^{(2)})I, \qquad (4.31)$$

where $|n\rangle$ represents the effective dimer at site n of the lattice and $I = \sum_n |n\rangle\langle n|$ is the identity operator. The Hamiltonian (4.31) is valid provided (i) $|U|/J \gg 1$ and (ii) the potential does not satisfy $v(n \pm 1) - v(n) \approx U$ for any n, since otherwise the dissociation (or a superposition of dimer-monomer states) would be a resonant process; this issue will become clearer when studying the dynamics of two particles with an external parabolic trap, which is the topic of sect. 4.4.

4.2. Two-particle states in the extended Hubbard model

The first, non-trivial generalization of the two-body problem on the lattice corresponds to the so-called extended Hubbard model [MRR90], which includes on-site interactions as well as nearest-neighbor interactions between particles (bosons or spin up-spin down fermions). Clearly, with spin-polarized fermions the inclusion of interactions has to start at a nearest-neighbor level, since the on-site potential does not affect them due to the Pauli principle. Moreover, the recent quest for the physics of dipolar atoms [GWH+05] and molecules [NOdM+08, OOH+06] in an optical lattice needs of course the inclusion of, to lowest order, nearest-neighbor interactions to take into account the effects of the long range potentials.

In this section we consider the physics of two particles in the extended Hubbard model. Instead of dealing with its original, fermionic version, we study the model for bosons, without loss of generality. Indeed, the two boson case is identical to one spin-up and one spin-down fermions, while the case of two spin-polarized fermions corresponds to the limit of infinitely strong on-site interaction of the bosonic case in one dimension [Gir60].

The Hamiltonian of the extended Hubbard model in a homogeneous lattice reads

$$H = \sum_n -J \sum_n (b_n^\dagger b_{n+1} + b_{n+1}^\dagger b_n)$$
$$+ \frac{U}{2} \sum_n \hat{N}_n(\hat{N}_n - 1) + V \sum_n \hat{N}_n \hat{N}_{n+1}, \qquad (4.32)$$

where V is the nearest-neighbor interaction, and both U and V can be attractive or repulsive.

After separation of center of mass and relative coordinates as $\psi(n_1, n_2) = e^{iKR}\phi_K(z)$ with $R = (n_1 + n_2)/2$ and $z = n_1 - n_2$, the eigenvalue problem $H|\psi\rangle = E|\psi\rangle$ reduces to the three-term difference equation

$$-J_K \left[\phi_K(z+1) + \phi_K(z-1) \right] + \left[U\delta_{z,0} + V(\delta_{z,1} + \delta_{z,-1}) - E_K \right]\phi_K(z) = 0. \qquad (4.33)$$

We show in this section that the solutions to the above equation can have resonances, in contrast to the problem of on-site interaction only. The existence of a resonance has two implications: first, the resonant eigenstate is asymptotically the non-interacting solution, which means that, for indistinguishable particles, there is a full transmission

after the collision; second, the "zero-energy" resonances mark the entry or exit of a bound state into or out of the continuum. Below we give a rigorous meaning to the term "zero-energy" resonance for particles on the lattice, which is qualitatively different from the properly called zero-energy resonances in continuous space. We characterize all the scattering properties of the system in detail, starting from the exact collisional states, and obtaining the scattering lengths (corresponding to top/bottom of the continuum) which describe the "low-energy" properties. As we have already noted, we will assume from now on that we deal with a pair of bosons (symmetric eigenstates of Eq. (4.33)), and we will obtain the corresponding fermionic states by applying the standard Bose-Fermi mapping theorem [Gir60].
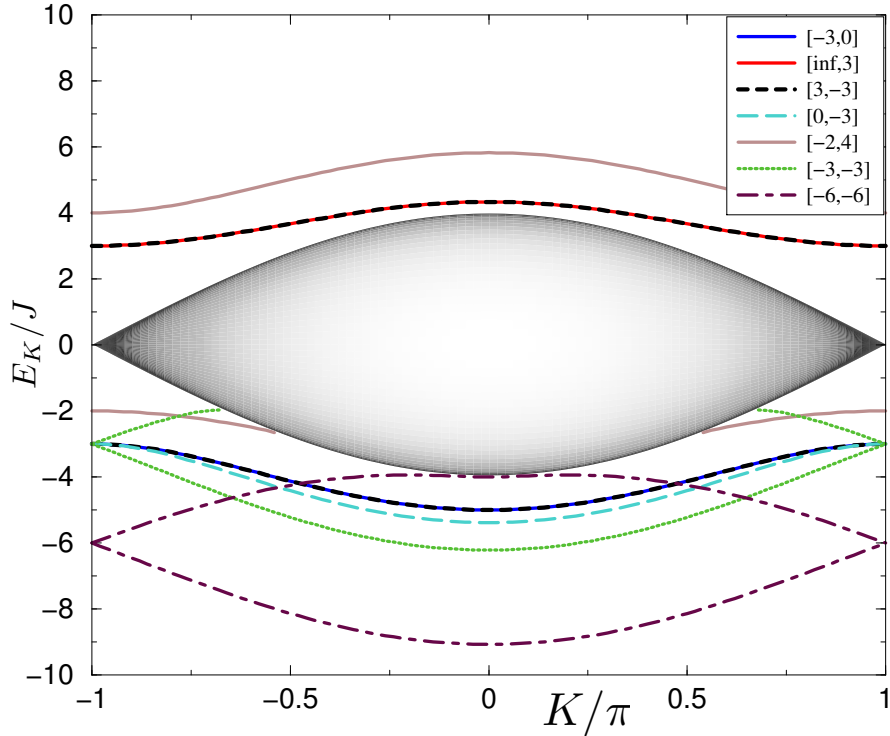
Figure 4.3.: Energies versus the center-of-mass momentum K for a pair of bosons in a 1D lattice described by the extended Hubbard model. The continuum spectrum corresponds to energies $E_{K,k}$ of the scattering states, with the shading proportional to the density of states $\rho(E, K)$. The lines correspond to energies E_K of the two particle bound states for various values of interaction strengths $[U/J, V/J]$.

4.2.1. Scattering states and resonances

The scattering solutions $|\phi\rangle$ of the Schrödinger equation (4.33) have the asymptotic form ($|z| \geq 1$)

$$\phi_{K,k}(z \neq 0) = e^{-\mathrm{i}k|z|} + e^{2\mathrm{i}\delta_{K,k}}e^{\mathrm{i}k|z|}, \tag{4.34}$$

where the effects of the collision are accounted for by the phase shift $\delta_{K,k}$. As for any finite range potential, the energies are given by the sum of two free-particle Bloch bands

$$E_{K,k} = -2J_K \cos(k).$$ (4.35)

The continuum of energies $E_{K,k}$ and the corresponding density of states $\rho(E, K) \propto \partial k/\partial E = [(2J_K)^2 - E^2]^{-1/2}$ are shown in Fig. 4.3. The wave functions of the scattering states for $\sin(k) \neq 0$ are given by

$$\phi_{K,k}(0) = \cos(\delta_{K,k}^{(0)}) \frac{\cos(k + \delta_{K,k})}{\cos(k + \delta_{K,k}^{(0)})},$$ (4.36)

$$\phi_{K,k}(z \neq 0) = \cos(kz + \delta_{K,k}),$$ (4.37)

where the phase shifts $\delta_{K,k}^{(0)}$ and $\delta_{K,k}$ are defined through

$$\tan(\delta_{K,k}^{(0)}) = -\frac{U}{2J_K \sin(k)},$$ (4.38)

$$\tan(\delta_{K,k}) = \frac{J_K U + [2J_K \cos(k) + U] V \cos(k)}{\{UV - 2J_K[J_K - V \cos(k)]\} \sin(k)}.$$ (4.39)
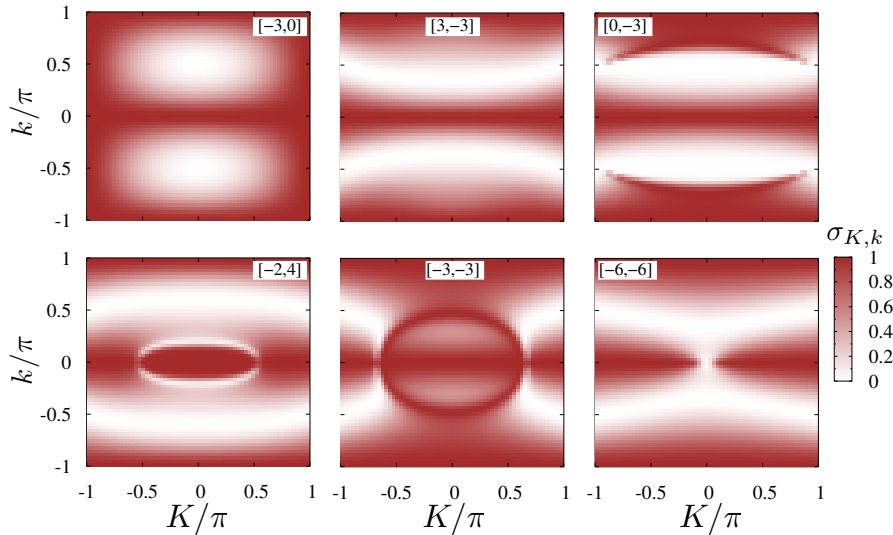
Figure 4.4.: Two-particle scattering cross-section $\sigma_{K,k}$ versus the center-of-mass K and relative k quasi-momenta for several values of interaction strengths $[U/J, V/J]$. Flipping simultaneously the sign of both U and V is equivalent to shifting $k \to k + \pi$.

Clearly, when the nearest-neighbor interaction vanishes, $V = 0$, the scattering states reduce to those studied in the previous section. We concentrate here on the role of non-vanishing nearest-neighbor interaction $V \neq 0$ in the two-body collisions. To this end, we define the scattering amplitude [Joa75] f as

$$f(\delta_{K,k}) = \frac{1}{2}(e^{2i\delta_{K,k}} - 1),$$ (4.40)

4. The two-body problem

so that the cross section $\sigma_{K,k}$ takes the form

$$\sigma_{K,k} = |f(\delta_{K,k})|^2 = \sin^2(\delta_{K,k}). \tag{4.41}$$

The cross sections for several values of U and V are plotted in Fig. 4.4. The cross section vanishes when the phase shift is zero, denoting therefore a resonance at energy $E_{K,k} = -2J_K \cos(k)$. By making use of Eq. (4.39), we see that, with the condition $8J_K^2/(UV) \leq 1$, there is a resonance at $E_{K,k}$ if

$$E_{K,k} = \frac{1}{2}U \left[1 \pm \sqrt{1 - 8\frac{J_K^2}{UV}} \right], \tag{4.42}$$

or, written more explicitly, if

$$\cos(k) = -\frac{U}{4J_K} \left[1 \pm \sqrt{1 - 8\frac{J_K^2}{UV}} \right]. \tag{4.43}$$

The other interesting limit to consider is that of the maximal cross section, i.e. $\sigma_{K,k} = 1$. This happens whenever $\delta_{K,k} = \pi/2$, and the asymptotic wave function corresponds to the state of two hard-core bosons ($U \to \infty$). Since we are considering here the case of $\sin(k) \neq 0$, there is a resonance whenever the denominator $[UV - 2J_K(J_K - V\cos(k))]\sin(k)$ in the expression (4.39) vanishes for $k \neq 0, \pm\pi$, that is, at energies

$$E_{K,k} = U - 2\frac{J_K^2}{V}, \tag{4.44}$$

or, more explicitly, whenever

$$\cos(k) = \frac{J_K}{V} - \frac{U}{2J_K}. \tag{4.45}$$

We now consider the "low-energy" behavior of the system, at $\sin(k) \to 0$. As in Eq. (4.19), we define two scattering lengths, given by

$$a_K^{\pm} = -\lim_{k \to 0, \pi} \frac{\partial \delta_{K,k}}{\partial k} = \frac{UV - 2J_K(J_K \mp V)}{UV \pm J_K(U + 2V)}. \tag{4.46}$$

"Zero-energy" resonances will be present for some value of the center of mass quasi-momentum K if any of the two scattering lengths $a_K^{\pm}$ diverges. The scattering lengths have a pole when

$$UV \pm J_K(U + 2V) = 0. \tag{4.47}$$

Defining

$$W = \frac{UV}{U + 2V}, \tag{4.48}$$

the scattering length diverges for

$$J_K = \lim_{k \to 0, \pi} \text{sgn}(\cos(k))W = \mp W. \tag{4.49}$$

In other words, the divergence of $a_K^\pm$ occurs when the absolute value of the center of mass quasi-momentum $|K|$ is equal to the critical value

$$K_R = 2\arccos\left(\mp\frac{W}{2J}\right), \tag{4.50}$$

under the condition $0 \le \mp W/2J \le 1$ for $k \to 0, \pi$, respectively. As will become apparent from the subsequent discussion, K_R indicates the emergence of scattering resonances associated with the bound states (see Fig. 4.5).

4.2.2. Bound states

We now consider the two-particle bound states. For bosons, using in Eq. (4.33) the exponential ansatz

$$\phi_K(z \ne 0) \propto \alpha_K^{|z|-1}, \tag{4.51}$$

we immediately see that the eigenenergies of the bound states have the already discussed form

$$E_K = -J_K \frac{1 + \alpha_K^2}{\alpha_K}. \tag{4.52}$$

From the Schrödinger equation for the wave function at $z = 0$,

$$\phi_K(0) = -\alpha_K + \frac{V}{J_K} + \frac{1 + \alpha_K^2}{\alpha_K}, \tag{4.53}$$

which, upon substitution back into the Schrödinger equation for $z = 0$, and applying the symmetry requirement $\phi_K(1) = \phi_K(-1)$, yields the cubic polynomial equation

$$J_K V \alpha_K^3 + (VU - J_K^2)\alpha_K^2 + J_K(V + U)\alpha_K + J_K^2 = 0. \tag{4.54}$$

The solutions $\alpha_K^{(i)}$ of Eq. (4.54) with $i \in \{1, 2, 3\}$ are physically acceptable if they imply normalizable eigenfunctions, $|\alpha_K^{(i)}| < 1$. In fact, if Eq. (4.54) admits a solution with $\alpha_K^{(i)} = \pm 1$, this solution corresponds to a "zero-energy" resonance. Indeed, setting $\alpha_K = \pm 1$ in Eq. (4.54), we find the relation between U, V and J_K to be

$$UV \pm J_K(U + 2V) = 0, \tag{4.55}$$

which is exactly the same relation derived from the requirement that the scattering length, Eq. (4.46), has a pole (cf. Eq. (4.47)).

Existence of at least one and at most two bound states. In the case where only the on-site interaction was present we showed, by explicitly calculating the wave functions and eigenenergies, that there is always one bound state, independently of the value of interaction $U \ne 0$. We now proceed to show that when the nearest-neighbor interaction is added, there is at least one and at most two symmetric bound states. Mathematically, we shall prove that Eq. (4.54) admits always at least one real solution whose absolute value is smaller than one, and that it has at most two such solutions.

- *Existence of at least one bound state.* Let us first fix V, and let it be positive (if

4. The two-body problem

$V < 0$ the result evidently holds, too). Consider the function

$$\mathcal{U}(\alpha_K) = \frac{-J_K V \alpha_K^3 + J_K^2 \alpha_K^2 - J_K V \alpha_K - J_K^2}{V \alpha_K^2 + J_K \alpha_K}, \qquad (4.56)$$

obtained by rearranging Eq. (4.54). We prove that for $K = 0$, $\mathcal{U}$ is a surjective function of $\alpha_{K=0} = \alpha_0$ in its domain $D(\mathcal{U}) \subset (-1, 1)$; we denote $R(\mathcal{U})$ as the range (or image) of $\mathcal{U}$. The function $\mathcal{U}$ has a singularity at $\alpha_0 = -2J/V$ whenever $V \geq 2J$, and a singularity at $\alpha_0 = 0$ for any value of V. $\mathcal{U}$ is a continuous function of α_0 with no singularities if $\alpha_0 > 0$. Thus, we have to consider the limits of $\mathcal{U}$ when $\alpha \to 0^+$ and $\alpha \to +1$,

$$\lim_{\alpha_0 \to 0^+} \mathcal{U}(\alpha_0) = -\infty \qquad (4.57)$$

$$\lim_{\alpha_0 \to +1} \mathcal{U}(\alpha_0) = -\frac{4JV}{V + 2J}, \qquad (4.58)$$

which proves that $(-\infty, -4JV/(V + 2J)) \subset R(\mathcal{U})$.

We consider first the case $V < 2J$. In this situation the two relevant limits are

$$\lim_{\alpha_0 \to 0^-} \mathcal{U}(\alpha_0) = +\infty \qquad (4.59)$$

$$\lim_{\alpha_0 \to -1} \mathcal{U}(\alpha_0) = -\frac{4JV}{2J - V}. \qquad (4.60)$$

Since the inequality

$$-\frac{4JV}{2J - V} < -\frac{4JV}{2J + V} \qquad (4.61)$$

holds, the range of $\mathcal{U}$ for $U < 2J$ is the real line, that is, $R(\mathcal{U}) = \mathbb{R}$. If, on the other hand, $V \geq 2J$, the relevant limit to take is

$$\lim_{\alpha_0 \to \left(-\frac{2J}{V}\right)^+} \mathcal{U}(\alpha_0) = -\infty, \qquad (4.62)$$

which proves that for any values of U and V there is at least one bound state at $K = 0$. Therefore, there is always at least one bound state for any value of K.

- *Existence of at most two bound states.* Since we have already proved that there is at least one bound state, we may use this result in the subsequent discussions. Define the polynomial

$$P(\alpha) = J_K V \alpha_K^3 + (VU - J_K^2)\alpha_K^2 + J_K(U + V)\alpha_K + J_K^2, \qquad (4.63)$$

whose roots are the bound state solutions for α_K. There are four different cases.

(a) $U, V < 0$ with $UV > -J_K(U + 2V)$. The polynomial at the positive edge of $[-1, 1]$ satisfies $P(1) > 0$. We also have $\lim_{\alpha_K \to +\infty} P(\alpha_K) = -\infty$. Therefore $P(\alpha_K)$ has a zero in $(1, +\infty)$. Since P is a cubic polynomial, it has three roots; hence there are at most two bound states.

(b) $U, V < 0$ with $UV < -J_K(U + 2V)$. In this case we have $P(-1) < 0$ and

$\lim_{\alpha_K \to -\infty} P(\alpha_K) = +\infty$. Thus, there are at most two bound states in this case.

(c) $U < 0, V > 0$ with $UV > -J_K(U+2V)$. We have $P(1) > 0$. If $U+2V > 0$ then $P(-1) < 0$ which, combined with $\lim_{\alpha_K \to -\infty} P(\alpha_K) = +\infty$ proves that there are at most two bound states. If $U + 2V < 0$, then $P(-1) > 0$, and so $P(-1)P(1) > 0$; since there is at least one and at most three roots in the interval $(-1, 1)$, then there are exactly two bound states in this case.

(d) $U < 0, V > 0$ with $UV < -J_K(U + 2V)$. We have that $P(1) < 0$ and $\lim_{\alpha_K \to +\infty} P(\alpha_K) = +\infty$, which completes the proof.
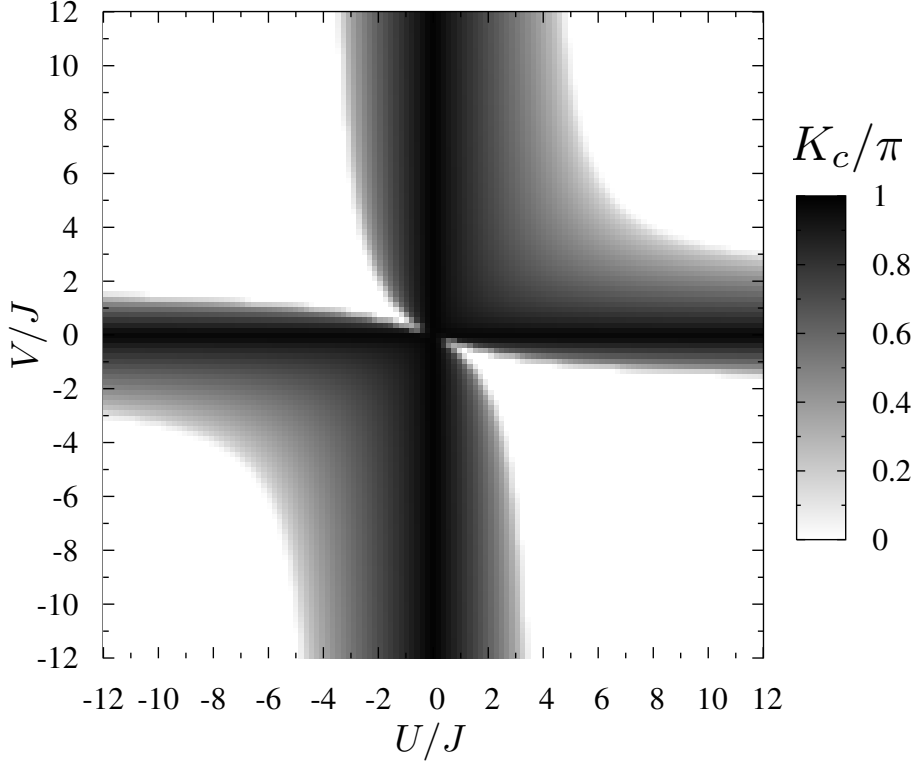
Figure 4.5.: The U, V diagram for the existence of the second bound solution $|\alpha_K^{(2)}| < 1$ of Eq. (4.54) with $K_c < |K| \leq \pi$, with shading proportional to $K_c \in [0, \pi]$.

As we have shown, Eq. (4.54) admits at most two solutions corresponding to bound states. Obviously, for non-interacting particles $U = V = 0$, there can be no bound state. For $U \neq 0$ and $V = 0$[6] [VP08b] as well as for $U = 0$ and $V \neq 0$, there is only one bound solution $\alpha_K^{(1)}$ at any K. For any other values of $U, V \neq 0$, the first bound solution $\alpha_K^{(1)}$ exists at any K, and the second bound solution $\alpha_K^{(2)}$ exists at $|K| > K_c$, where the critical K_c is shown in Fig. 4.5 and is defined as

$$K_c = \begin{cases} K_R & \text{if } |W/2J| \leq 1 \\ 0^- & \text{otherwise} \end{cases}. \tag{4.64}$$

---

[6]See sect. 4.1.

We thus see that the scattering length diverges when the second bound state approaches the edge of the scattering continuum. This signifies the appearance of the scattering resonance at $|K| = K_R$ which is determined by Eq. (4.50) under the condition $|W/2J| \leq 1$. If, however, this condition is not satisfied, no scattering resonance is present, and the second bound state exists for all $K \in (-\pi, \pi]$ with the energy below or above the scattering continuum depending on whether $W \equiv UV/(U + 2V)$ is negative or positive, respectively (see Fig. 4.3).

Some solutions for the bound states. In general, analytic expressions for the bound solutions of Eq. (4.54) are too cumbersome for detailed inspection, but several special cases yield simple instructive results. (i) With only the on-site interaction $U \neq 0$ and $V = 0$, there is one bound solution $\alpha_K^{(1)} = (U - E_K)/(2J_K)$ with the corresponding energy $E_K = \text{sgn}(U)\sqrt{U^2 + 4J_K^2}$, as was discussed in the previous section. (ii) With very strong on-site interaction $|U| \to \infty$ and $V \neq 0$, the first bound solution is trivial, $\alpha_K^{(1)} = 0$ and $E_K = U$. It represents an infinitely bound pair. The second, more relevant (non-trivial) solution $\alpha_K^{(2)} = -J_K/V$ and $E_K = V + J_K^2/V$ describes a pair of hard-core bosons, $\phi_K(0) = 0$, that are bound by the nearest-neighbour interaction V provided $|J_K/V| < 1$ [SEG94]. Note that in this limit we have $W = V$, and the last condition for the existence of the second bound state again reduces to $|K| > K_c$. This solution is relevant to spin-polarized fermions as well. According to the Bose-Fermi mapping theorem [Gir60], the eigenenergies and eigenfunctions for fermions are those corresponding to bosons, except for the symmetry of the wave functions: call $\phi_B(z)$ the relative hard-core bosonic eigenfunction; then the fermionic eigenfunction $\phi_F(z)$ has the form

$$\phi_F(z) = \text{sgn}(z)\phi_B(z). \tag{4.65}$$

Note that the above equation also applies to the stationary scattering states. (iii) Finally, a rather curious and simple case is realized with $U = -V$. The first bound solution is similar to that in (i), but with U replaced by V, $\alpha_K^{(1)} = (V - E_K)/(2J_K)$ and the energy $E_K = \text{sgn}(V)\sqrt{V^2 + 4J_K^2}$, which corresponds to binding mainly by the off-site interaction. The second bound solution is similar to that in (ii), but now with V replaced by U, $\alpha_K^{(2)} = -J_K/U$ and $E_K = U + J_K^2/U$, provided $|J_K/U| < 1$ (note that now $W = U$). This solution corresponds to the on-site interaction binding.

More generally, when the on-site U and off-site V interactions have different sign, the first bound state is associated mainly with larger interaction in absolute value, and the second bound state with the weaker one. When, however, U and V have the same sign and comparable strength, the bound states have mixed nature in the sense that both interactions significantly contribute to the binding. To illustrate the foregoing discussion, in Fig. 4.6 we show the wave functions of bound states for several cases pertaining to the on-site, off-site and mixed binding, while the corresponding energy dispersion relations are plotted in Fig. 4.3.
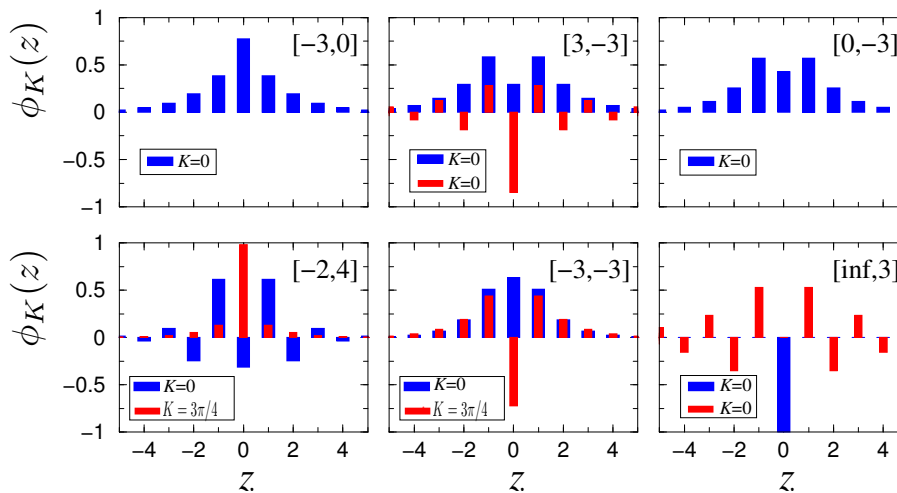
Figure 4.6.: Relative coordinate wave functions $\psi_K(z)$ of the two-particle bound states for several values of interaction strengths $[U/J, V/J]$. Thick bars correspond to the first bound solution of Eq. (4.54) at $K = 0$. Thinner bars correspond to the second bound solution at $K = 0$, if it exists for all K, or at $K = 3\pi/4$, if it exists for $|K| > K_c$ (cf. Figs. 4.3 and 4.5).

4.3. The two-body problem with arbitrary finite-range interactions

In this chapter we have so far solved two models[7] of two interacting one-dimensional lattice particles, drawing several conclusions about them: (i) bound states can be calculated via a certain polynomial equation of different degree that depends on the range of the interaction, (ii) the scattering states, both symmetric (bosonic) or antisymmetric (spin-polarized fermionic), are well described, asymptotically, by a single phase shift which depends again on the range of the potential, (iii) the "low-energy" properties of those systems, characterized by the scattering lengths, can always be calculated, leading to rather simple expressions of the corresponding interaction potentials.

Therefore, the next relevant question to ask is whether there is a general pattern followed by the solutions and properties of the two-body problem when the interactions are of arbitrary but finite range. In this section we deal with this question and find that, indeed, there is a well defined pattern for the bound states, and that all scattering properties can be calculated efficiently. For the particular, yet very important case of low-energy scattering (which we define as scattering at the top or bottom of the energy band) we show how to obtain the scattering lengths accurately even without knowing the phase shift.

Below we deal with both identical and distinguishable particles which can, of course, have different tunneling rates, using a generalization of the center of mass separation ansatz for the two-body problem.

---

[7]See sects. 4.1 and 4.2.

4.3.1. General separation of the two-body problem

We consider two particles, labeled A and B, in general having different tunneling rates[8] J_A and J_B, and interacting via a symmetric two-body potential $V(z) = V(-z)$. The reduction of the two-body to a one-body problem was also carried out by Piil and collaborators in [PNM08], in quasi-momentum space. Here we show how to separate the problem in direct lattice space, which is much more convenient in order to obtain the exact results in the remainder of this section.

The two-body one dimensional discrete Schrödinger operator H, acting on $\ell^2(\mathbb{Z}) \otimes \ell^2(\mathbb{Z})$ is, in first-quantized form,

$$
\begin{aligned}
(Hu)(n_A, n_B) = & -J_A \left[u(n_A + 1, n_B) + u(n_A - 1, n_B) \right] \\
& - J_B \left[u(n_A, n_B + 1) + u(n_A, n_B - 1) \right] \\
& + V(|n_A - n_B|) u(n_A, n_B),
\end{aligned} \tag{4.66}
$$

For the moment, we do not allow V to be infinitely large, $|V(|n|)| < \infty$ for all $n \in \mathbb{Z}$; this condition will be relaxed afterwards. Moreover, we assume that V is an arbitrary potential of finite range $\rho \in \mathbb{Z}$, that is, $V(|n| > \rho) = 0$ with at least $V(\rho) \neq 0$.

In order to solve the Schrödinger equation exactly we need to transform the Hamiltonian H to a single particle operator. For this purpose, consider the ansatz

$$
u(n_A, n_B) = u_K(z) e^{-i\beta_K z + iKR}, \tag{4.67}
$$

where $R = (n_A + n_B)/2$, $z = n_A - n_B$ and

$$
\tan \beta_K = \frac{J_A - J_B}{J_A + J_B} \tan(K/2). \tag{4.68}
$$

After introducing u in the Schrödinger equation $Hu = Eu$ we arrive at the desired single-particle Hamiltonian

$$
(\tilde{H} u_K)(z) = -|J^{(K)}| [u_K(z + 1) + u_K(z - 1)] + V(|z|) u_K(z), \tag{4.69}
$$

where the so-called collective tunneling rate [PNM08] has the form

$$
|J^{(K)}| = \sqrt{J_A^2 + J_B^2 + 2 J_A J_B \cos K}. \tag{4.70}
$$

At this point it is convenient to introduce a dimensionless Hamiltonian by dividing it by the collective tunneling, which is equivalent to setting $J^{(K)} \equiv 1$ in Eq. (4.69), and rename $u_K \equiv u$ for simplicity.

4.3.2. Bound states

We pursue the exact solution for the bound states of two-body systems on the lattice with finite range interactions.

We define a bound state of $\tilde{H}$ as any square-summable solution $u(z)$ of the discrete stationary Schrödinger equation $\tilde{H}u = Eu$ with its associated eigenvalue E lying outside

---

[8]In continuous space this is equivalent to particles with different masses.

the essential spectrum of $\tilde{H}$, $\sigma_{\text{ess}} = [-2, 2]$. Recall that "outside the essential spectrum" can actually mean both above [WTL^{+}06, PSAF07, PM07, VP08b, VP08a, VP09] or below the continuum.

It is already known that for any finite range potential V there exists at least one symmetric bound state;[9] it is also known that the maximum number of symmetric (antisymmetric) bound states of $\tilde{H}$ is $\rho + 1$ (ρ) [Tes00]. Now we show rigorously *how* to calculate all these bound states exactly. The formulation of this result is as follows.

Theorem:

Let $\tilde{H}$ be the Hamiltonian (4.69) with V a range-ρ ($< \infty$) potential. Then all bound states $u(z)$ of $\tilde{H}$ have the decay property $u(z) = \alpha^{|z|-\rho}$ for $|z| \geq \rho$, $0 < |\alpha| < 1$; the energies of the bound states are given by $E = -\alpha - 1/\alpha$. If $u(z)$ is symmetric then α is a root of a polynomial of degree $2\rho + 1$ if $\rho \geq 1$ and, if $\rho = 0$, its degree is 2; if $u(z)$ is antisymmetric and $\rho > 0$ then α is the root of a polynomial of degree $2\rho - 1$.

Proof. Applying the exponential ansatz for $u(z)$ with $|z| \geq \rho$ yields immediately

$$E = -\alpha - 1/\alpha \equiv f(\alpha). \tag{4.71}$$

Since $f((-1, 0) \cup (0, 1)) = (-\infty, -2) \cup (2, \infty)$ and f is injective in $(-1, 0) \cup (0, 1)$, we have that the exponential ansatz is the only possible form for the bound states outside the range of V. It can be shown by induction that α is a root of a polynomial: for $\rho \geq 2$, if $u(z)$ is exponentially decaying, then $\alpha^n u(\rho - n) = Q_{2n-1}^{(n)}(\alpha)$ and $\alpha^{n-1} u(\rho - n - 1) = Q_{2n-3}^{(n-1)}(\alpha)$, where $Q_k^{(m)}$ are polynomials of degree k. For symmetric solutions the polynomial equation is then obtained by setting $u(1) = u(-1)$ and, for antisymmetric solutions, by setting $u(0) = 0$, which proves our statement. For $\rho = 0$ and $\rho = 1$ the result can be proved by explicitly obtaining the polynomial equation [VP08b, VP09] as done in subsects. 4.1 and 4.2.

The theorem presented here implies that for any finite range potential we have to solve a polynomial equation whose degree grows slowly with increasing ρ. The way of obtaining such polynomials is, as can be observed from the proof, inductive: we start by setting $u(\rho) = 1$ and proceed to calculate $u(\pm 1)$ and $u(0)$ by recurrence and solve the respective symmetry constrains $u(1) = u(-1)$ or $u(0) = 0$. Certainly, if ρ gets too large it becomes inconvenient to get such polynomials for a general potential V, and we should obtain the coefficients of the polynomial equation for the given particular potential. We have calculated both polynomials $P(\alpha)$ for the symmetric and antisymmetric bound states numerically, with their roots characterizing the bound states, for the specific choice of the potential

$$V(z) = \left\{ \begin{array}{rl} -\frac{1}{|z|^3} & \text{if } 0 < |z| \leq 10 \\ 0 & \text{if } |z| > 10 \\ -9.7313 & \text{if } |z| = 0 \end{array} \right\} \tag{4.72}$$

which represents a dipolar potential with a cutoff. The results are shown in Fig. 4.7. For symmetric bound states the polynomial has only one root in $(-1, 1)$, and therefore only one bound state.[10] The polynomial has a root at $\alpha = 1$, which means that it has

---

[9]This result is a generalization of what we proved in subsect. 4.2. See [DHKS03], where the authors make use of simple variational estimates with perturbation theory-inspired trial functions.

[10]Note that since $V(z) \leq 0$ for all $z \in \mathbb{Z}$, there can be no roots for $-1 < \alpha < 0$.

low-energy resonance. We will discuss resonances in subsect. 4.3.4. The polynomial for antisymmetric bound states has also one and only one root in $(-1, 1)$, in agreement with the discrete Bargmann's bound [HS02].
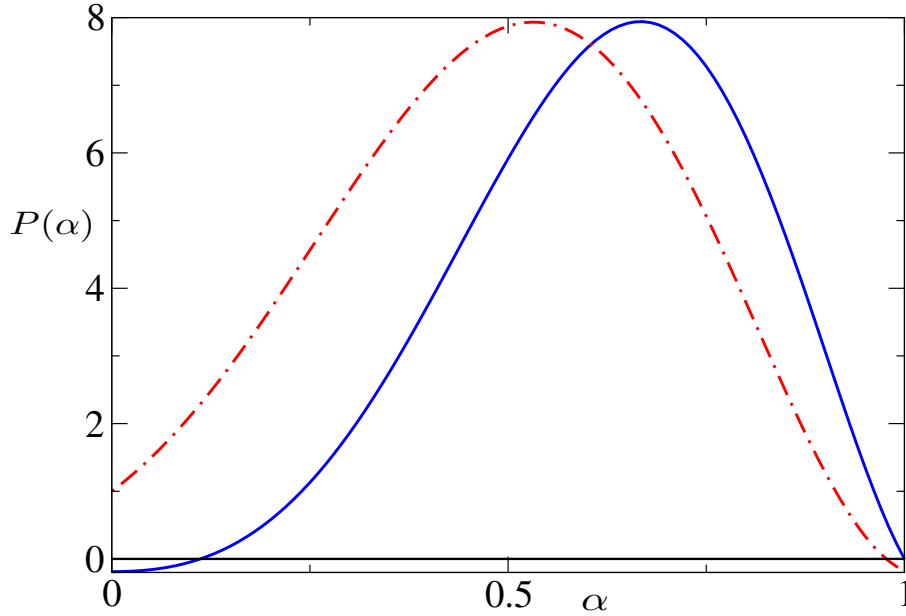

Figure 4.7.: Polynomials for symmetric (solid line) and antisymmetric (dashed-dotted line) bound states whose roots α characterize the bound states with energy $E = -\alpha - 1/\alpha$.

4.3.3. Scattering states

For finite range potentials, the scattering states of Hamiltonian $\tilde{H}$ are asymptotically plane waves, that is, for $|z| \geq \rho$ we have

$$u_S(z) \propto \cos(k|z| + \delta_S), \tag{4.73}$$

$$u_A(z) \propto \text{sgn}(z)\cos(k|z| + \delta_A), \tag{4.74}$$

where S and A denote, respectively, the symmetric and antisymmetric solutions. Their associated eigenenergies are given by the standard energy dispersion [AM76]

$$E = -2\cos(k). \tag{4.75}$$

However, a general result concerning the phase shifts δ_S and δ_A does not seem feasible, and it is quite cumbersome to obtain them in closed form for rather large ρ. We can, however, calculate the phase shifts (and the exact solution at all z) numerically by recurrence. To this end, we set $u_S(\rho+1) = \cos(k(\rho+1)+\delta_S)$ and $u_S(\rho) = \cos(k\rho+\delta_S)$ and analogously for antisymmetric solutions. We then calculate $u_S(-1)$ and $u_S(1)$ for symmetric solutions with the help of Eq. (4.69) and solve $u_S(-1) = u_S(1)$. In the case of antisymmetric solutions, the relevant equation is $u_S(0) = 0$. We have done so for the potential of Eq. (4.72), as plotted in Fig. 4.8. There, we clearly observe

that the main differences between the two phase shifts are at low quasi-momenta where the symmetric solution is resonant (see Fig. 4.7); at slightly higher quasi-momentum we observe little difference between the two phase shifts. This means that far from $k = 0$ fermionization appears rapidly, and is due to the large on-site interaction $V(0)$, while at low momenta the longer-range part of the potential plays an important role. In the insets of Fig. 4.8, we compare the phase shifts for the potential in Eq. (4.72) and a model range-1 potential, whose analytic solution is known[11] [VP09]. The model potential W is chosen so as to be consistent with Bargmann's bound [HS02], and to be resonant for the lowest-energy symmetric solution. We obtain [VP09]

$$W(1) = \sum_{n=1}^{\infty} V(n) = -1.19753$$
$$W(0) = -12.125. \tag{4.76}$$

The qualitative agreement between the results using V or W for the symmetric eigenstates is manifest in Fig. 4.8 and, as expected, the differences are most noticeable in the high quasi-momentum regime. For antisymmetric eigenstates the agreement is very good, even quantitatively, until $|k| \simeq \pi/2$.

4.3.4. Scattering lengths and zero-energy resonances

The "low" energy $(k \to 0, \pi)$ scattering properties of the two-body system can be understood via a simple, yet exact, calculation of the scattering lengths. Indeed, the solution of the stationary Schrödinger equation for $k \to 0$ and $k \to \pi$ has the corresponding energy $E = -2$ and $E = +2$, and the asymptotic $(|z| \geq \rho)$ behavior

$$u_S(z) = (\mp 1)^z \frac{|z| - a_S^{\pm}}{\rho - a_S^{\pm}} \tag{4.77}$$

$$u_A(z) = \mathrm{sgn}(z)(\mp 1)^z \frac{|z| - a_A^{\pm}}{\rho - a_A^{\pm}}, \tag{4.78}$$

where a_i^- (a_i^+) is the scattering length, $i = S, A$. It must be noted that on the lattice, there can be *four* different scattering lengths, two for bosons and two for (spin-polarized) fermions. In order to calculate the scattering lengths we proceed as follows : using the recurrence relation from $z = \rho$ by setting $u_i(\rho + 1) = (\mp 1)^{\rho+1}[1 + 1/(\rho - a^{\pm})]$, $u_i(\rho) = (\mp 1)^{\rho}$ and $E \equiv E_{\pm} = \pm 2$, the scattering lengths for the symmetric states are obtained by solving the equation $(V(0) - E_{\pm})u_S(0) - 2u_S(1) = 0$ (see proof of the theorem in subsect. 4.3.2), while for the antisymmetric states the equation to be solved is $u_A(0) = 0$. It is remarkable that the resulting equations for the scattering lengths as functions of the potential are linear in $a^{\pm}$, that is, are of the form $s_0 a^{\pm} + b_0 = 0$ with s_0 and b_0 real constants which depend on $V(z)$. In fact, this is an alternative way of defining the four lattice scattering lengths, completely equivalent to the definition $a^{\pm} = -\lim_{k \to \pi, 0} \partial_k \delta$, with the advantage of not needing to know the phase shift explicitly. It must be noted at this point that, strictly speaking, scattering lengths are singular properties of one-dimensional lattices since the radial symmetry is lost in dimensions $D > 1$.
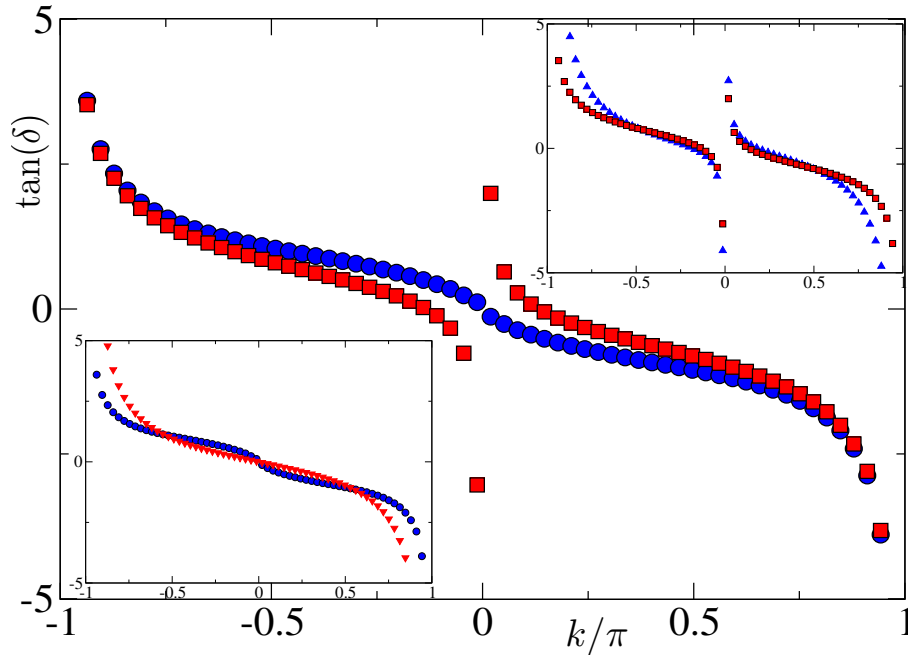
---

[11]See sect. 4.2.

Figure 4.8.: The calculated phase shifts ($\tan(\delta)$ with $\delta = \delta_S$ or $\delta = \delta_A$) for symmetric (circles) and antisymmetric (squares) scattering wave functions, Eqs. (4.73) and (4.74) as a function of the relative quasi-momentum k, for the potential (4.72). Left inset: comparison of the symmetric phase shift (circles) with the one obtained with a model range-1 potential (triangles), Eq. (4.76). Right inset: antisymmetric phase shift (squares) compared to the result with the model range-1 potential (triangles). The axes of the insets have the same meaning as those of the main figure.

As an example, we have calculated a_S^- for a quickly decaying potential $V(0 < |z| \leq \rho) = -1/|z|^3$ with a cutoff, $V(|z| > \rho) = 0$, and $V(0)$ as a free parameter. The results are shown in Fig. 4.9 for range $\rho = 10$, where we observe a clearly marked resonance at the point where the scattering length diverges.

The divergence of one of the scattering lengths can happen for different values of the total quasi-momentum K.[12] In the simplest case of a zero range interaction with $V(0) = U$, we know that the system has no zero-energy resonances, subsect. 4.1. For longer ranges, already starting with $\rho = 1$ [VP09], these resonances can occur (see subsect. 4.2). With the method outlined in this section we are then able to predict when, for a given range-ρ potential with one or more free parameters $\{V(z_1), V(z_2), \ldots, V(z_n)\}$, there is such a resonance. To do so, one sets $u(z \geq \rho) = (\mp 1)^z$ and iterates recursively as has been explained, and then solves the resulting equation for symmetric and antisymmetric states, obtaining a relation between the free potential parameters corresponding to a resonance.

We consider again the example of Fig. 4.9. As we have already noted, the system admits one resonance at the bottom of the continuum for the symmetric states. The

---

[12]Recall that we have normalized the Hamiltonian as $\tilde{H} = H/|J^{(K)}|$.
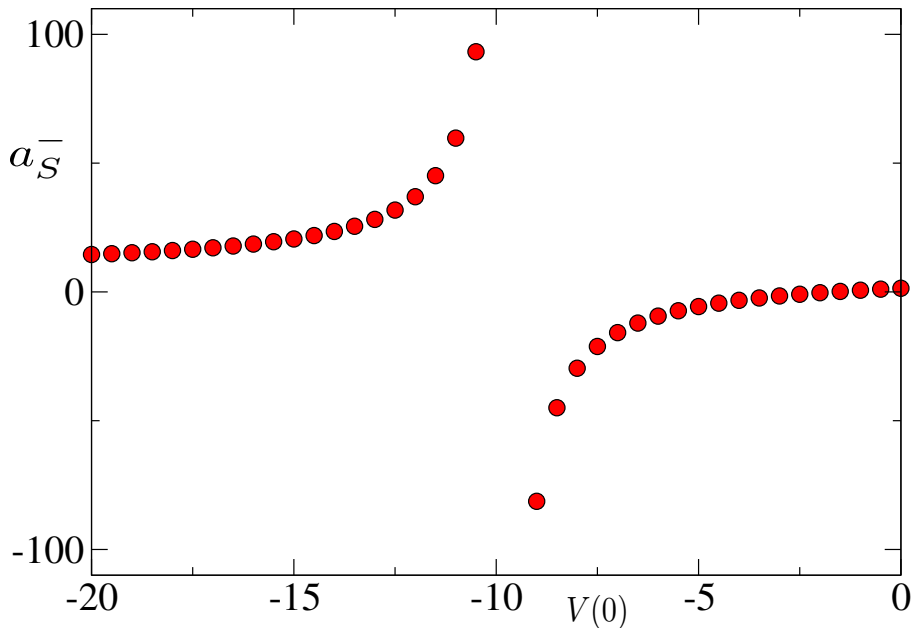
Figure 4.9.: Scattering length a_S^- (see text) as a function of the free parameter $V(0)$, with $V(0 < |z| \leq 10) = -1/|z|^3$ and $V(|z| > 10) = 0$.

approximate location of the resonance can be inferred from Fig. 4.9. However, once the scattering length starts to diverge, it becomes very hard (if not impossible) to accurately locate the resonance grafically, especially if the resonance is a very sharp function of $V(0)$. With our method, we are able to locate the resonance very precisely, obtaining for the above discussed example a value of $V(0) = -9.7313$.[13] This is exactly the value chosen in the previous subsections to match this resonance.

4.3.5. The number of bound states

The scattering lengths are very useful quantities in the sense that their precise values imply the knowledge of the total number of bound states with energies lying below or above the continuum. For this purpose, we use the discrete analog of Sturm oscillation theory [Tes00]. In simple terms, oscillation theory states that the number of nodes[14] of the zero-energy ($E = E_- = -2$) symmetric (antisymmetric) solution u_0 of $\tilde{H} u_0 = E u_0$ in $\mathbb{Z}_+$ is exactly the number of symmetric (antisymmetric) eigenstates below $E_- = -2$. Since any state with energy below E_- is a bound state, the number of nodes of u_0 is the number of bound states below the continuum. To see how many bound states there are with energies above the continuum, we make use of the transformation $\hat{G}$, Eq. (2.71), or, equivalently, count the number of missing nodes.

We apply oscillation theory now to our example with the potential of Eq. (4.72) leaving again $V(0)$ as a free parameter. We calculate the symmetric zero-energy solution for a

---

[13]If the calculation is implemented with a symbolic package, the value of $V(0)$ at which the resonance occurs can be calculated exactly (with no machine precission limit). In our example, $V(0)$ is a rational number whose (large) numerator and denominator can be calculated exactly this way.

[14]On the lattice, a function f is said to have a node between n and $n+1$ iff $f(n)f(n+1) < 0$.

given scattering length a_S^- with the methods introduced in this section and see that for $V(0) < -9.7313$ there are two bound states with energies below E_-, and for $V(0) \geq -9.7313$ there is exactly one bound state below the continuum.

4.3.6. A generalization

More general Hamiltonians with exchange operators appear when dealing with the problem of one "free" boson and a bound pair [VPS10], which is the topic of the next chapter. We will then see that the effective particles are distinguishable, there is a hardcore on-site interaction, an effective range-1 potential and a first-order exchange interaction. We consider now the following one-body Schrödinger operator

$$(H_{\text{ex}}u)(z) = -[u(z+1) + u(z-1)] + V(|z|)u(z) + \Omega(|z|)(\hat{P}u)(z), \qquad (4.79)$$

where $V(0)$ can be finite or infinite and $\hat{P}$ is the discrete parity operator. We further assume that $\Omega(|z|)$ has a finite range ρ_{ex} with no on-site exchange, $\Omega(0) = 0$, since it can be included in $V(0)$.

Obviously $[\hat{P}, H_{\text{ex}}] = 0$, and therefore we can look for symmetric and antisymmetric eigenfunctions. However, the Hamiltonian does not commute with the exchange operator $\Omega\hat{P}$. With the parity being a good quantum number it is straightforward to generalize the theorem in subsect. 4.3.2 to include the exchange. To see this, take $\rho_M \equiv \max(\rho, \rho_{\text{ex}})$. If $u(z)$ is symmetric, the exchange shifts the potential to $V(|z|) + \Omega(|z|)$, while if $u(z)$ is antisymmetric it shifts the potential to $V(|z|) - \Omega(|z|)$. Therefore, obtaining the bound states of H_{ex} reduces again to a polynomial equation of degree $2\rho_M \pm 1$, and all the results of our theorem apply by changing ρ to ρ_M. However, it is no longer true that the hardcore condition maps "bosons" onto "fermions". Indeed, the non-trivial dependence of H_{ex} on the parity of the eigenstates makes it possible for the states to be above as well as below the continuum even if V and Ω have both the same definite sign. This makes H_{ex} violate the hypotheses of the Bose-Fermi mapping theorem (BFMT) [Gir60], and it explains the appearance of exotic three-body bound states in a 1D lattice [VPS10], studied extensively in chapter 5.

4.4. Dynamics of two bosons in a combined lattice and parabolic potential

This section is a natural continuation of sect. 3.3; however, for the understanding of the following discussions, the results obtained in the previous sections of this chapter are valuable.

Here, our goal is to study the quantum transport of a single bound pair on the harmonically trapped lattice. We have shown in subsect. 4.1 that a two-body bound state with strong on-site interaction has a very large effective mass. We also developed the effective theory that treats, under certain conditions, a single pair as essentially unbreakable, constituting a new particle. We will show that this is indeed a very good approximation for the dynamics when the lattice is superimposed with a weak parabolic potential.

On a flat lattice, both repulsive and attractive on-site interactions are totally equivalent, as we saw in subsect. 2.7. However, this is no longer true when the trapping

potential is switched on; this fact makes the repulsively bound pairs more stable than their attractive counterparts.

Apart from the main goal of this section, we also study, in a time-dependent fashion, two-body collisions and partial trapping of two-body wave packets due to the larger effective mass of the portion of the initial state that has some population of two particles at the same site.

4.4.1. The model

We thus consider cold bosonic atoms in a combined tight-binding periodic and weak parabolic potential. In 1D, the system is described by the trapped, interacting Bose-Hubbard Hamiltonian

$$H = \sum_n \left[\tilde{\Omega} n^2 \hat{N}_n + \frac{U}{2} \hat{N}_n (\hat{N}_n - 1) - J(b_n^\dagger b_{n+1} + b_{n+1}^\dagger b_n) \right] , \qquad (4.80)$$

where $\tilde{\Omega} > 0$ quantifies the strength of the superimposed parabolic potential due to which site $n = \pm 1, \pm 2, \ldots$ acquires energy offset $\tilde{\Omega} n^2$ with respect to site $n = 0$ corresponding to the minimum of the potential.

4.4.2. Two particle dynamics

Clearly, in the simplest case of feeble interaction $|U| \ll J$, we have two independent particles for which the results of sect. 3.3 apply. But even for strong on-site interaction U, some aspects of the combined dynamics of two low-energy particles can be inferred from the independent particle picture modified by short range collisions. This applies when the initial state $|\Psi(0)\rangle = |\psi\rangle \otimes |\psi'\rangle$ is composed of two non-overlapping single-particle wave packets, $|\langle\psi|\psi'\rangle|^2 \ll 1$, which upon collision with each other are reflected by the potential barrier $|U| \gtrsim J$. Examples of such a situation with large on-site attractive interaction energy $U = -10J$ are shown in Figs. 4.10(a) and 4.10(b). Analogous dynamics is observed for the repulsive interaction $U = 10J$.

More intriguing is the case of initial state $|\Psi(0)\rangle = |\psi\rangle \otimes |\psi\rangle$ consisting of two overlapping single-particle wavepackets shown in Fig. 4.10(c). This state has a significant population of the two-particle states $|2_n\rangle$ given by $\sum_n |\langle 2_n|\Psi\rangle|^2 \simeq \sum_n |a_n|^4$, where a_n are the single-particle probability amplitudes. Clearly, the population of two-particle states is largest in the central part of the initial density distribution. As seen in Fig. 4.10(c), this part exhibits slow dynamics, characterized by the effective tunnelling constant $J^{(2)} = -2J^2/U$, and separates from the wings of the initial density profile. The wings, formed by the single-particle states $|1_n\rangle$, oscillate between the two sides of parabolic potential with the usual period τ.[15]

Interaction-bound dimers. At this point, let us recall[16] [WTL$^+$06, PSAF07, VP08b, VP08a, PM07] that two bosonic particles occupying the same site n can form an effective "dimer" bound by the on-site interaction U. Thus, when $|U| \gg J$, the first-order

---

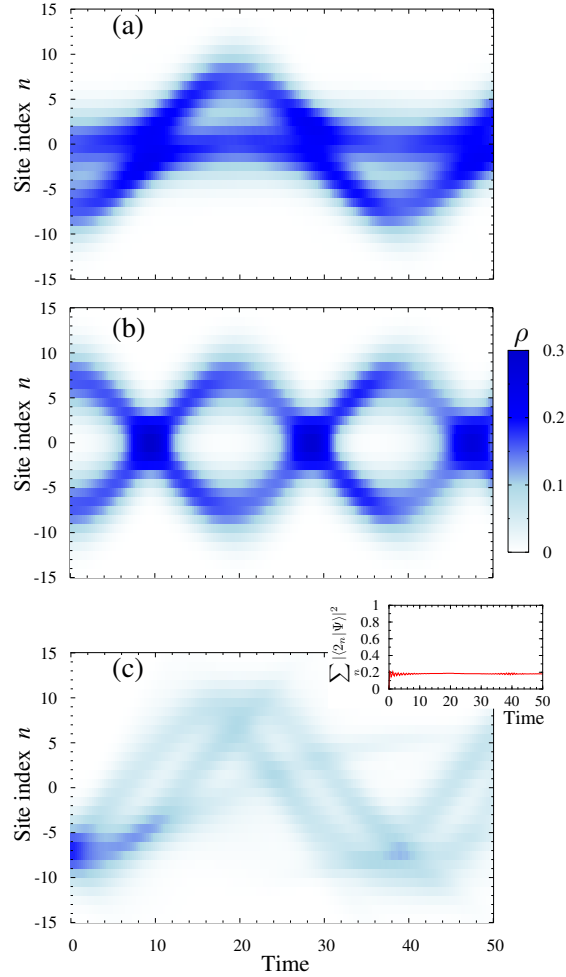[15]See sect. 3.3.
[16]See sect. 4.1.

Figure 4.10.: Time evolution of density $\rho_n \equiv \langle \hat{N}_n \rangle$ for two particles in a combined periodic and parabolic potential with $J/\tilde{\Omega} = 140$ and $U = -10J$. (a) Initial state $|\Psi(0)\rangle$ corresponds to one particle in the ground state $|\chi_0\rangle$ and the other particle in state $|\chi_0\rangle$ shifted from the trap center by 7 sites. (b) Initially both particles in state $|\chi_0\rangle$ are shifted from the trap center by 7 sites in opposite directions. (c) Initial state corresponds to both particles in state $|\chi_0\rangle$ shifted from the trap center by 7 sites in the same direction. Inset in (c) shows the projection $\sum_n |\langle 2_n|\Psi\rangle|^2$.

transitions $|2_n\rangle \rightarrow |1_n\rangle |1_{n\pm1}\rangle$ effected by the last term of Hamiltonian (4.80) are non-resonant and the particles cannot separate. However, the second-order in J transitions $|2_n\rangle \rightarrow |2_{n\pm1}\rangle$ via virtual intermediate states $|1_n\rangle |1_{n\pm1}\rangle$ are resonant. Consequently, the dimer can tunnel as a whole with the effective rate $J^{(2)} = -2J^2/U \ll J$ [PSAF07, VP08a], as was also derived from the exact energy band in sect. 4.1. This explains the dynamics seen in Fig. 4.10(c) where the initial density distribution splits into slow and fast propagating components, the former composed of the dimer states $|2_n\rangle$ while the latter containing the monomer states $|1_n\rangle$.

If the initial state is prepared in such a way that only two-particle (dimer) states are

populated, as implemented in, e.g., [WTL$^+$06], for $|U| \gg J$ the system can, to a good approximation, be described by an effective dimer Hamiltonian derived in the second order in J/U, Eq. (4.31). In terms of the dimer creation $c_n^\dagger = (b_n^\dagger)^2 [1/\sqrt{2(\hat{N}_n + 1)}]$ and annihilation $c_n = [1/\sqrt{2(\hat{N}_n + 1)}](b_n)^2$ operators, and number operator $\hat{m}_n = c_n^\dagger c_n = \hat{N}_n/2$, the effective Hamiltonian for a single dimer reads

$$H_{\text{eff}} = \sum_n \left[\Omega^{(2)} n^2 \hat{m}_n + (U - 2J^{(2)}) \hat{m}_n - J^{(2)} (c_n^\dagger c_{n+1} + c_{n+1}^\dagger c_n) \right], \qquad (4.81)$$

where $\Omega^{(2)} = 2\tilde{\Omega}$ is the strength of the parabolic potential felt by the dimer, while $(U - 2J^{(2)})$ represents the "internal" energy of a dimer. Note that Eq. (4.81) is a particular case of Eq. (4.31), but in second quantized form.

Before proceeding, let us note that, differently from the flat lattice situation considered in [VP08b, PSAF07] and sect. 4.1, here the effective Hamiltonian H_{eff} is not applicable in the vicinity of sites $|n| \simeq |U|/(2\tilde{\Omega})$ where near-resonant dissociation of a dimer can occur via transitions $|2_n\rangle \to |1_n\rangle |1_{n\pm1}\rangle$. But since we are interested in the dynamics of low-energy dimers with $|U| \gg J \gg \tilde{\Omega}$, such high-$n$ states cannot be reached.

Figure 4.11.: Time evolution of atom density $\rho_n \equiv \langle \hat{N}_n \rangle$ for an attractively-bound dimer in a combined periodic and parabolic potential with $J/\tilde{\Omega} = 140$ and $U = -10J$. Initial state $|\Psi(0)\rangle$ corresponds to the ground state $|\chi_0^D\rangle$ of the effective Hamiltonian (4.81) with the dimer amplitudes $a_n^D(0)$ shown in the left inset. Right inset is the projection $\sum_n |\langle 2_n | \Psi \rangle|^2$.

Consider first the case of strong attractive interaction $U < 0$ leading to a positive tunnelling constant $J^{(2)} > 0$. Then the effective Hamiltonian (4.81) has the same form as the Hubbard Hamiltonian (3.15) for a single particle in a combined periodic and parabolic potential. We can therefore immediately write the lowest energy eigenvalues

and eigenstates for an effective dimer as

$$E_k^D \approx -2J^{(2)} + 2\sqrt{J^{(2)}\Omega^{(2)}}\left(k + \tfrac{1}{2}\right), \tag{4.82}$$

$$|\chi_k^D\rangle \approx \mathcal{N}\sum_n (2^k k!)^{-1/2} e^{-\xi_n^2/2} H_k(\xi_n) |1_n^D\rangle, \tag{4.83}$$

where energies E_k^D are relative to the dimer internal energy $(U - 2J^{(2)})$, $\xi_n = n\sqrt[4]{\Omega^{(2)}/J^{(2)}}$ is the discrete coordinate, and $|1_n^D\rangle \equiv c_n^\dagger |0\rangle$ denotes a state with a single dimer at site n; obviously $|1_n^D\rangle = |2_n\rangle$. The modified Bloch band $-2J^{(2)} \leq E_k^D \leq 2J^{(2)}$ for the dimer is restricted to the sites with

$$|n| \leq n_{\max}^D \equiv \sqrt{\frac{2J^{(2)}}{\Omega^{(2)}}}, \tag{4.84}$$

thus containing $N_{\max}^D = 2\lfloor n_{\max}^D \rfloor + 1$ energy levels E_k^D with $0 \leq k < N_{\max}^D$. The effective harmonic oscillator frequency at the bottom of the modified Bloch band is $\hbar\omega^D = 2\sqrt{J^{(2)}\Omega^{(2)}}$ and the dimer effective mass $\mu^D = \hbar^2/(2J^{(2)})$ is large $(J^{(2)} \ll J)$ and positive. We have verified these conclusions by numerically solving the Schrödinger equation using the exact Hamiltonian (4.80) with the initial conditions corresponding to eigenstates (4.83) of the effective Hamiltonian (4.81). As an example, in Fig. 4.11 we show the time evolution, or nearly complete absence thereof, of the system in the ground state of (4.81),

$$|\chi_0^D\rangle \simeq \sqrt[8]{\frac{\Omega^{(2)}}{\pi^2 J^{(2)}}}\sum_n e^{-\xi_n^2/2} |1_n^D\rangle = \sqrt[8]{\frac{\tilde{\Omega}|U|}{\pi^2 J^2}}\sum_n e^{-\xi_n^2/2} |2_n\rangle, \tag{4.85}$$

with energy $E_0^D = -2J^{(2)} + \sqrt{J^{(2)}\Omega^{(2)}}$.

We next turn to the case of strong repulsive interaction $U > 0$. The dimer tunneling constant is negative, $J^{(2)} < 0$, corresponding to a negative effective mass μ^D [PSAF07]. As a result, $|\chi_0^D\rangle$ in Eq. (4.85) is no longer the ground state of Hamiltonian (4.81), as attested in Fig. 4.12(a). To see this, consider for a moment a single particle in a flat lattice of L sites with $J < 0$. It follows from Eqs. (3.1), (3.2) that the lowest energy state with $\bar{E}_{L-1} = -2J\cos[\pi L/(L+1)] = -2|J|\cos[\pi/(L+1)]$ is

$$|\bar{\chi}_{L-1}\rangle = -\mathcal{N}\sum_{l=1}^L \sin\left[\frac{l\pi}{L+1}\right] e^{il\pi} |1_l\rangle. \tag{4.86}$$

Thus, in the limit of infinite lattice $L \to \infty$, the ground state corresponds to the Bloch wave with quasi-momentum $q = \pi$. Returning back to the repulsively-bound dimer in the combined periodic and parabolic potential, we find that the low-energy eigenvalues are those of Eq. (4.82) with the replacement $J^{(2)} \to |J^{(2)}|$, while the corresponding eigenstates are given by

$$|\tilde{\chi}_k^D\rangle \approx \mathcal{N}\sum_n (2^k k!)^{-1/2} e^{-\xi_n^2/2} H_k(\xi_n) e^{i\pi n} |1_n^D\rangle. \tag{4.87}$$
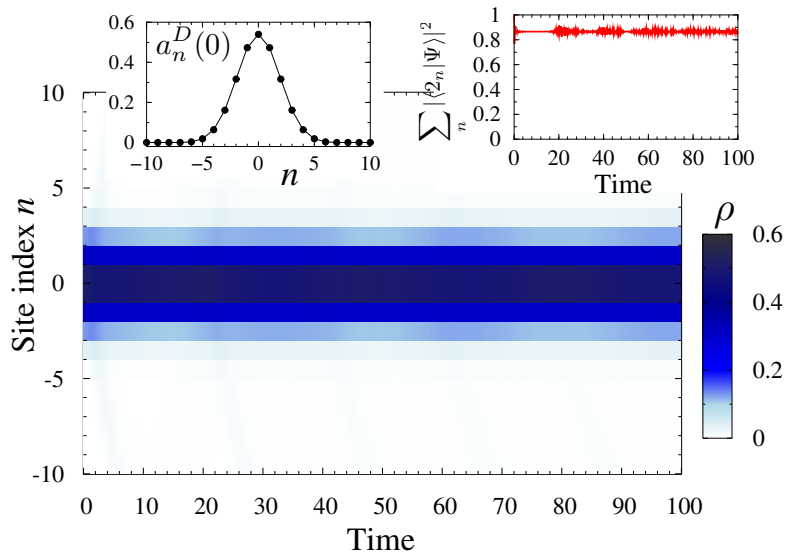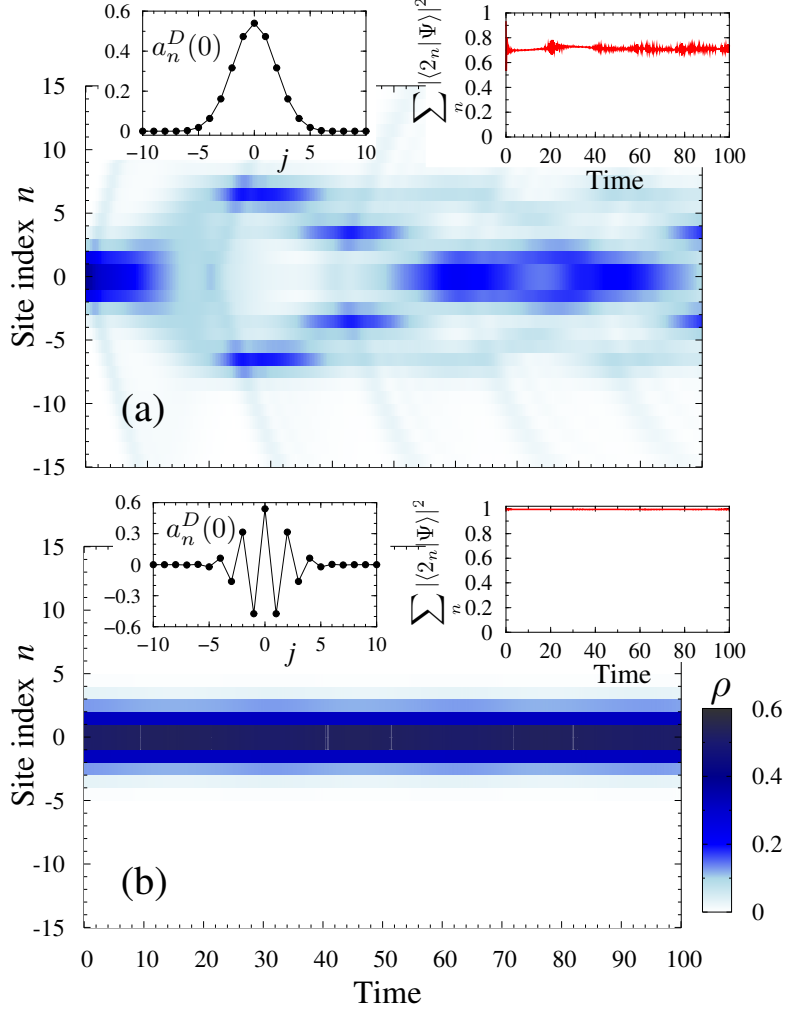
Figure 4.12.: Time evolution of density $\rho_n \equiv \langle \hat{N}_n \rangle$ for repulsively-bound dimer in a combined periodic and parabolic potential with $J/\tilde{\Omega} = 140$ and $U = 10J$. (a) Initial state $|\Psi(0)\rangle$ is the ground state $|\chi_0^D\rangle$ of attractive dimer, Eq. (4.85), with amplitudes $a_n^D(0)$ shown in the left inset. (b) Initial state $|\Psi(0)\rangle$ is the ground state $|\tilde{\chi}_0^D\rangle$ of repulsive dimer, Eq. (4.88), with amplitudes $a_n^D(0)$ shown in the left inset. Right insets are the projections $\sum_n |\langle 2n|\Psi\rangle|^2$.

The ground state with $E_0^D = -2|J^{(2)}| + \sqrt{|J^{(2)}|\Omega^{(2)}}$ is then

$$|\tilde{\chi}_0^D\rangle \simeq \sqrt[8]{\frac{\Omega^{(2)}}{\pi^2|J^{(2)}|}} \sum_n e^{-\xi_n^2/2} e^{i\pi n} |1_n^D\rangle$$

$$= \sqrt[8]{\frac{\tilde{\Omega}|U|}{\pi^2 J^2}} \sum_n e^{-\xi_n^2/2} (-1)^n |2_n\rangle, \qquad (4.88)$$

which is confirmed by our numerical simulations illustrated in Fig. 4.12(b). Remarkably, the repulsive dimer appears to be tighter bound than the attractive one. The symmetry

4. The two-body problem

between the cases of $U < 0$ and $U > 0$ is broken due to the presence of a parabolic potential, in which the ground state of the repulsive dimer has quasi-momentum $K = \pi$ leading, according to Eq. (4.21), to almost completely colocalized bosons.
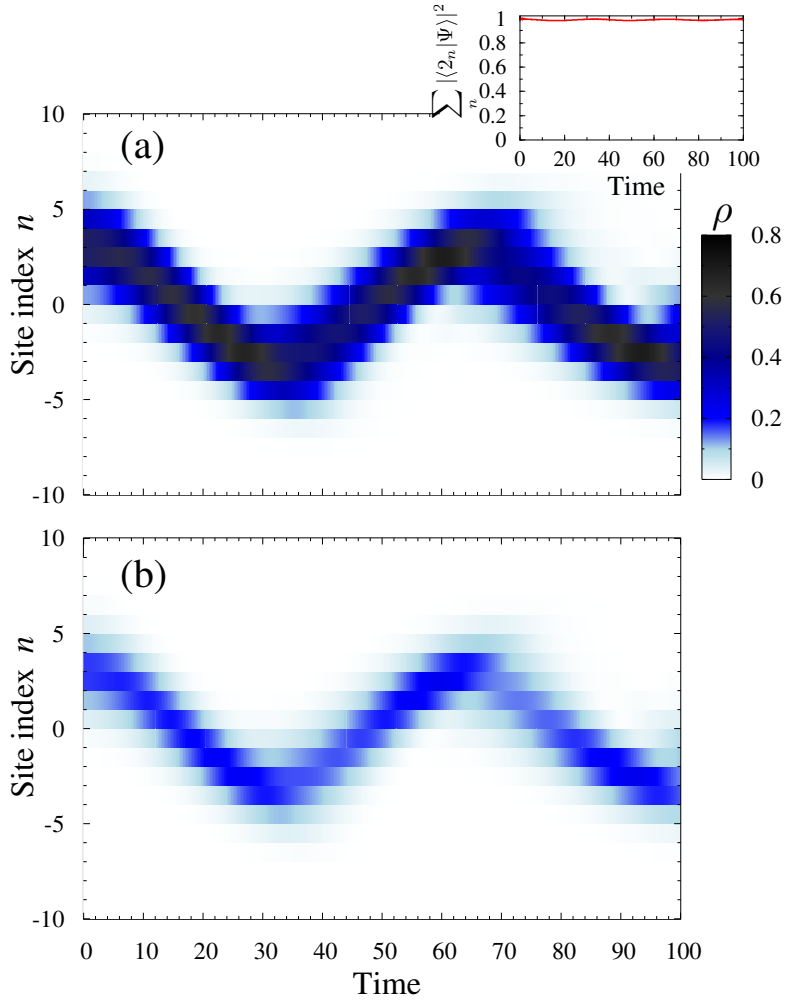
Figure 4.13.: Time evolution of (a) atom density $\rho_n \equiv \langle \hat{N}_n \rangle$, and (b) dimer density $\rho_n^D \equiv \langle \hat{m}_n \rangle \simeq \rho_n/2$ in a combined periodic and parabolic potential with $J/\tilde{\Omega} = 140$ and $U = 10J$. Initial state $|\Psi(0)\rangle$ corresponds to the dimer ground state $|\tilde{\chi}_0^D\rangle$ shifted by 3 sites from the trap center. (a) is the numerical solution of the Schrödinger equation with the exact Hamiltonian (4.80), while (b) is obtained with the effective Hamiltonian (4.81). Inset in (a) shows the projections $\sum_n |\langle 2_n | \Psi \rangle|^2$.

Finally, in Fig. 4.13 we show the dynamics of a dimer wave packet $|\Psi\rangle$, represented by the ground state $|\tilde{\chi}_0^D\rangle$ initially shifted by 3 sites from the trap center (for these parameters, $n_{\max}^D \simeq 4.9$). Our simulations using the exact Hamiltonian (4.80) and the effective Hamiltonian (4.81) yield practically identical results, which amount to periodic oscillations of the dimer wavepacket between the two sides of parabolic potential with period $\tau^D \simeq 2\pi/\omega^D = (\pi\hbar/2J)\sqrt{|U|/\tilde{\Omega}}$. Numerical simulations for attractively bound

dimers reveal similar behaviour but with considerably larger admixture of the single-particle states, $\sum_n |\langle 1_n | \Psi \rangle|^2 \lesssim 0.2$. This is another manifestation of the fact that the repulsive dimer in a combined periodic and weak parabolic potential is bound tighter than the attractive dimer under the otherwise similar conditions.

4.5. Conclusions and outlook

To summarize, in this chapter we have studied in detail the two-body problem on a one-dimensional (1D) tight-binding lattice.

We have given complete analytical solutions of the eigenvalue problem for, first, the simplest case of on-site interaction only, then the extended Hubbard model which includes also nearest-neighbor interaction, and then the general two-body problem with finite range interactions, although involving some more numerical work. We have shown that, in 1D, in order to obtain two-body resonances – which can be important for many-body applications – we need to include, at least, nearest-neighbor interactions. We have shown that all two-body bound states with any finite range interaction are characterized by roots of an algebraic equation and we have developed a complete formalism for exact calculation of resonance positions, scattering lengths and phase shifts.

Apart from the static results, we have studied the dynamics of two interacting bosons on a lattice under the influence of an external harmonic potential. We have shown that coherent – non-dispersive – transport of an interaction-bound pair can be achieved between the two sides of the trap. Moreover, we have seen that, due to the internal structure of the bound pairs, the repulsive dimers in the trap are bound tighter than their attractive counterparts. Our results are relevant to current experiments with cold alkali atoms in optical lattices and weak magnetic (or optical) traps [MO06, Blo05].

In higher dimensions, the two-body problem has been studied in [Mat86], however mostly at zero total quasi-momentum. It would be very interesting to study the effects of anisotropy – different quasi-momenta in each of the lattice directions –, especially the crossover between three and two dimensions; and from two to one dimension. The reduction of the effective tunneling in one direction compared to the other direction when the projection of the total quasi-momentum in this direction is close to the edge of the Brillouin zone may lead to the so-called geometric resonances [Ols98, FBZ04], even when the lattice is actually isotropic.

The most natural extension of our work is, without any doubts, the three-body problem. Our results in this direction [VPS10] are explained in detail in the following chapter.

5. The three-body problem

'For historical reasons, there is a great deal of satisfaction in solving the three-body problem, or at least in reducing it to quadrature, in *any* context'.
(Daniel C. Mattis [Mat86])

The three-body problem on a lattice has a long history. The study of the three-magnon problem, for the Heisenberg model (HM) in one dimension, can be carried out analytically with great detail thanks to the Bethe ansatz [KM97]. These magnons, the quasi-particles of the HM, behave as lattice hard-core bosons with nearest-neighbor pairwise interactions. For three spin-polarized fermions the situation is not different, since the Heisenberg model and the many-fermion problem are unitarily equivalent. Even the case of spin-1/2 fermions with two spins up and one spin down (or the other way around), with on-site softcore interactions (which is nothing but the three-body problem in the Hubbard model), can be solved analytically [LW68], and no three-body bound states are present.

Given the success of the Bethe ansatz to describe essentially all three-body problems on one-dimensional lattices, Rudin and Mattis [RM84] studied the problem only in higher (two and three) dimensions for soft-core bosons and spin-1/2 fermions; however, they did it only for vanishing total quasi-momentum $\mathbf{K} \equiv 0$. For fermions, they realized that no three-body bound state exists, whatever (strong or weak) the interaction strength is. In the case of three bosons, they found two results. First of all, that the Efimov effect [Efi70] also appears on the lattice around the $\mathbf{K} = 0$ two-body resonance in three dimensions, although no qualitative or quantitative analysis was carried out. Second, and more important, that the three-body bound state in three dimensions with an asymptotic energy $3U$ (U is the on-site interaction strength) appears discontinuously[1] and already in the strong coupling regime. In two dimensions no Efimov effect was reported, and the three-body bound states have no threshold, as in one dimension. Most of these results are treated in detail, with a great pedagogical value, in the review article [Mat86].

We study here the three-boson problem on the lattice, when the motion of the particles is restricted to one spatial dimension. This case (for *bosons*) has been overlooked for more than 20 years, and only recently the present author and his collaborators studied this problem in detail in [VPS10].

Apart from the simple strongly bound trimer of three particles essentially co-localized at the same lattice site, we find two other kinds of weakly bound three-boson states corresponding to a "free" particle attached to a bound pair. Their binding will be shown to be qualitatively explained by an effective theory in the strong coupling regime. This theory suggests that the binding mechanism is an effective particle exchange interaction between the dimer and the third particle, the monomer.

---

[1]It has a finite size at the formation threshold.

5.1. Bound states

In order to study the properties of the three-boson bound states exactly , we will make use of the so-called Mattis equation [Mat86], which we derive in the next subsection for general lattice dimensions. We then solve it in one dimension in subsect. 5.1.2, finding new bound states whose physics will be revealed by our effective model in subsect. 5.1.3.

5.1.1. Mattis equation

Let us consider three interacting bosons on a D dimensional homogeneous, hypercubic lattice with the single band energy dispersion

$$\epsilon(\mathbf{k}_i) \equiv \epsilon(k_{i_1}, k_{i_2}, \ldots, k_{i_D}) = \sum_{j=1}^{D} \epsilon(k_{i_j}), \tag{5.1}$$

which is assumed to have the period of the first Brillouin zone $\Omega = (-\pi, \pi]^D$, that is, we define

$$\epsilon(k_{i_j} + 2\pi) = \epsilon(k_{i_j}). \tag{5.2}$$

The interaction potential $\hat{V}$ between each pair of particles acts like

$$\hat{V} |\mathbf{k}_1, \mathbf{k}_2, \mathbf{k}_3\rangle = \frac{1}{(2\pi)^D} \int_\Omega d\mathbf{k} V(\mathbf{k}) \big[|\mathbf{k}_1 + \mathbf{k}, \mathbf{k}_2 - \mathbf{k}, \mathbf{k}_3\rangle$$
$$+ |\mathbf{k}_1 + \mathbf{k}, \mathbf{k}_2, \mathbf{k}_3 - \mathbf{k}\rangle$$
$$+ |\mathbf{k}_1, \mathbf{k}_2 + \mathbf{k}, \mathbf{k}_3 - \mathbf{k}\rangle \big] \tag{5.3}$$

on the non-symmetrized eigenstates of the free three-body Hamiltonian $\hat{T}$,

$$\hat{T} = \sum_{i=1}^{3} \hat{T}_i, \tag{5.4}$$

$$\hat{T}_i = \epsilon(-\mathrm{i}\partial_{\mathbf{k}_i}). \tag{5.5}$$

In solving the stationary Schrödinger equation $H |\psi\rangle = E |\psi\rangle$, for $H = \hat{T} + \hat{V}$, we need to calculate the matrix elements of the form

$$\langle \mathbf{k}_1', \mathbf{k}_2', \mathbf{k}_3'| \hat{V} |\psi\rangle. \tag{5.6}$$

For the bosonic bound states, the eigenfunctions can be expanded as

$$|\psi\rangle = \iiint_{\Omega^3} d\mathbf{k}_1 d\mathbf{k}_2 d\mathbf{k}_3 \psi(\mathbf{k}_1, \mathbf{k}_2, \mathbf{k}_3) |\mathbf{k}_1, \mathbf{k}_2, \mathbf{k}_3\rangle, \tag{5.7}$$

with ψ being symmetric with respect to exchange of any pair of quasi-momenta. The formal solution to the Schrödinger equation has the form

$$|\psi\rangle = -[\hat{T} - E]^{-1}\hat{V} |\psi\rangle, \tag{5.8}$$

where $\hat{T}$ is the non-interacting Hamiltonian (5.4) with energy dispersion given by Eq. (5.1). We then obtain the bound state equation

$$[E - \epsilon(\mathbf{k}_1, \mathbf{k}_2, \mathbf{k}_3)]\psi(\mathbf{k}_1, \mathbf{k}_2, \mathbf{k}_3) = \bar{M}(\mathbf{k}_1; \mathbf{k}_3) + \bar{M}(\mathbf{k}_1; \mathbf{k}_2) + \bar{M}(\mathbf{k}_3; \mathbf{k}_1), \qquad (5.9)$$

where the functions $\bar{M}$ are defined as

$$\bar{M}(\mathbf{k}_1; \mathbf{k}_2) = \frac{1}{(2\pi)^D} \int_\Omega d\mathbf{k} V(\mathbf{k})\psi(\mathbf{k}_1 + \mathbf{k}, \mathbf{k}_2 - \mathbf{k}, \mathbf{K} - \mathbf{k}_1 - \mathbf{k}_2), \qquad (5.10)$$

and similarly for any pair of quasi-momenta k_i and k_j. We have defined above the (conserved) total quasi-momentum $\mathbf{K} \equiv \mathbf{k}_1 + \mathbf{k}_2 + \mathbf{k}_3$ of the three-body system which is introduced to eliminate the dependence of each $\bar{M}$ on one of the three quasi-momenta.

We can simplify Eq. (5.9) further by assuming the following two properties:
(i) The interaction potential preserves the symmetry of the lattice,

$$V(\mathbf{k}) = V(k_{i_1}, \ldots, k_{i_j}, \ldots, k_{i_D}) = V(k_{i_1}, \ldots, k_{i_j} + 2\pi, \ldots, k_{i_D}), \qquad (5.11)$$

that is, V is periodic with the period of the Brillouin zone.
(ii) The potential is invariant under the change $\mathbf{k} \to -\mathbf{k}$, that is

$$V(\mathbf{k}) = V(-\mathbf{k}). \qquad (5.12)$$

This last condition is of course natural. The first of these conditions is usually not a problem when it concerns either one-dimensional systems (e.g. the $|n|^{-1}$ potential in 1D satisfies condition (i)), or short-range interactions. It is, however, more problematic when long range interactions in $D > 1$ occur. To illustrate this point, let us consider the Coulomb interaction between two electrons in continuous space. The three-dimensional Coulomb potential V_C in momentum space reads

$$V_\mathrm{C}(\mathbf{k}) = 4\pi e^2 \frac{1}{\mathbf{k}^2}. \qquad (5.13)$$

Of course, if used in this form as an electron-electron interaction on the lattice, it violates condition (i). The Coulomb problem on a three-dimensional (3D) lattice has not been solved analytically, that is, the solution of the discrete Poisson equation

$$(\Delta V_\mathrm{C})(\mathbf{n}) = -\delta_{\mathbf{n},0}, \qquad (5.14)$$

is not known analytically in three dimensions. However, if one still needs a Coulomb-like interaction which satisfies the requirement (i), and behaves at low momenta as the continuous space Coulomb interaction, the following choice for the potential is possible [Mat86],

$$V_\mathrm{C}(\mathbf{k}) \propto \frac{1}{\cos(k_x) + \cos(k_y) + \cos(k_z) - 3}, \qquad (5.15)$$

since for $\mathbf{k} \to 0$ (i.e. the continuum limit), $V_\mathrm{C}(\mathbf{k}) \sim \mathbf{k}^{-2}$. This way of parametrizing lattice potentials to respect the lattice symmetry (i), by replacing $\mathbf{k}^2$ by $\sum \cos(k_i) - d$, is indeed very useful for numerical (finite-difference) simulations of problems in the continuum in the low-momentum regime.

5. The three-body problem

Having discussed the conditions that a "good" interaction potential on the lattice should satisfy, we proceed to simplify Eq. (5.9). If (i) and (ii) are met, then the eigenfunctions ψ also have the periodicity of V in each of their arguments $\mathbf{k}_i$, $i = 1, 2, 3$. Therefore, we can choose freely the origin of integrations in Eq. (5.9), and the functions $\bar{M}$ become

$$\bar{M}(\mathbf{k}_i; \mathbf{k}_j) = \frac{1}{(2\pi)^D} \int_\Omega d\mathbf{k} V(\mathbf{k} - \mathbf{k}_i) \psi(\mathbf{k}, \mathbf{k}_j, \mathbf{K} - \mathbf{k} - \mathbf{k}_j). \tag{5.16}$$

There are only three different $\bar{M}$'s thanks to conditions (i) and (ii), since the following relation

$$\bar{M}(\mathbf{k}_i; \mathbf{k}_j) = \bar{M}(\mathbf{k}_s; \mathbf{k}_j), \tag{5.17}$$

where $i \neq j$ and $i \neq s \neq j$, holds. Finally, we have derived a system of three coupled integral equations, namely (5.16), with the wave function ψ given by Eq. (5.9). A major simplification of Eq. (5.16) is then achieved if the interaction potential has zero range, that is, for $V(\mathbf{k}) \equiv U$. In this case, the functions $\bar{M}(\mathbf{k}_i; \mathbf{k}_j)$ cease to depend on the first variable $\mathbf{k}_i$ and simply become

$$\bar{M}(\mathbf{k}_i; \mathbf{k}_j) \equiv M(\mathbf{k}_j) = \frac{U}{(2\pi)^D} \int_\Omega d\mathbf{k} \psi(\mathbf{k}, \mathbf{k}_j, \mathbf{K} - \mathbf{k} - \mathbf{k}_j), \tag{5.18}$$

so they satisfy the following integral equation,

$$M(\mathbf{k}_j) = \frac{U}{(2\pi)^D} \int_\Omega d\mathbf{k} \frac{M(\mathbf{k}) + M(\mathbf{k}_j) + M(\mathbf{K} - \mathbf{k} - \mathbf{k}_j)}{E - \epsilon(\mathbf{k}, \mathbf{k}_j, \mathbf{K} - \mathbf{k} - \mathbf{k}_j)}. \tag{5.19}$$

The single final integral equation for the Mattis functions $M(\mathbf{k}_j)$, the Mattis equation [Mat86], is then obtained by making use of the symmetry in the denominator in Eq. (5.19), so we can make the replacement $M(\mathbf{K} - \mathbf{k} - \mathbf{k}_j) \rightarrow M(\mathbf{k})$ in the numerator, obtaining

$$M(\mathbf{k}_j)[1 + I_E(\mathbf{k}_j)] = \frac{2U}{(2\pi)^D} \int_\Omega d\mathbf{k} \frac{M(\mathbf{k})}{E - \epsilon(\mathbf{k}, \mathbf{k}_j, \mathbf{K} - \mathbf{k} - \mathbf{k}_j)}, \tag{5.20}$$

where I_E is a generalized Watson's integral [Wat39] and has the form

$$I_E(\mathbf{k}_j) = -\frac{U}{(2\pi)^D} \int_\Omega d\mathbf{k} \frac{1}{E - \epsilon(\mathbf{k}, \mathbf{k}_j, \mathbf{K} - \mathbf{k} - \mathbf{k}_j)}. \tag{5.21}$$

5.1.2. Three-boson bound states on a one-dimensional lattice

Formalism. We restrict ourselves now to the case of three bosons on an infinitely long one-dimensional (1D) lattice interacting via a zero range potential of strength U, as described by the Bose-Hubbard Hamiltonian in 1D,

$$H = -J \sum_n (\hat{b}_n^\dagger \hat{b}_{n+1} + \hat{b}_{n+1}^\dagger \hat{b}_n) + \frac{U}{2} \sum_n \hat{N}_n(\hat{N}_n - 1). \tag{5.22}$$

We will use the formalism developed in the previous subsection; we work in the three-particle subspace and write the eigenfunctions in quasi-momentum representation ex-

plicitly for $D = 1$,

$$|\psi\rangle = \int_{\Omega^3} dk_1 dk_2 dk_3 \psi(k_1, k_2, k_3) |k_1, k_2, k_3\rangle, \qquad (5.23)$$

where $\Omega \equiv (-\pi, \pi]$ is the one-dimensional Brillouin zone, and where k_i is the quasi-momentum of particle i ($i = 1, 2, 3$). We saw in the previous subsection that the bound-state wave functions have the simple form

$$\psi(k_1, k_2, k_3) = -\frac{M(k_1) + M(k_2) + M(k_3)}{\epsilon(k_1) + \epsilon(k_2) + \epsilon(k_3) - E}, \qquad (5.24)$$

where $\epsilon(k) = -2J\cos(k)$ is the single particle energy band of the tight-binding lattice Hamiltonian, Eq. (5.22), while the functions M satisfy the one-dimensional Mattis equation

$$M(k)[1 + I_E(k)] = -\frac{U}{\pi} \int_{-\pi}^{\pi} dq \frac{M(q)}{\epsilon(k) + \epsilon(q) + \epsilon(K - k - q) - E}, \qquad (5.25)$$

where I_E is the one-dimensional generalized Watson's integral

$$I_E(k) = \frac{U}{2\pi} \int_{-\pi}^{\pi} dq \frac{1}{\epsilon(k) + \epsilon(q) + \epsilon(K - k - q) - E}. \qquad (5.26)$$

The Watson's integral (5.26) can be performed analytically by using contour integration [PM07]. However, with the methods already introduced in the previous chapter, we can calculate it easily by simple comparison. This is very useful in order to do numerical calculations efficiently. To this end, consider the two-boson problem on a 1D lattice with on-site interaction only. The bound state solutions, after separation of center of mass and relative coordinates, are obtained as

$$\langle k|\phi\rangle = -\frac{1}{2\cos(K/2)\epsilon(k) - E} \langle k| \hat{V} |\phi\rangle, \qquad (5.27)$$

where k is the relative momentum, ϕ is the relative wave function and K is the total quasi-momentum. After simple algebraic manipulations we arrive at the integral equation

$$1 = -\frac{U}{2\pi} \int_{-\pi}^{\pi} dk \frac{1}{2\cos(K/2)\epsilon(k) - E} \qquad (5.28)$$

for the energy E. The solutions are, of course, those obtained in coordinate space, so that the bound state energies are given by

$$E = \text{sgn}(U)\sqrt{U^2 + (4J\cos(K/2))^2}. \qquad (5.29)$$

Conversely, for Eq. (5.28) to have a solution, U must have the form

$$U = \text{sgn}(E)\sqrt{E^2 - (4J\cos(K/2))^2}. \qquad (5.30)$$

Therefore, for a general value of E, the integral in Eq. (5.28) is given by

$$\int_{-\pi}^{\pi} dk \frac{1}{2\cos(K/2)\epsilon(k) - E} = -\text{sgn}(E)\frac{2\pi}{\sqrt{E^2 - (4J\cos(K/2))^2}}. \tag{5.31}$$

By comparison, the 1D generalized Watson's integral (5.26) has the form

$$I_E(k) = -\frac{\text{sgn}[E - \epsilon(k)]U}{\sqrt{[E - \epsilon(k)]^2 - 16J^2\cos^2[(K-k)/2]}}. \tag{5.32}$$

The Mattis integral equation, Eq. (5.25), is a homogeneous Fredholm equation of the second kind with a fixed eigenvalue $\lambda = 1$. Note that it can be written formally as

$$\mathcal{K}M = \lambda M, \tag{5.33}$$

subject to $\lambda = 1$ and with the kernel $\mathcal{K}$ defined as

$$\mathcal{K}(q, k) = -\frac{U}{\pi}\frac{1}{[1 + I_E(k)][\epsilon(k) + \epsilon(q) + \epsilon(K - k - q) - E]}. \tag{5.34}$$

Therefore, Eq. (5.25) is a highly non-linear equation for the energy E for a given value of U/J and a fixed total quasi-momentum K. Note also that Eq. (5.25) does not imply $M(k)$ to be an even or odd function of k; in fact, there is no symmetry with respect to $k = 0$ unless $|K| = 0$ or $|K| = \pi$.

The numerical solution of Eq. (5.33) combines two methods. First of all, one has to solve the eigenvalue problem, therefore obtaining a set of λ's, by means of Nystrom's method [Nys30]. Then the correct solution is obtained by minimizing

$$f_E(\{\lambda\}) = |\lambda_1 - 1|, \tag{5.35}$$

with respect to E, where $\{\lambda\}$ is the set of eigenvalues of $\mathcal{K}$ for a given energy E, and λ_1 is the eigenvalue which is closest to 1 among the set.

Spectrum of the three-boson problem. Before solving Eq. (5.25), we can already describe a large part of the spectrum of three bosons interacting via on-site repulsion or attraction on a 1D lattice, since we know the full two-body spectrum in detail. First, the continuous spectrum of three scattered (unbound) bosons, with energies denoted by $E_{c3}(k_1, k_2, K - k_1 - k_2)$ is simply the sum of three single-particle energy bands,

$$E_{c3}(k_1, k_2, K - k_1 - k_2) = \epsilon(k_1) + \epsilon(k_2) + \epsilon(K - k_1 - k_2). \tag{5.36}$$

We will refer to this subset of the spectrum as the "three-body continuum". Next, there is a continuum (which we call "two-body continuum") consisting of energies which are the sum of a single particle band and a dimer (bound pair) energy. If Q is the quasi-momentum of the dimer and $k = K - Q$ is the quasi-momentum of a monomer (single particle), the energies E_{c2} in the two-body continuum are given by

$$E_{c2}(K, Q) = \text{sgn}(U)\sqrt{U^2 + [4J\cos(Q/2)]^2} - 2J\cos(K - Q). \tag{5.37}$$

There is still another part of the spectrum which is well-known and, at least in 1D, trivial. When the on-site interaction is strong enough, $|U|/J \gg 1$, three bosons occupying the same site are forced to stay together as a bound "on-site" trimer with energy $E_b \approx 3U$, since the energy required to dissociate it is approximately $|\Delta_E| \approx |3U - U| = 2|U| \gg J$. Consequently, there is a narrow band of on-site bound states with energies lying at around $3U$.
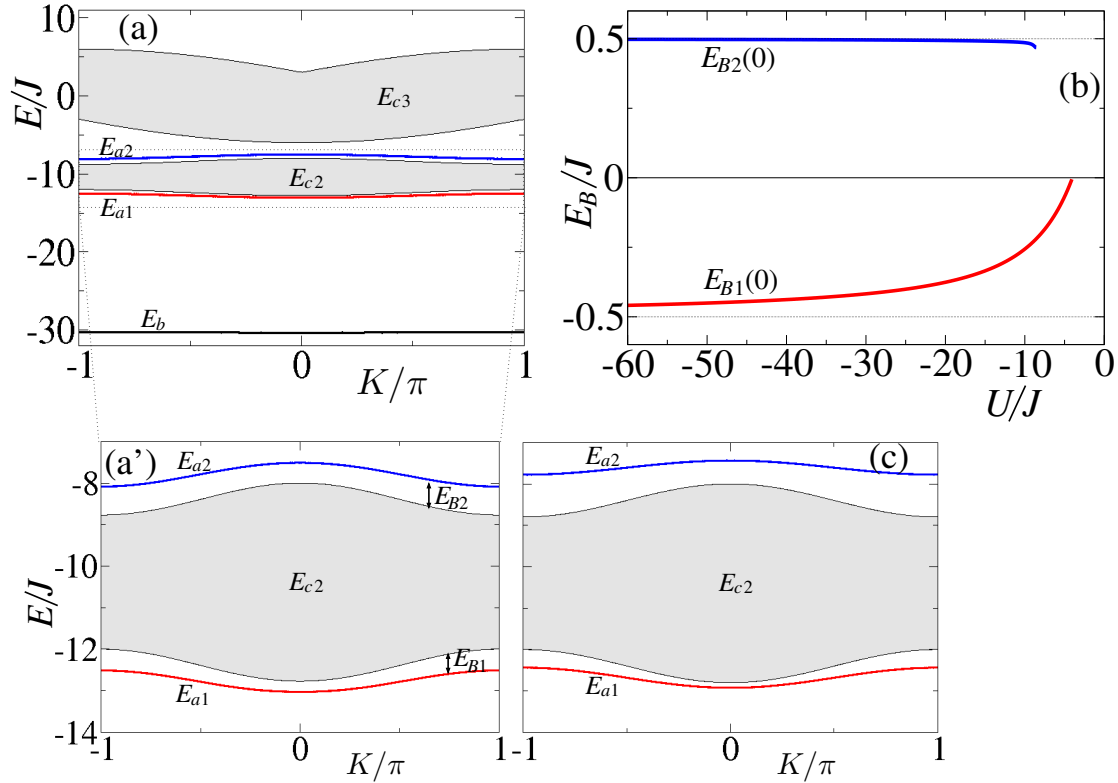

Figure 5.1.: (a) Full three-particle energy spectrum of Hamiltonian (5.22) with U=-10J, versus the total quasi-momentum K. All bound states are obtained via exact numerical solution of Eq. (5.25). (a') Magnified part of the spectrum corresponding to dimer-monomer states. (b) Binding energies E_B for the off-site (weakly bound) trimers at $K = 0$ versus the interaction strength $U < 0$. (c) Dimer-monomer spectrum of the effective Hamiltonian (5.53). The two bound states are obtained via numerical solution of Eq. (5.58).

We solve Eq. (5.25) numerically, concentrating for concreteness on the case of attractive interactions, $U < 0$. We note, however, that our results also apply to the case of repulsive interactions, since the spectrum for $U > 0$ is obtained from that for $U < 0$ by mirror reflection against the $E = 0$ axis and shifting of the quasi-momentum k_j of each particle by π, so that the total quasi-momentum is $K \to K + 3\pi \pmod{2\pi}$. The full spectrum of Hamiltonian (5.22) is shown in Fig. 5.1. Apart from the already discussed three- and two-body continua, and the band of on-site bound states, we see that two new kinds of bound states arise, with energies lying below (E_{a1}) and above (E_{a2}) the two-body continuum. We can already deduce certain properties of these states by

simply looking at the spectrum. First, these are not on-site bound states, since their energies $E_{a1(2)} \approx U + O(J)$ are very far from $E_b \approx 3U$. This means that these states must populate very little the Fock states of the form $|3_n\rangle$, so it is appropriate to call them "off-site" bound states. Next, their binding energies with respect to the two-body continuum are $E_{B1(2)} \approx \mp J/2$, which suggests that these states are composed of a dimer and a monomer weakly bound to each other. It is remarkable that the state above the two-body continuum is bound stronger than the state below the continuum. Finally, they are not the so-called Efimov trimers [Efi70, NFJG01], since their existence seems attached to $D = 3$, close to a two-body resonance (in 1D, Hamiltonian (5.22) has no resonances), and the states calculated here will be shown to persist deep in the strong coupling regime, where the Efimov effect cannot be present.

In Fig. 5.2 we show the quasi-momentum distributions $|\psi(k_1, k_2, K - k_1 - k_2)|^2$ at $K = 0$ for the three different bound states, with the on-site interaction set to $U/J = -10$, together with the reduced single particle quasi-momentum distributions ρ_K, defined as

$$\rho_K(k) = \int_{-\pi}^{\pi} dq |\psi(k, q, K - k - q)|^2. \tag{5.38}$$

As seen in the figure, the bound state below the two-body continuum has a quasi-momentum distribution which is centered at $k = 0$, resembling then the quasi-momentum distribution of an attractively bound pair [WTL$^+$06], and is weakly bound since it has a rather peaked quasi-momentum distribution. On the other hand, the bound state above the two-body continuum has a momentum distribution peaked at around $k \approx \pi$, similarly to the case of repulsively bound pairs. Hence, if the intuitive picture of these bound states as dimer-monomer pairs is valid, there must be another mechanism, apart from the on-site interaction alone, capable of binding the system together into attractively- and repulsively-bound states of a dimer and a monomer. Finally, the on-site bound states have a very flat quasi-momentum distribution, indicating that they are strongly bound, as we already saw in the full spectrum, Fig. 5.1, and by strong-coupling arguments ($E_b - E_{c2} \sim 2U$).

As can be seen from Fig. 5.1(b), where we plot the binding energies $E_{B1(2)}$ at $K = 0$, there are thresholds for the existence of full bands of the off-site bound states. For the trimer below the two-body continuum, the binding energy vanishes when $|U| \approx 4J$: at this critical value of U the trimer energy E_{a1} approaches the edge of the dimer-monomer scattering continuum $E_{c2} = -\sqrt{U^2 + 16J^2} - 2J$. On the other hand, the trimer above the two-body continuum ceases to exist already for $|U| \approx 8.5J$, since then its energy E_{a2} approaches the bottom of the three-body continuum $E_{c3} = 3\epsilon(0) = -6J$ (the two continua, E_{c2} and E_{c3}, overlap for $|U| \leq 8J$). Thus, at $K = 0$, the trimer state with energy E_{a2} starts to appear well in the strong interaction regime, while for larger K the threshold is smaller: $|U| \approx 4J$ for $|K| \to \pi$.

5.1.3. Effective theory in the strong-coupling regime

In the previous chapters, where mostly analytical expressions for the bound state energies were derived, it was only a matter of applying Peierls' substitution to the bound state energy bands and expanding them in Taylor series in order to obtain effective single-particle theories for the bound composites. Now, we want to derive an effective Hamiltonian for the dimer-monomer system which can describe to a good approxima-
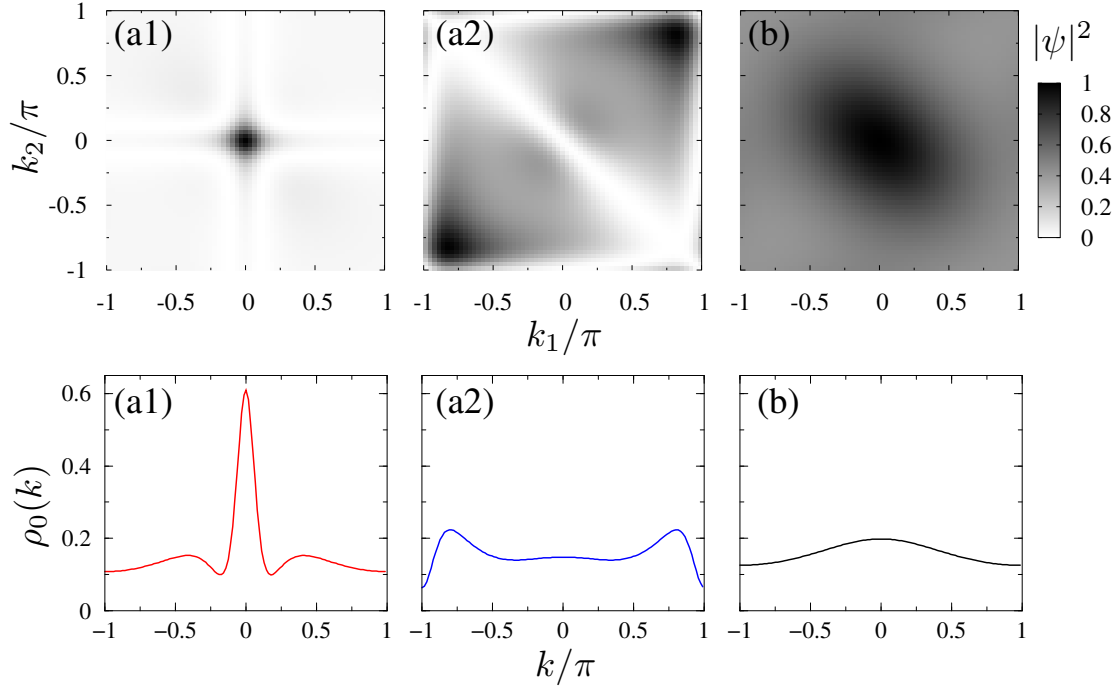
Figure 5.2.: Top panel: Quasi-momentum distributions $|\psi(k_1, k_2, K - k_1 - k_2)|^2$ of the three-particle bound states for $U = -10J$ and $K = 0$; (a1) and (a2) correspond to the off-site (weakly bound) trimers with energies below and above the two body dimer-monomer continuum, while (b) corresponds to the on-site (strongly bound) trimer. Lower panel: Reduced single-particle momentum distributions $\rho_0(k)$ for the cases of (a1), (a2), and (b).

tion the properties of the off-site bound states, as well as the scattering states of the system, in the strong interaction regime, $|U|/J \gg 1$.

The dimer-monomer effective theory. We now apply the effective strongly coupled theory outlined in Appendix A to the problem of the dimer-monomer system in a one-dimensional lattice. We split the Bose-Hubbard Hamiltonian (5.22) in the following way

$$H = H_0 + \xi V, \tag{5.39}$$

with $\xi \equiv -J$ and

$$V = \sum_n (\hat{b}_{n+1}^\dagger \hat{b}_n + \hat{b}_n^\dagger \hat{b}_{n+1}), \tag{5.40}$$

$$H_0 = \frac{U}{2} \sum_n \hat{N}_n(\hat{N}_n - 1). \tag{5.41}$$

In our case, the subspace we are interested in to derive an effective Hamiltonian consists of the unperturbed Fock states of the form

$$|n_1, n_2\rangle \equiv |2_{n_1}\rangle |1_{n_2}\rangle, \tag{5.42}$$

with $n_1 \neq n_2$. For the first order correction given in Eq. (A.13) we need

$$\langle 2_{m_1} 1_{m_2} | \, V \, | 2_{n_1} 1_{n_2} \rangle = \langle 2_{m_1} 1_{m_2} | \, [(\hat{b}^\dagger_{n_1+1} + \hat{b}^\dagger_{n_1-1})\hat{b}_{n_1} + (\hat{b}^\dagger_{n_2+1} + \hat{b}^\dagger_{n_2-1})\hat{b}_{n_2}] \, | 2_{n_1} 1_{n_2} \rangle, \quad (5.43)$$

obtaining the effective Hamiltonian to first order

$$H^{(1)}_{\text{eff}} = H_1 + H_{\text{ex}}, \quad (5.44)$$

with

$$H_1 = -J \sum_{n_1 \neq n_2} [\, |2_{n_1} 1_{n_2+1}\rangle(1 - \delta_{n_1,n_2+1}) + |2_{n_1} 1_{n_2-1}\rangle(1 - \delta_{n_1,n_2-1})]\langle 2_{n_1} 1_{n_2}|, \quad (5.45)$$

and

$$H_{\text{ex}} = -2J \sum_{n_1 \neq n_2} |2_{n_2} 1_{n_1}\rangle(\delta_{n_1+1,n_2} + \delta_{n_1-1,n_2})]\langle 2_{n_1} 1_{n_2}|. \quad (5.46)$$

We define now creation and annihilation operators for the dimer ($\hat{c}$, $\hat{c}^\dagger$) and monomer ($\hat{a}$, $\hat{a}^\dagger$) as [PSAF07]

$$\hat{c}_n = \frac{1}{\sqrt{2(\hat{N}_n + 1)}}(\hat{b}_n)^2(\hat{N}_n - 1)(3 - \hat{N}_n), \quad (5.47)$$

$$\hat{c}^\dagger_n = (\hat{N}_n - 1)(3 - \hat{N}_n)(\hat{b}^\dagger_n)^2 \frac{1}{\sqrt{2(\hat{N}_n + 1)}}, \quad (5.48)$$

$$\hat{a}_n = \hat{b}_n \frac{(2 - \hat{N}_n)(3 - \hat{N}_n)}{2}, \quad (5.49)$$

$$\hat{a}^\dagger_n = \frac{(2 - \hat{N}_n)(3 - \hat{N}_n)}{2}\hat{b}^\dagger_n, \quad (5.50)$$

which can be verified to obey the bosonic commutation relation. Indeed,

$$[\hat{c}_n, \hat{c}^\dagger_m] \, |\psi_D\rangle = \delta_{n,m} \, |\psi_D\rangle, \quad (5.51)$$

$$[\hat{a}_n, \hat{a}^\dagger_m] \, |\psi_M\rangle = \delta_{n,m} \, |\psi_M\rangle, \quad (5.52)$$

where $|\psi_D\rangle = \sum_n f^D(n) \, |2_n\rangle$ and $|\psi_M\rangle = \sum_n f^M(n) \, |1_n\rangle$. If they act on any ket which does not belong to their subspace, they map it onto the zero vector. We also define the number operators $\hat{N}^D_n \equiv \hat{c}^\dagger_n \hat{c}_n$ and $\hat{N}^M_n \equiv \hat{a}^\dagger_n \hat{a}_n$.

With the above definitions, and after carrying out the calculation of the second order correction to the unperturbed Hamiltonian, we arrive at the effective dimer-monomer Hamiltonian,

$$H_{\text{eff}} = H_1 + H_2 + H_{\text{int}}, \quad (5.53)$$

where H_1 reads

$$H_1 = -J \sum_n (\hat{a}^\dagger_n \hat{a}_{n+1} + \text{H.c.}), \quad (5.54)$$

describing the kinetic energy term of the monomer with single particle energy band $\epsilon(k)$;

$$H_2 = \mathcal{E}^{(2)} \sum_n \hat{N}^D_n - J^{(2)} \sum_n (\hat{c}^\dagger_{n+1} \hat{c}^\dagger_n + \text{H.c.}) \quad (5.55)$$

is the dimer internal energy, $\mathcal{E}^{(2)} = U - 2J^{(2)}$, with the second order tunneling rate $J^{(2)} = -2J^2/U$ giving rise to the single dimer Bloch band $\epsilon^{(2)}(Q) = -2J^{(2)}\cos(Q)$; and finally,

$$H_{\text{int}} = V^{(2)} \sum_n \hat{N}_n^D \hat{N}_{n\pm1}^M - W \sum_n (\hat{c}_{n+1}^\dagger \hat{c}_n \hat{a}_n^\dagger \hat{a}_{n+1} + \text{H.c.}) \tag{5.56}$$

describes effective short-range interactions between the dimer and the monomer, including a weak repulsive (or attractive, if $U > 0$) nearest-neighbor interaction $V^{(2)} = -7J^2/2U$, and an exchange interaction with the rate $W = 2J$. We emphasize here that a hard-core on-site interaction between the dimer and monomer is assumed.

In Fig. 5.1(c) we plot the spectrum of the effective Hamiltonian (5.53). It involves a two-body scattering continuum, with the energy given by the sum of the energies of (asymptotically) free dimer and monomer,

$$E_{c2} = [U - 2J^{(2)}] - 2J^{(2)}\cos(Q) - 2J\cos(K - Q), \tag{5.57}$$

and two bound states with energies E_{a1} and E_{a2} below and above E_{c2}. These effective dimer-monomer bound states are obtained using the stationary Schrödinger equation for the two-body wavefunction $\Psi(Q, k)$ in quasi-momentum space, which leads to the integral equation

$$\Psi(Q, k) = -\frac{1}{2\pi} \int_{-\pi}^{\pi} dq \frac{U_{12} + V_{\text{C}}(Q, q) + V_{\text{S}}(Q, q)}{\mathcal{E}^{(2)} + \epsilon^{(2)}(q) + \epsilon(K - q) - E} \Psi(q, k), \tag{5.58}$$

where $K = Q + k$ is the total quasi-momentum of the system, and

$$V_C(Q, q) = [2V^{(2)}\cos(q) - 4J\cos(K - q)]\cos(Q) \tag{5.59}$$

$$V_S(Q, q) = [2V^{(2)}\sin(q) - 4J\sin(K - q)]\sin(Q). \tag{5.60}$$

We have included an artificial on-site interaction $U_{12} \to \infty$ to impose the hard-core condition on Hamiltonian (5.53). It is possible to reduce Eq. (5.58) to a non-linear equation for the energy E by making use of the properties of the free lattice Green's functions. However, the resulting equation is rather cumbersome and we omit it here. After solving Eq. (5.58) numerically, we obtain the two bands of bound states E_{a1} and E_{a2} of Fig. 5.1(c). Comparison with Fig. 5.1(a') reveals good qualitative agreement with the exact spectrum of the three-body problem. The energies of the two-body continuum are very well reproduced, while the bound state energies differ quantitatively from those obtained by the exact Hamiltonian (5.22). These differences are associated with the internal structure of the dimer, which is not accounted for by the effective model. However, the discrepancies disappear progressively with increasing value of the on-site interaction, as second order perturbation theory becomes more accurate.

There are two special but important cases for which the bound states of the effective model can be calculated analytically. These correspond to the dimer-monomer system having total quasi-momentum $K = 0$ or $K = \pi$. We seek the eigenstates $|\Psi\rangle$ of Hamiltonian (5.53) in position space,

$$|\Psi\rangle = \sum_{n_1 \neq n_2} \Psi(n_1, n_2) |n_1, n_2\rangle, \tag{5.61}$$

5. The three-body problem

where we have redefined $|n_1\rangle \equiv |1^D_{n_1}\rangle$ and $|n_2\rangle \equiv |1^M_{n_2}\rangle$. We can map the resulting difference equation into a one-body problem by using the ansatz we introduced in the previous chapter for distinguishable particles with different masses,

$$\Psi(n_1, n_2) = e^{iK(n_1+n_2)/2}e^{-i\beta_K z}\phi_K(z), \tag{5.62}$$

with $z \equiv n_1 - n_2$ the dimer-monomer relative distance, and

$$\tan(\beta_K) = \frac{J - J^{(2)}}{J + J^{(2)}} \tan\left(\frac{K}{2}\right). \tag{5.63}$$

After separation of coordinates, and using the hardcore condition $\phi_K(0) = 0$, we obtain the one-body difference equation

$$\bar{J}_K \phi_K(\pm 2) + W_K \phi_K(\mp 1) + [\bar{E} - V^{(2)}]\phi_K(\pm 1) = 0,$$
$$\bar{J}_K[\phi_K(z+1) + \phi_K(z-1)] + \bar{E}\phi_K(z) = 0, \tag{5.64}$$

with $|z| > 1$, $\bar{J}_K \equiv \sqrt{J^2 + (J^{(2)})^2 + 2JJ^{(2)}\cos(K)}$, $W_K \equiv W\cos(K)$, and $\bar{E} \equiv E - \mathcal{E}^{(2)}$.

The bound solution is obtained by applying the exponential ansatz

$$\phi_K^{(\mathcal{P})}(z \neq 0) = [\text{sgn}(z)]^{(1-\mathcal{P})/2}\alpha_K^{|z|-1}, \tag{5.65}$$

where $\mathcal{P} = \pm 1$ is the parity of the state ($\mathcal{P} = 1$ for symmetric and $\mathcal{P} = -1$ for antisymmetric ϕ_K). The solution of the resulting equation yields

$$\alpha_K^{(\mathcal{P})} = -\frac{\bar{J}_K}{V^{(2)} - \mathcal{P}W_K}, \tag{5.66}$$

with the energy given by the usual expression $E - \mathcal{E}^{(2)} = -\bar{J}_K(1 + \alpha_K^2)/\alpha_K$. In the limit of infinitely strong interaction, $|U|/J \to \infty$, second order perturbation theory is exact, and predicts limiting values of the binding energies below and above the two-body continuum, being $E_{b,\infty} = \mp J/2$, as can be inferred from Fig. 5.1 at large values of the interaction $|U|/J$.

We now show how, without the exchange interaction, it is not possible to have bound states in the range of validity of the effective Hamiltonian, but even if it were possible, we could not explain the existence of a second bound state. To see this, assume the hypothetical situation of no exchange term, $W = 0$. Then, the problem becomes that of two hard-core bosons in the extended Hubbard model (though with a collective tunneling rate $\bar{J}_K \neq 2J\cos(K/2)$) discussed in full detail in chapter 4. The only possible bound state would be $\phi_K = \alpha_K^{|z|-1}$, with

$$\alpha_K = \frac{\bar{J}_K}{V^{(2)}}. \tag{5.67}$$

However, $|\alpha_K| < 1$ if and only if $|U|/J < 3/2$ for $K = 0$ and $|U|/J < 11/2$ for $K = \pi$. Since the effective Hamiltonian can only be valid for $|U|/J > 8$ – the value that defines when the three- and two-body continua overlap and no adiabatic elimination is sensible – there can be no bound states at all if the exchange is not present. Moreover, as we

have already noted, the model without exchange cannot describe the presence of a bound state located below (for $U < 0$) the scattering continuum of Hamiltonian (5.53). We therefore can conclude that the off-site bound states arise due to the effective exchange of a particle, with the rate $2J$, when the bound pair and the "free" particle are close to each other.

5.2. Scattering states

Quantum collision theory, on and off the lattice, for three particles does not differ much from that for two particles [Joa75]. However, the inclusion of a third particle is by no means trivial. In most cases, there are no analytical solutions of the three-body problem, however with notable exceptions, such as the Bethe ansatz-solvable models we discussed in the beginning of this chapter.

On a one dimensional lattice with soft-core pairwise interactions, and due to the equivalence between attractive and repulsive interactions,[2] there is not a single scattering problem that can be dealt with exactly in a simple manner[3], since two-body bound states (above or below the continuum) are always present and, unavoidably, have to appear as one of the "products" of scattering whenever the energy of the incident wave is sufficiently large to form bound states. Moreover, the scattering of a dimer and a monomer on a lattice, even in 1D, has not been studied rigorously to the date of writing. Therefore approximate methods to study three-body collisions, allowing a physical understanding of the results, are needed.

Here we present an approximate solution to the elastic scattering of a bound pair and an unbound third boson on a 1D lattice in the strong coupling regime for two special cases for which the scattering problem is exactly solvable. Therefore, we make use of the effective Hamiltonian (5.53) of the previous section, qualitatively valid for $|U|/J > 8$. The two cases are those which appeared to be exactly solvable for the bound state problem, that is, for total quasi-momenta $K = 0$ and $K = \pi$. We restrict ourselves from now on to these two special values. We have an effective problem where the two particles involved are distinguishable, and therefore we can now study the proper scattering problem of an incident wave scattered off a potential which includes exchange. First of all, we realize that the parity is conserved, so we can solve first for antisymmetric and symmetric eigenfunctions, and we will then use them to construct the scattering "experiment", and calculate the reflection and transmission rates.

The symmetric scattering eigenfunctions ϕ_K^S of Hamiltonian (5.53) have the form

$$\phi_K^S(z) = \cos(k|z| + \delta_S), \tag{5.68}$$

for $|z| \neq 0$, together with the hard-core condition $\phi_K^S(0) = 0$. After tedious but simple algebra we obtain the symmetric phase shift δ_S,

$$\tan \delta_S = \frac{\bar{J}_K \cos(2k) + (W_K + \bar{E} - V^{(2)}) \cos(k)}{\bar{J}_K \sin(2k) + (W_K + \bar{E} - V^{(2)}) \sin(k)}, \tag{5.69}$$

---

[2]See subsect. 2.7.

[3]Not even in a complicated one.

where the scattering energies are given by

$$\bar{E} = -2\bar{J}_K \cos(k). \tag{5.70}$$

The antisymmetric wave functions are constructed similarly, as

$$\phi_K^A(z) = \text{sgn}(z)\cos(k|z| + \delta_A), \tag{5.71}$$

which obviously yield the same eigenenergies, Eq. (5.70), and the antisymmetric phase shift has the form

$$\tan\delta_A = \frac{\bar{J}_K\cos(2k) + (-W_K + \bar{E} - V^{(2)})\cos(k)}{\bar{J}_K\sin(2k) + (-W_K + \bar{E} - V^{(2)})\sin(k)}. \tag{5.72}$$

In order to obtain wave functions that consist of incident, transmitted and reflected waves, we consider the eigenstates which are superpositions of symmetric and antisymmetric wave functions,

$$\phi_K(z) \propto \cos(k|z| + \delta_S) + B\text{sgn}(z)\cos(k|z| + \delta_A)$$
$$= \left[e^{i\delta_S} + B\text{sgn}(z)e^{i\delta_A}\right]e^{ik|z|} + \left[e^{-i\delta_S} + B\text{sgn}(z)e^{i\delta_A}\right]e^{-ik|z|}. \tag{5.73}$$

Requiring the wave function for $z > 0$ to be the transmitted wave, we impose the condition

$$B = -e^{-i(\delta_S - \delta_A)}, \tag{5.74}$$

so that the final wave function has the form

$$\phi_K(z > 0) = te^{ikz}, \tag{5.75}$$
$$\phi_K(z < 0) = e^{ikz} + re^{ikz}, \tag{5.76}$$

where the reflection and transmission coefficients are given by

$$t = \frac{1}{2}\left[e^{2i\delta_S} - e^{2i\delta_A}\right], \tag{5.77}$$
$$r = \frac{1}{2}\left[e^{2i\delta_S} + e^{2i\delta_A}\right]. \tag{5.78}$$

One immediately realizes that the coefficients are normalized so that the sum of transmission (T) and reflection (R) probabilities is unity, $T + R \equiv |t|^2 + |r|^2 = 1$, with T and R given by the expressions

$$T \equiv |t|^2 = \sin^2(\delta_S - \delta_A), \tag{5.79}$$
$$R \equiv |r|^2 = \cos^2(\delta_S - \delta_A). \tag{5.80}$$

Therefore, the transmission will be maximal when the difference between the symmetric and antisymmetric phase shifts is close to $\pm\pi/2$. In Fig. 5.3 we plot the transmission and reflection probabilities as functions of the relative quasi-momentum k, for the value $U/J = -10$ at total quasi-momenta $K = 0$ and $K = \pi$. We observe that full transmission is never obtained, but rather high transmission probabilities can be achieved at relative momenta close to $\pi/2$. We have checked (numerically) that there can never be

complete transmission with U/J in the range of validity of the model, contrary to the conclusions obtained in [JCS09], where the authors did not derive a consistent effective Hamiltonian to second order in J/U, and seemingly replaced the exchange rate $W = 2J$ by the (incorrect) value of $W = J$.
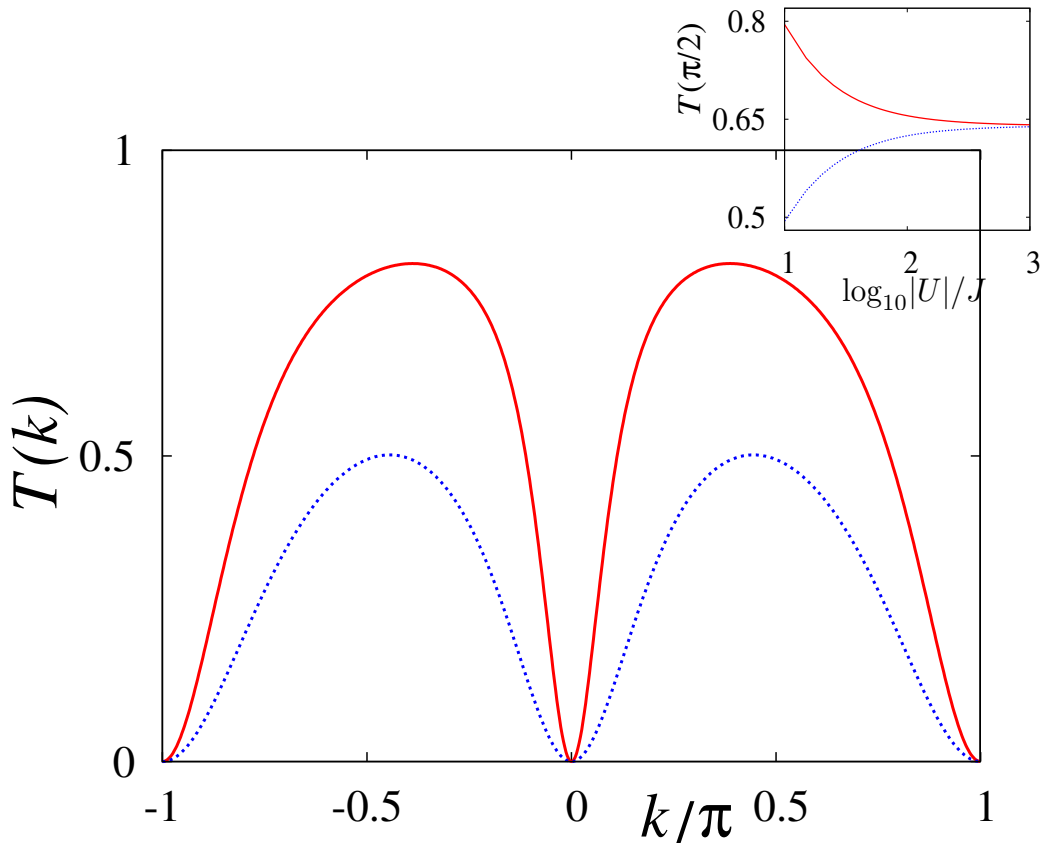

Figure 5.3.: Transmission probabilities for a monomer colliding with a dimer in the effective model with $U/J = -10$; $K = 0$ corresponds to solid line and $K = \pi$ to dotted line.

5.3. Conclusions and outlook

In this chapter we have studied the three-boson problem on a one-dimensional lattice in detail. We have shown that, for strong interactions, two types of non-trivial bound states essentially composed of a dimer and a monomer exist for any value of the total three-body quasi-momentum. One of these states appears to have the "wrong" binding energy: above (below) the relevant continuum for attractive (repulsive) interactions, showing a quasi-momentum distribution according to this binding. We have explained the nature of these bound states as a consequence of an effective exchange interaction between dimer and monomer in the strong coupling regime. Moreover, these states have asymptotic, universal binding energies in the limit of very large on-site interaction.

5. The three-body problem

The universal binding energies are equal, in absolute value, to half the single-particle hopping rate.

We have also studied the exact scattering properties of the dimer-monomer system in our strong coupling effective theory. Our results prove that dimer-monomer scattering cannot be resonant, that is, no full transmission of a monomer through a dimer (or conversely) can happen. This is contrary to what was incorrectly predicted in [JCS09].

The next natural step in the three-body problem on the lattice is the systematic study of the Efimov effect. Efimov states were proven, numerically, to exist on a 3D lattice by Rudin and Mattis [RM84]. More rigorously, Lakaev and collaborators proved, mathematically, that the Efimov effect occurs on a 3D lattice loaded with three short range interacting bosons, and estimated the spectrum asymptotics [LM03, ALM04, ADL07]. However, there is neither quantitative nor physical understanding of the Efimov effect on the lattice. More dramatically, the case of finite quasi-momentum in some (one or two) of the three directions of the lattice, which is equivalent to certain degree of anisotropy, has not been studied, and should reveal even more exotic states than we have so far observed. As a last remark I would like to launch a rather exotic question: is there a three-magnon Efimov effect in a real material?

6. Collision theory on a model superlattice

Superlattices are superpositions of two or more lattices with different periods. The interplay between the different subperiods of the new system gives rise to what is known as mini-bands – splitting of the original bands of the problem.

In semiconductor physics, superlattices are formed by periodically arranged layers of semiconducting materials with different band gaps [ET70]. Upon application of a static electric field, superlattices can show resonant tunneling effects of an electron from one mini-band to the other or Bloch oscillations due to the Wannier-Stark ladder [Wan60],[1] depending on the relative strength of the electric field with respect to the gap between the mini-bands.

For cold atoms, superlattices can be formed by superimposing two optical lattices with different periods [PPT$^+$03]. The resulting system can have a whole range of subperiods and, consequently, a richer mini-band structure compared to that achievable with semiconductors.

The theory of ultracold atoms in optical superlattices and strongly correlated electrons in superlattice structures is currently attracting much interest [RMO06, RAR$^+$06, BPH$^+$07, CLH$^+$08, HR09, TNB09], since the periodicity of the superlattice gives rise to new and striking correlated quantum phases and quantum phase transitions.

Optical superlattices can be used to prepare and detect certain phases not achievable with homogeneous optical lattices. The phenomenon of d-wave Cooper pairing with ultracold fermionic gases loaded in an optical superlattice, which may be of relevance to the physics of high-T_c superconductors, might be observed in this system [RSF$^+$09]. Moreover, a scheme for producing magnetic quantum phases with cold spinor gases in a superlattice has been recently proposed [RGB$^+$07].

One-dimensional tight-binding superlattice Hamiltonians describe the transmission of microwaves through long arrays of scatterers (micrometer screws) inserted in a waveguide. In [KS98], the authors were able to experimentally observe the Hofstadter butterfly [Hof76], the fractal spectrum of Harper's equation describing the single-particle Schrödinger equation on a superlattice.

From a purely theoretical point of view, and given the success in solving the one-dimensional lattice many-fermion problem [LW68] and the Heisenberg model [KM97] by means of the Bethe ansatz, one may be tempted to proceed to the solution of the many-body problem on the simplest possible tight-binding superlattice with a period of twice the natural lattice period. But even before that, it is necessary to understand a much simpler, yet important problem, which is that of a single particle colliding with a fixed impurity on a superlattice. This problem is closely related to "dimerized" fermionic systems,[2] which arise as a consequence of the so-called Peierls' instability [Pei55, KL87] in one dimensional crystals.

---

[1] See subsect. 3.2.1.

[2] The non-interacting Hamiltonians of the dimerized and superlattice models have identical band structures.

In this chapter we give the exact solution of the problem of a single particle scattering off and binding to a single immobile impurity where the interaction is given by a zero range potential. We find that a simple modification of the usual (homogeneous lattice) solutions, involving periodic modulation of the scattering and bound state wave functions, is sufficient to obtain the full spectrum and eigenstates of the system. But contrary to the flat lattice case, for any parameters of the system there are two bound states, one of which lying in the band gap and the other one outside of it. These interesting solutions can serve as conceptual building blocks for the more important cases of two- and many-body physics on a superlattice. Our findings can be observed with standard experimental techniques in microwave scattering in waveguides [KS98] or with ultracold atoms in optical superlattices.

6.1. The free particle

In the tight-binding approximation, the Hamiltonian H_0 of a period-τ ($\in \mathbb{Z}$) superlattice acting on a wave function ψ is defined through

$$(H_0\psi)(n) = (\hat{T}\psi)(n) + \lambda \cos\left(\frac{2\pi}{\tau}n\right)\psi(n), \tag{6.1}$$

where $\hat{T}$ is the discrete kinetic energy operator, Eq. (2.34), and we set, by convention, $\lambda > 0$. Since the superlattice Hamiltonian is periodic, we can apply Bloch's theorem [AM76] and the eigenfunctions of H_0 can be written as

$$\psi(n) = e^{ikn}\phi_k(n), \tag{6.2}$$

where $\phi_k(n + \tau) = \phi_k(n)$ has the periodicity of the superlattice, and k is the particle's quasi-momentum.[3] The periodicity of ϕ_k allows one to perform exact calculations for superlattice band structures even for very large periods, since for each value of the quasi-momentum k one can simply diagonalize the Hamiltonian with periodic boundary conditions for ϕ_k. This can be seen more clearly in quasi-momentum representation. Applying the canonic transformation $n \to i\partial_k$ – the inverse Peierls' substitution – we obtain the transformed Hamiltonian

$$H_0\left|k\right\rangle = \epsilon(k)\left|k\right\rangle + \frac{\lambda}{2}\left(\left|k + \frac{2\pi}{\tau}\right\rangle + \left|k - \frac{2\pi}{\tau}\right\rangle\right), \tag{6.3}$$

from which we see that the potential operator couples $\left|k\right\rangle$ with only a finite number (2) of other states. This means that in order to solve the eigenvalue problem exactly, we need to diagonalize a finite matrix for each value of the quasi-momentum.

6.1.1. The simplest superlattice: three solutions

The simplest possible superlattice is the one with period $\tau = 2$, which is sketched in Fig. 6.1. For the rest of this chapter, we will deal exclusively with this model, for which

---

[3]This quasi-momentum is *not* the same quasi-momentum used in the previous chapters, but should, strictly speaking, be called quasi- quasi-momentum. In a discrete theory it plays the role of a quasi-momentum while the usual quasi-momentum plays the role of the true momentum.

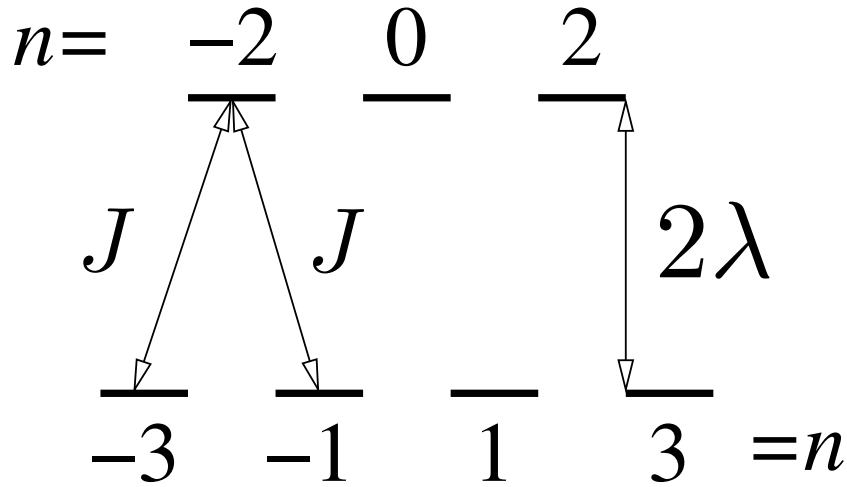mostly exact analytical solutions can be obtained.

Figure 6.1.: Sketch of the tunneling and potential with period $\tau = 2$ for Hamiltonian (6.1).

We begin with the free particle problem. There are at least three different ways of solving the stationary Schrödinger equation $H_0 |\psi\rangle = E |\psi\rangle$. We start from the one that makes use of Bloch's theorem explicitly. Assume $\psi(n) = \exp(ikn)\phi_k(n)$, with $\phi_k(n+2) = \phi_k(n)$, and the Schrödinger equation becomes

$$-J(e^{ik}\phi_k(n+1) + e^{-ik}\phi_k(n-1)) + \lambda(-1)^n\phi_k(n) = E(k)\phi_k(n). \tag{6.4}$$

Since $\phi_k(n+1) = \phi_k(n-1)$, we have

$$-2J\cos(k)\phi_k(n+1) + \lambda(-1)^n\phi_k(n) = E(k)\phi_k(n). \tag{6.5}$$

We set $n = 0$ and take $\phi_k(0) = 1$ since its value is arbitrary. We then obtain the relation

$$\phi_k(1) = -\frac{E(k) - \lambda}{2J\cos(k)}, \tag{6.6}$$

and by setting $n = 1$ we get

$$\phi_k(1) = -\frac{2J\cos(k)}{E(k) + \lambda}, \tag{6.7}$$

by solving the set of two equations we obtain for the energy

$$E_s(k) = (-1)^s\sqrt{(2J\cos(k))^2 + \lambda^2}, \tag{6.8}$$

with $s = 1, 2$, which shows explicitly that the model we are dealing with has two bands. Note that the two bands are "mirror symmetric", that is, $E_1(k) = -E_2(k)$.

We can solve the Schrödinger equation in a much more elegant way which, however,

lacks generality and can only be applied to the present model. First note that the superlattice potential $V(n) = \lambda(-1)^n$ anticommutes with the kinetic energy operator, $\{V, \hat{T}\} = 0$. By squaring the Hamiltonian we then obtain

$$H_0^2 = \hat{T}^2 + V^2 + \{V, \hat{T}\} = \hat{T}^2 + \lambda^2, \tag{6.9}$$

and, since the eigenvalues of the kinetic energy squared are $(2J\cos(k))^2$, we immediately see that the eigenvalues of H_0 are given by (6.8) as they should.

The third method to obtain the eigenstates of the superlattice Hamiltonian is, perhaps, the most useful, since introducing interactions within this method is usually simpler, especially in higher (two or three) dimensions. We diagonalize the Hamiltonian now in quasi-momentum space. As was discussed in the previous subsection, the superlattice potential (which is off-diagonal in quasi-momentum space) only couples $|k\rangle$ with $|k + \pi\rangle = |k - \pi\rangle$. We diagonalize H_0 in the basis $\{|k\rangle, |k + \pi\rangle\}$ for each value of the quasi-momentum k. The eigenfunctions are given by

$$|s, k\rangle \equiv |\psi_{s,k}\rangle = \frac{\lambda}{E_s(k) - \epsilon(k)} |k\rangle + |k - \pi\rangle = \frac{E_s(k) + \epsilon(k)}{\lambda} |k\rangle + |k - \pi\rangle, \tag{6.10}$$

where $s = 1, 2$ labels the two bands, E_s is given by Eq. (6.8) and $\epsilon(k) = -2J\cos(k)$ is the usual single-particle Bloch band in a flat lattice.

When there is no superlattice potential (if $\lambda \equiv 0$), all single-particle properties are periodic, in quasi-momentum space, with the period (2π) of the first Brillouin zone $\Omega = (-\pi, \pi]$. The superlattice induces what we can call Brillouin *subzones* (BsZ).[4] We see that all properties of the eigenstates of the superlattice Hamiltonian are invariant under a quasi-momentum translation $k \to k \pm \pi$: $E_s(k \pm \pi) = E_s(k)$ and $|s, k \pm \pi\rangle = |s, k\rangle$ (up to a normalization constant). Therefore we define the first Brillouin subzone of the period-2 superlattice as the interval $\Omega_{1\text{BsZ}} = (-\pi/2, \pi/2]$ and the second Brillouin subzone as $\Omega_{2\text{BsZ}} = (-\pi, -\pi/2] \cup (\pi/2, \pi]$.

The eigenfunctions (6.10), after normalization, take the form

$$|s, k\rangle = A_s(k) \left(\frac{E_s(k) + \epsilon(k)}{\lambda} |k\rangle + |k - \pi\rangle \right), \tag{6.11}$$

where the normalization constant $A_s(k)$ is given by

$$A_s(k) = \frac{1}{\sqrt{1 + \left(\frac{E_s(k) + \epsilon(k)}{\lambda}\right)^2}}. \tag{6.12}$$

It is easy to check that two states from the same band with different quasi-momenta are orthogonal, and that any two states from different bands are also orthogonal, so we have

$$\langle s, q | s', k \rangle = \delta_{s,s'} \delta(q - k). \tag{6.13}$$

We discuss now two important cases, namely, the limits of small and large gap $\Delta_G = $

---

[4]These play the role of Brillouin zones in discrete theories, while the actual Brillouin zone Ω plays the role of $\mathbb{R}$.

2λ. If the gap is large, $\lambda \gg J$, then the eigenenergies (6.8) are approximately given by

$$E_s(k) \approx (-1)^s \left[\lambda + \frac{(\epsilon(k))^2}{2\lambda} \right], \tag{6.14}$$

and their associated wave functions (6.10) are approximated by

$$|s,k\rangle \approx B_s(k) \left[\left((-1)^s + \frac{\epsilon(k)}{\lambda} \right) |k\rangle + |k-\pi\rangle \right], \tag{6.15}$$

with $B_s(k)$ a normalization constant. We observe that when the gap is large, the eigenstates of H_0 are essentially a superposition of $|k\rangle$ and $|k-\pi\rangle$ with equal weights, and the energy bands are flat – they almost do not vary as a function of k. In Fig. 6.2 we compare the approximate band structure (6.14) with the exact one, Eq. (6.8).

For a small gap, $\lambda \ll J$, the energies can be expanded as

$$E_s(k) \approx (-1)^s \frac{2(\epsilon(k))^2 + \lambda^2}{2|\epsilon(k)|}. \tag{6.16}$$

As can be observed in Fig. 6.3, the concept of Brillouin zones is then very useful: we can interpret the small gap limit as a single energy band with a discontinuity (gap) of magnitude Δ_G at the edges of the first BsZ $k = \pm\pi/2$.
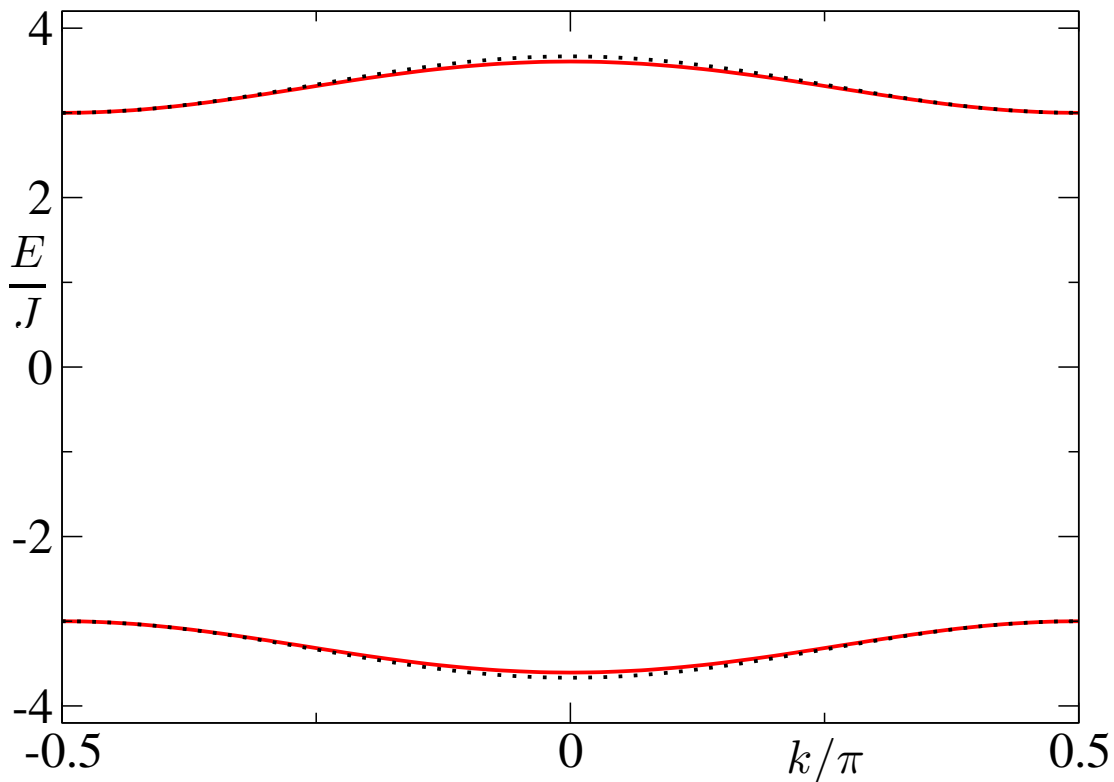

Figure 6.2.: The exact band structure (solid lines) for $\lambda/J = 3$ and the approximation (dots), Eq. (6.14).
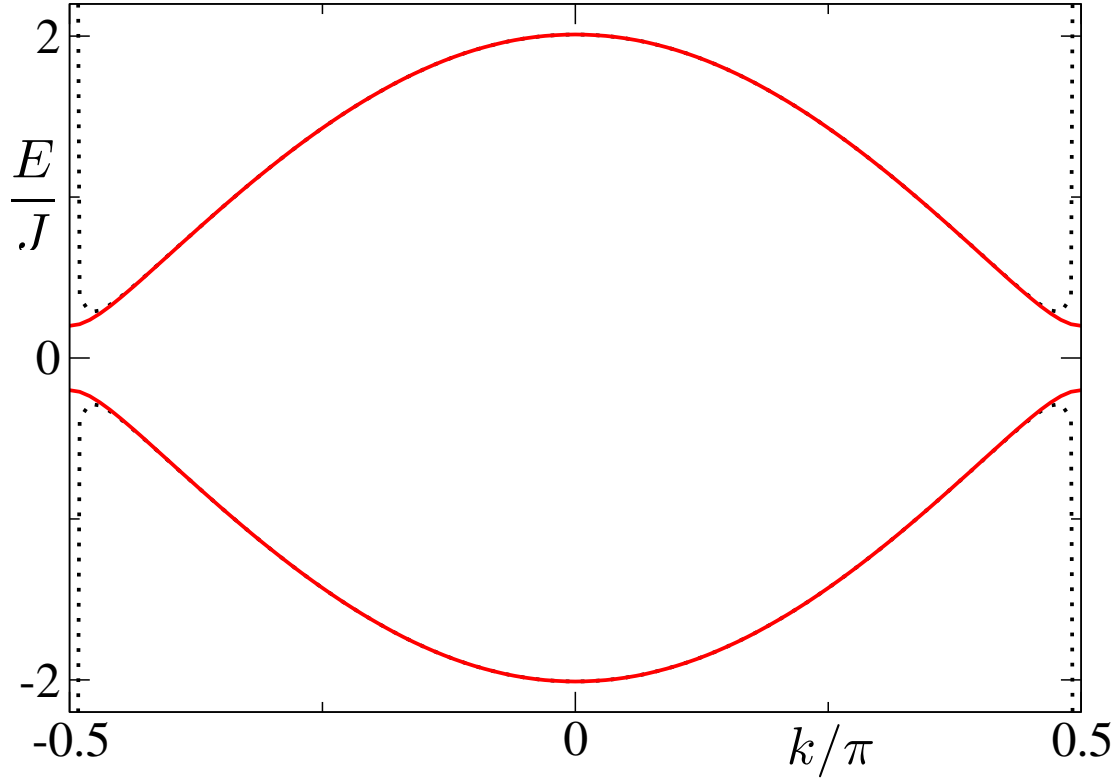
Figure 6.3.: The exact band structure (solid lines) for $\lambda/J = 1/5$ and the approximation (dots), Eq. (6.16).

The effective mass of a single particle in the s-th band of the superlattice is given by

$$m_s^* = \hbar^2 \left[\frac{\partial^2 E_s(k)}{\partial k^2} \right]_{k=0}^{-1} = (-1)^{s+1} \hbar^2 \sqrt{\left(\frac{\lambda}{4J^2} \right)^2 + \frac{1}{4J^2}}, \qquad (6.17)$$

which is positive for the lower band and negative for the upper band. As can be observed in Fig. 6.4, the effective mass is approximately constant and equal to the case of no superlattice for $\lambda \ll J$, while for large λ it grows (in absolute value) linearly with increasing the magnitude of the gap. This essentially means that the larger the gap, the slower the low-energy dynamics of a single particle on the superlattice, as expected. Moreover, hopping between nearest neighbors is suppressed while second-order tunneling is slow but resonant.

6.2. The single impurity problem on the superlattice

We consider now the simplest interacting problem for a particle on the period-2 super-lattice, corresponding to its collision with a single localized impurity. The impurity is assumed to be an infinitely heavy particle (with zero tunneling rate), located at a fixed lattice position. The impurity and the mobile particle interact via a zero range potential. Moreover, since the two bands of the superlattice are mirror symmetric, we can assume,
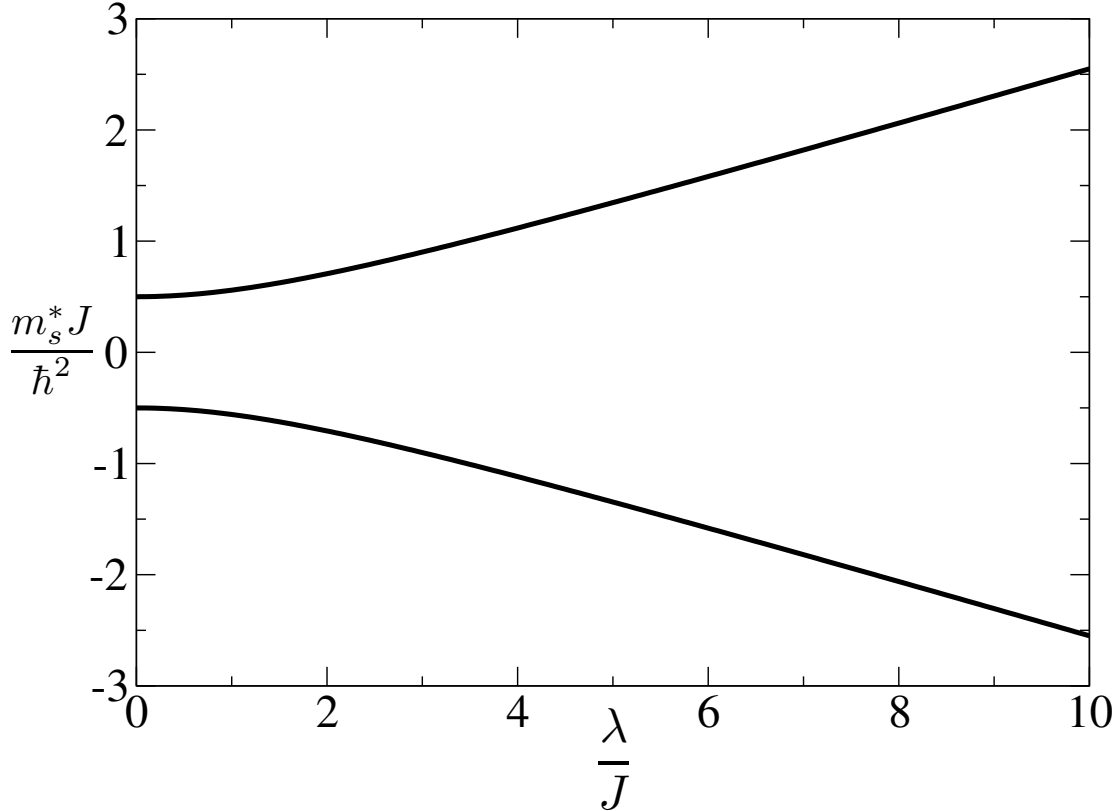
Figure 6.4.: Effective mass of a particle in the $\tau = 2$ superlattice. The upper branch corresponds to $s = 1$ (lower band) and the lower branch to $s = 2$ (upper band).

without loss of generality, that the impurity is located at the centre of the lattice (in our convention, it lies at a site with $v(0) = +\lambda$). Therefore the new Hamiltonian has the form

$$H = H_0 + U \, |0\rangle\langle 0| \,, \tag{6.18}$$

where H_0 is the single particle Hamiltonian of the superlattice with $\tau = 2$, Eq. (6.1), and U is the particle-impurity interaction, which can be attractive or repulsive.

6.2.1. Bound states

Bound states in quasi-momentum representation. We first treat the problem in the quasi-momentum representation, for which the extension to higher dimensions is easier. The discrete Fourier transform (DFT) of H_0 is given by Eq. (6.3), and the DFT of the potential $\hat{V} \equiv U \, |0\rangle\langle 0|$ provides its action in k-space

$$\hat{V} \, |k\rangle = \frac{U}{2\pi} \int_{-\pi}^{\pi} dq \, |q\rangle, \tag{6.19}$$

on any eigenstate $|k\rangle$ of the free particle with no superlattice.

We study now the stationary states of the system. To this end, it is more convenient

6. Collision theory on a model superlattice

to work in the basis of eigenstates of the superlattice Hamiltonian H_0, $\{\,|1,k\rangle,\,|2,k\rangle\}$ given by Eq. (6.11). The matrix elements of the interaction potential are given by

$$\langle s,k'|\,\hat{V}\,|s',k\rangle = \frac{U}{2\pi}A_s(k')A_{s'}(k)[f_s(k')+1][f_{s'}(k)+1], \qquad (6.20)$$

where $A_s(k)$ is given by Eq. (6.12) and $f_s(k) \equiv \lambda^{-1}(E_s(k)+\epsilon(k))$. Recall the matrix elements of the free superlattice Hamiltonian

$$\langle s,k'|\,H_0\,|s',k\rangle = E_s(k)\delta_{s,s'}\delta(k'-k). \qquad (6.21)$$

The bound state wave functions have the form

$$|\psi\rangle = \int_{-\pi/2}^{\pi/2} dk\,(\psi_1(k)\,|1,k\rangle + \psi_2(k)\,|2,k\rangle), \qquad (6.22)$$

and therefore we have

$$\langle s,k'|\,\hat{V}\,|\psi\rangle = \frac{U}{2\pi}A_s(k')[f_s(k')+1]\times$$
$$\int_{-\pi/2}^{\pi/2} dk[\psi_1(k)A_1(k)(f_1(k)+1) + \psi_2(k)A_2(k)(f_2(k)+1)]. \qquad (6.23)$$

By taking now the brackets $\langle s,k'|\,H\,|\psi\rangle$ and using the stationary Schrödinger equation $H\,|\psi\rangle = E\,|\psi\rangle$ we obtain a set of two coupled integral equations

$$\psi_s(k') = \frac{U}{2\pi}\frac{A_s(k')(f_s(k')+1)}{E-E_s(k')}\int_{-\pi/2}^{\pi/2} dk F(k), \qquad (6.24)$$

for $s=1,2$, where we have defined the function

$$F(k) = \psi_1(k)A_1(k)(f_1(k)+1) + \psi_2(k)A_2(k)(f_2(k)+1). \qquad (6.25)$$

We proceed now to decouple the two equations. Defining

$$\psi_s(k) \equiv \frac{A_s(k)(f_s(k)+1)}{E-E_s(k)}\chi_s(k), \qquad (6.26)$$

trivially yields $\chi_1(k) = \chi_2(k) = C \in \mathbb{C}$, and therefore the final equation for the bound states reads

$$1 = \frac{U}{2\pi}\int_{-\pi/2}^{\pi/2} dk\left[\frac{(A_1(k))^2(f_1(k)+1)^2}{E-E_1(k)} + \frac{(A_2(k))^2(f_2(k)+1)^2}{E-E_2(k)}\right]. \qquad (6.27)$$

The above equation can be solved numerically with the same methods introduced in subsect. 5.1.2. We will however solve the problem in direct lattice space, which yields a much simpler, transcendental equation for the bound state energies, and is the subject of the following paragraph.

Bound states in position representation. Recall that, in a flat lattice ($\lambda \equiv 0$), the following conformal transformation,

$$E = -J\frac{1+\alpha^2}{\alpha}, \tag{6.28}$$

with $0 < |\alpha| < 1$ and $\alpha \in \mathbb{R}$, maps unambiguously the range $|\alpha| < 1$ into $\mathbb{R} - [-2J, 2J]$. Therefore, if the desired eigenstate represents a bound state, with energy outside the continuum, it can be fully characterized by a single parameter α. This form of the energy as a function of α immediately gives the correct wave functions $\psi(n) = \alpha^{|n|}$ for zero range interaction, and one finally obtains a system of two equations with two unknowns.

For the $\tau = 2$ superlattice, we now apply the following reasoning:
(i) The energies of the continuum are given by $E_s(k) = (-1)^s \sqrt{[\epsilon(k)]^2 + \lambda^2}$, with $s = 1, 2$ and $\epsilon(k) = -2J\cos(k)$.
(ii) For the case of $\lambda = 0$, the bound state energies are obtained by replacing $\epsilon(k)$ by expression (6.28).
(iii) We need a new conformal transformation that maps a subset $S \subset \{\alpha \in \mathbb{C} \mid |\alpha| < 1\}$ onto $\mathbb{R} - \sigma_{\mathrm{ess}}$, where the continuous spectrum is now given by

$$\sigma_{\mathrm{ess}} = [-\sqrt{4J^2 + \lambda^2}, -\lambda] \cup [\lambda, \sqrt{4J^2 + \lambda^2}]. \tag{6.29}$$

From (iii) it is clear that the functional form of the energy must depend only on α and λ. Keeping in mind (i) and (ii), we propose the following functional form for the two energies

$$E_s = (-1)^s \sqrt{\left(J\frac{1+\alpha^2}{\alpha}\right)^2 + \lambda^2}. \tag{6.30}$$

The domain of the transformation (6.30) can no longer be a subset of $\mathbb{R}$. Part $\mathcal{D}_1$ of the domain $\mathcal{D}$ which is mapped onto $(-\infty, -\sqrt{4J^2 + \lambda^2}) \cup (\sqrt{4J^2 + \lambda^2}, \infty)$ is easily seen to be

$$\mathcal{D}_1 = (0, 1). \tag{6.31}$$

The other part $\mathcal{D}_2$ which is mapped onto $(-\lambda, \lambda)$ consists of a set of purely imaginary numbers $\alpha = \mathrm{i}a$, with $a > 0$,

$$\mathcal{D}_2 = \{\mathrm{i}a \in \mathbb{C} \mid (\sqrt{\lambda^2 + 4J^2} - \lambda)/2J < a < 1\}. \tag{6.32}$$

We now assume the following form for the bound state wavefunctions ψ,

$$\psi(n) = f(\alpha; n)\phi_\alpha(n), \tag{6.33}$$

where $\phi_\alpha(n+2) = \phi_\alpha(n)$. This assumption will be justified if the final equations obtained for ϕ_α and E have non-trivial, consistent solutions. With these ansätze, and using the energy (6.30) in the Schrödinger equation $H|\psi\rangle = E|\psi\rangle$, we find that the function f has the form

$$f(\alpha; n) = \alpha^{|n|}, \tag{6.34}$$

and the periodic part of the eigenfunctions is simply

$$\phi_\alpha(1) = \frac{U}{J}\frac{\alpha}{\alpha^2 - 1}, \tag{6.35}$$

with $\phi_\alpha(0) \equiv 1$. The consistency equation for the energies becomes

$$E = \frac{1 + \alpha^2}{1 - \alpha^2}U + \lambda. \tag{6.36}$$

By equating Eqs. (6.30) and (6.36), we obtain the two final equations

$$(-1)^s\sqrt{\left(J\frac{1 + \alpha^2}{\alpha}\right)^2 + \lambda^2} = \frac{1 + \alpha^2}{1 - \alpha^2}U + \lambda, \tag{6.37}$$

for $s = 1, 2$, and the physically relevant solutions lie in the domain $\mathcal{D} \equiv \mathcal{D}_1 \cup \mathcal{D}_2$. We can also extend the domain to include negative values of α (if $-\alpha \in \mathcal{D}_1$) and a (if $-ia \in \mathcal{D}_2$), giving rise to different wave functions for which the phase changes from site to site while their associated eigenenergies are equal to those of the solutions lying in $\mathcal{D}$.

In Fig. 6.5 we plot the bound state energies as functions of λ for a fixed value of the zero range particle-impurity interaction $U = -2J$. As can be inferred from the figure, there are two bound states, one below the lowest scattering continuum and one in the gap. Although the bound state below the band quickly approaches the bottom of the continuum for larger λ/J, it does not disappear but remains very weakly bound for all gap sizes. We will show in the next subsection that there are no zero-energy resonances.

6.2.2. Scattering theory

Let us now calculate the symmetric continuum states (note that $[H, \hat{P}] = 0$ for the $\tau = 2$ superlattice). We assume that they can be factorized as

$$\psi^{(S)}(n) = \cos(k|n| + \delta)\phi_k(n), \tag{6.38}$$

with $\phi_k(n+2) = \phi_k(n)$. After substitution into the Schrödinger equation $H|\psi\rangle = E|\psi\rangle$ and some algebra we obtain that the phase shift, $\delta \equiv \delta_s(k)$, must satisfy

$$\tan \delta_s(k) = \frac{U}{E_s(k) - \lambda}\cot(k), \tag{6.39}$$

where $s = 1, 2$ is the band index, $\phi_k(0) \equiv 1$, $\phi_k(1)$ is given by Eq. (6.7) and the energy bands $E_s(k)$ are given by Eq. (6.8). For $\lambda = 0$, the above relation, Eq. (6.39), reduces to the flat lattice result. Moreover, there are no resonances in the system for any value of λ, U or k. The antisymmetric scattering states[5] are readily calculated by applying the ansatz

$$\psi^{(A)}(n) = \sin(kn)\phi_k(n), \tag{6.40}$$

where again ϕ_k are given by $\phi_k(0) \equiv 1$ and $\phi_k(1)$ in Eq. (6.7).

---

[5]The antisymmetric states do not feel the delta interaction at all: they are free states.
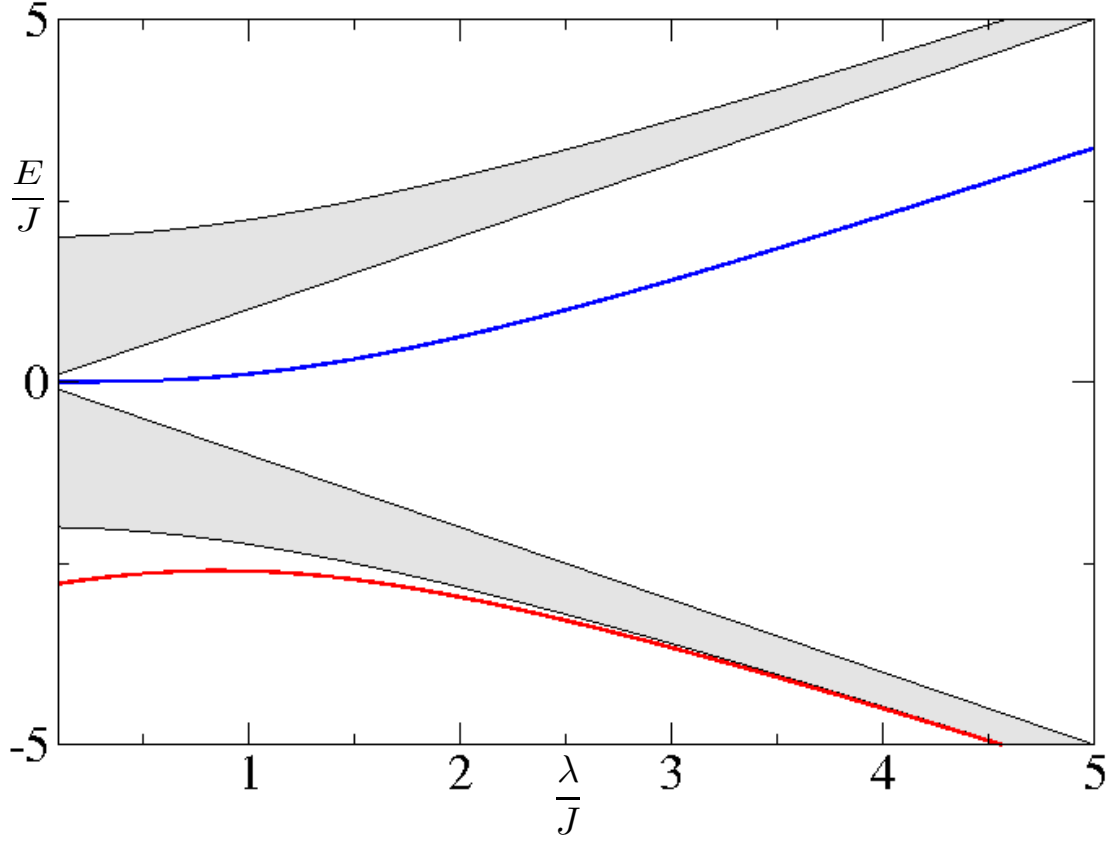
Figure 6.5.: The bound state energies (curves) as a function of λ for $U/J = -2$. The continuum of scattering states is plotted as shaded surfaces, and the gap is clearly observed.

Having both symmetric and antisymmetric scattering states we can now give the solution in terms of incident, reflected and transmitted waves[6] as

$$\psi(n) = \phi_k(n)[A\cos(k|n| + \delta_s(k)) + B\sin(kn)] = \begin{cases} \phi_k(n)(e^{ikn} + re^{-ikn}), & n < 0 \\ \phi_k(n)\, te^{ikn}, & n > 0. \end{cases}$$

$$(6.41)$$

In order for the second equality to hold, the coefficients must satisfy

$$B/A = ie^{-i\delta_s(k)}, \tag{6.42}$$

and we find for the transmission and reflection coefficients

$$t = \frac{1}{2}(e^{2i\delta_s(k)} + 1) \tag{6.43}$$

$$r = \frac{1}{2}(e^{2i\delta_s(k)} - 1). \tag{6.44}$$

Hence, the transmission and reflection probabilities are given by $T \equiv |t|^2 = \cos^2(\delta_s(k))$

---

[6]On the superlattice, these are no longer plane waves.

and $R = |r|^2 = 1 - T = \sin^2(\delta_s(k))$.

The solutions above are of course not well defined for "zero-energy" states, with $k = 0$ $(s = 1, 2)$ or $k = \pi/2$ $(s = 2)$. The "low-energy" scattering properties $(k = 0)$ are described in terms of the scattering length of the system, a_s

$$a_s \equiv -\lim_{k \to 0} \frac{\partial \delta_s(k)}{\partial k} = \frac{E_s(0) - \lambda}{U}. \tag{6.45}$$

$$\tag{6.46}$$

The solution at zero quasi-momentum is then given by

$$\psi_0(n) = \phi_0(n) \left(1 - \frac{|n|}{a_s}\right), \tag{6.47}$$

with ϕ_0 the periodic Bloch's function of the given band $s = 1$ or $s = 2$. For the case of $k = \pi/2$ and $s = 2$ we have not found a non-trivial (i.e. $\psi \neq 0$) solution.

6.3. Conclusions and outlook

In this chapter we have focused our attention to the simplest case of scattering on the superlattice, a single particle colliding with an immobile impurity. The superlattice we have used is the simplest one as well, described by a tight-binding Hamiltonian. This system, however, exhibits new physics such as the possibility of having, simultaneously, bound states inside and outside the energy gap induced by the superlattice. Moreover, our results can be generalized to any other period of the superlattice and with longer range (but still finite) interactions; this would require more involved algebraic manipulations but the physics will be similar.

One might be tempted to generalize our results to two-body scattering by employing a slight modification of the usual two-body ansatz studied in detail in chapter 4. Since on the superlattice the two-body problem does not separate into the center of mass and relative coordinates, it is indeed rather obvious that a natural generalization for the two-boson scattering states with zero range interaction could simply be

$$\psi(n_1, n_2) = \mathcal{S}\phi_{k_1}(n_1)\phi_{k_2}(n_2)e^{ik_1 n_1 + ik_2 n_2} + C\,\mathrm{sgn}(n_1 - n_2)\mathcal{A}\phi_{k_1}(n_1)\phi_{k_2}(n_2)e^{ik_1 n_1 + ik_2 n_2}, \tag{6.48}$$

where n_1 and n_2 are the coordinates of the two particles, ϕ_k is the Bloch's function with periodicity of the superlattice, $\mathcal{S}$ is the symmetrization operator, $\mathcal{A}$ is the antisymmetrization operator and C a constant to determine.

It is easy to see by direct substitution into the Schrödinger equation that the ansatz (6.48) cannot be an eigenstate of the two-body problem on the superlattice with period $\tau = 2$. The reason is that we have two sublattices, A and B, composed of even and odd sites, respectively. It turns out that, in addition to C, we need a second constant in Eq. (6.48). This means that we need a third function having the same (asymptotic) energy as the functions conforming Eq. (6.48) to build a correct ansatz. We have already proved that such functions exist and are unique. Moreover, physically acceptable solutions of the Schrödinger equations can be constructed analytically, with very little numerical effort – no more than solving a system of two linear equations! – and show

very interesting features such as unconventional paired states. Needless to say, the single particle-impurity collision is a fundamental building block for the two-body problem.

To the best of our knowledge, this would be the first two-body problem in a periodic potential[7] to be solved analytically, and might be a first step towards the exact solution of the many fermion problem on the superlattice.

---

[7]The tight-binding superlattice is a finite-difference problem with a periodic potential.

7. Lattice oscillator model, scattering theory and a many-body problem

The quantum harmonic oscillator is a paradigmatic model with applications in all branches of physics, too numerous to be counted. Due to the special structure of its Hamiltonian, it is possible to obtain its eigenstates exactly in several different ways. Perhaps the most celebrated one is the algebraic solution by means of the creation-annihilation (ladder) operators [CKS95], which is by far the simplest and most elegant and, moreover, it is the first step towards field quantization [Mes99].

For more complicated problems the use of numerical methods becomes necessary. One of the most popular techniques is the finite-difference discretization, which is often employed in high-energy physics to obtain non-perturbative results [Rot05]. However, this method has severe problems, since the symmetries of the original problem are usually lost on the lattice and can only be recovered once the continuum limit is taken which, in practice, is numerically impossible. As an important example, the lattice harmonic oscillator, subsect. 3.2.2, though it can be written as the Mathieu equation in quasi-momentum space [CGM86, Mat86], is not factorizable and not even its ground state can be obtained in closed form. This fact is very disappointing, since then the SUSY structure of the system is not transparent (in fact, not even present) until the continuum limit is taken.

In this chapter, we construct a model for the lattice harmonic oscillator which has a correct continuum limit. Its Hamiltonian is shape invariant [CKS95] and, though the excitations cannot be accessed analytically, its ground state is exactly solvable for any value of the oscillator frequency and the lattice spacing. The excitations can, however, be obtained by solving an equation which is analogous to the Hermite equation. We propose then a definition of coherent states, finding that their correct continuum limit cannot be obtained if they are defined as eigenstates of the lattice annihilation operators, so their definition has to be given in terms of the displacement operator. Our model is completely analogous to that for a single particle in a periodic potential, and we use it to calculate the lowest band zero energy scattering length in a particle-impurity collision. We then make further use of the analogy of the model with a many-body system with anharmonic interactions on a finite ring which can be solved exactly for the ground state.

7. Lattice oscillator model, scattering theory and a many-body problem

7.1. Position and momentum operators on the lattice

We define the following operators in quasi-momentum space as the momentum $(\hat{p})$ and position $(\hat{x})$ operators,

$$\hat{p} \equiv \frac{\hbar}{d} \sin kd \tag{7.1}$$

$$\hat{x} \equiv i\frac{\partial}{\partial k}, \tag{7.2}$$

where d (> 0) is the lattice spacing and $k \in (-\pi/d, \pi/d]$ is the quasi-momentum. The operators $\hat{p}$ and $\hat{x}$ are constructed in analogy with their continuous space counterparts.[1] We can write the lattice analog of the harmonic oscillator annihilation $\hat{a}$ and creation $\hat{a}^{\dagger}$ operators as

$$\hat{a} = (\hat{X} + i\hat{P})/\sqrt{2} \tag{7.3}$$

$$\hat{a}^{\dagger} = (\hat{X} - i\hat{P})/\sqrt{2}, \tag{7.4}$$

where the quadrature operators are defined as

$$\hat{X} \equiv (m\omega/\hbar)^{1/2}\hat{x}, \tag{7.5}$$

$$\hat{P} \equiv (m\hbar\omega)^{-1/2}\hat{p}. \tag{7.6}$$

However, by using the lattice operators of Eqs. (7.1) and (7.2) we see that $[\hat{X}, \hat{P}] = i\cos(kd)$ and $[\hat{a}, \hat{a}^{\dagger}] = \cos(kd)$. In other words, the canonic commutation relations are valid up to a factor of $\cos(kd)$. In the limit of small lattice spacing, we obtain the correct commutation relation of the continuous space case $\lim_{d\to 0}[\hat{X}, \hat{P}] = i$. The commutation relation $[\hat{X}, \hat{P}]$ yields a generalized uncertainty principle (GUP) of the form

$$\Delta X \Delta P \geq \frac{1}{2}|\langle\cos(kd)\rangle|, \tag{7.7}$$

which resembles the GUP of systems with a minimal length [Hos06]. The GUP (7.7) does not imply any minimal ΔX (it can be zero). However, we have a maximal dispersion for the momentum,

$$\Delta P \leq \Delta P_{\max} = \sqrt{\frac{\hbar\pi}{m\omega d^3}}, \tag{7.8}$$

which is infinite in the continuum limit, as it should.

7.2. The lattice harmonic oscillator

If we wish to construct a lattice theory for the harmonic oscillator having a similar structure as its continuum limit, we have to consider the operator

$$\hat{N} \equiv \hat{a}^{\dagger}\hat{a} = \frac{1}{2}(\hat{P}^2 + \hat{X}^2 + i[\hat{X}, \hat{P}]). \tag{7.9}$$

---

[1]Note that they have the correct continuum limit, i.e. they tend to the continuous space operators when $d \to 0$.

So far, the "number" operator, Eq. (7.9), has exactly the same appearance as in continuous space. Its explicit form is given by

$$\hat{N} = \frac{1}{2}\left(-\frac{m\omega}{\hbar}\frac{\partial^2}{\partial k^2} + \frac{\hbar}{m\omega d^2}\sin^2(kd) - \cos(kd)\right). \tag{7.10}$$

The number operator written in this way looks rather unusual. If we rewrite $\sin^2(kd) = (1 - \cos(2kd))/2$, and perform Fourier transform to direct lattice space, then we see that the number operator $\hat{N}$ acts as

$$(\hat{N}\psi)(x) = \frac{1}{2}\Big[\frac{m\omega}{\hbar}x^2\psi(x) - \frac{\psi(x+d) + \psi(x-d)}{2}$$
$$+ \frac{\hbar}{2m\omega d^2}\big(\psi(x) - \frac{\psi(x+2d) + \psi(x-2d)}{2}\big)\Big] \tag{7.11}$$

where $n = x/d \in \mathbb{Z}$ are the lattice points. Thus, the number operator corresponds to a lattice with nearest-neighbor and next-nearest-neighbor hoppings with an external harmonic trap, plus a trivial constant. After taking the continuum limit $d \to 0$, one easily verifies that $\hbar\omega\hat{N} \to \hat{p}^2/2m + m\omega^2 x^2/2 - \hbar\omega/2$.

7.2.1. Ground state and lattice Hermite equation

From now on we consider the Hamiltonian

$$H \equiv \hbar\omega(\hat{N} + \frac{1}{2}). \tag{7.12}$$

If operator $\hat{a}$ annihilates a wave function in k-space which is 2π-periodic,[2] then it is the ground state of H with energy $E_0 = \hbar\omega/2$. Equation $\hat{a}\psi_0(k) = 0$ is readily solved and the ground state wave function has the form

$$\psi_0(k) = \mathcal{N}e^{-\gamma_d}e^{\gamma_d\cos(kd)}, \tag{7.13}$$

where $\gamma_d \equiv \hbar/(m\omega d^2)$. In the continuum limit, Eq. (7.13) reduces to the well-known harmonic oscillator ground state, $\psi_0(k) \sim \exp(-\hbar k^2/m\omega)$. We use this result to verify the uncertainty principle on the lattice, and find that in the ground state of the lattice harmonic oscillator, the uncertainty relation is also minimal,

$$\Delta X \Delta P = \frac{1}{2}\left|\frac{\langle\psi_0|\cos(kd)|\psi_0\rangle}{\langle\psi_0|\psi_0\rangle}\right|, \tag{7.14}$$

since in general $\Delta X \Delta P \geq |\langle[\hat{X},\hat{P}]\rangle|/2$.

Further analogy with the harmonic oscillator in continuous space can be observed by solving the eigenvalue problem for the number operator $\hat{N}\psi(k) = \tilde{N}\psi(k)$ with the ansatz $\psi(k) = \psi_0(k)\phi(k)$. The eigenvalue problem is then transformed to the equation

$$\phi''(k) - 2\frac{\hbar}{m\omega}\frac{\sin(kd)}{d}\phi'(k) + 2\frac{\hbar}{m\omega}\tilde{N}\phi(k) = 0 \tag{7.15}$$

---

[2]For simplicity, we will call a function 2π-periodic when it is actually $2\pi/d$-periodic.

that determines the unknown $\phi(k)$ for which periodic boundary conditions (PBC) $\phi(k + 2\pi/d) = \phi(k)$ are assumed. Note the analogy of Eq. (7.15) with the Hermite equation: the naive substitution $\sin(kd)/d \sim k$, valid for $kd \ll 1$, yields the well-known continuum limit, in which the eigenvalues $\tilde{N}$ become natural numbers.

In Fig. 7.1 we plot the low-energy eigenvalues $\tilde{N}$ of $\hat{N}$, Eq. (7.10), for a small value of the lattice spacing d. We see that the lowest eigenvalue is indeed zero, while the rest of the eigenvalues appear to be quasi-degenerate but almost linearly spaced as $\tilde{N}_{s+2} - \tilde{N}_s = 1$. The reason is that, in direct lattice space, the number operator includes tunneling to nearest and second nearest neighbors, therefore inducing the quasi-degeneracy, except for the ground state. The relevant eigenstates for the continuum limit are those labeled by even quantum numbers s and, in direct lattice space, appear to be essentially a superposition of the discretized Hermite functions $\psi_{s/2}(x = 2nd) - \psi_{s/2}(x = -(2n+1)d)$.
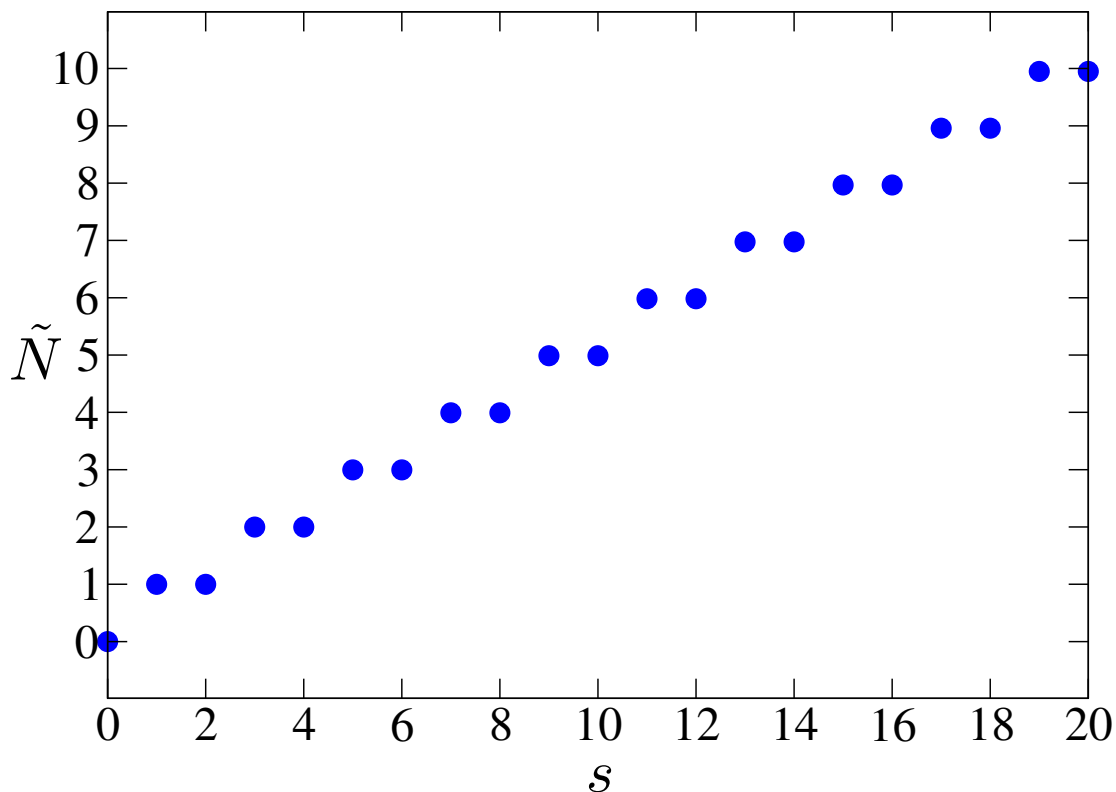

Figure 7.1.: Eigenvalues of $\hat{N}$, Eq. (7.10), for $d = \frac{1}{10\sqrt{5}}\sqrt{\frac{\hbar}{m\omega}}$.

7.2.2. Coherent states

It is natural to define now the coherent states for the lattice harmonic oscillator. First, we try the eigenstates of the annihilation operator, $\hat{a}\psi_\alpha = \alpha\psi_\alpha$, with $\alpha \in \mathbb{C}$. The solution of this equation is

$$\psi_\alpha(k) = \exp\left[-\mathrm{i}2\sqrt{\frac{\hbar}{m\omega}}\alpha k\right]\psi_0(k) \tag{7.16}$$

with $\psi_0(k)$ being the ground state, Eq. (7.13). If we assumed α to be *any* complex number, ψ_α would not fulfill the PBC. Hence, if we insist on ψ_α to be correct, we have no choice but to restrict the values of α to $\alpha_j = \frac{1}{2}\sqrt{\frac{m\omega}{\hbar}}j$, $j \in \mathbb{Z}$, which is a very unsatisfactory answer since the coherent states would then be restricted to equally spaced real numbers. Therefore the coherent states ψ_α do not present a very convenient definition. This apparently difficult situation can be resolved in a rather elegant way, however, relaxing the requirement that the coherent states be eigenstates of the lattice annihilation operator $\hat{a}$. To this end, we *define* the coherent states Ψ_α as solutions of the equation $\hat{a}\Psi_\alpha(k) = \alpha\cos(kd)\Psi_\alpha(k)$,

$$\Psi_\alpha(k) = \exp\left[-\mathrm{i}2\alpha\sqrt{\frac{\hbar}{m\omega}}\frac{\sin(kd)}{d}\right]\psi_0(k), \tag{7.17}$$

which are obviously 2π-periodic for all $\alpha \in \mathbb{C}$, and have the correct continuum limit. We can further justify Eq. (7.17) as a definition since even in the continuum the coherent states are solutions of $(\hat{a} + \alpha\mathrm{i}[\hat{X}, \hat{P}])\Psi_\alpha = 0$. The only issue we cannot generalize to the lattice case is the usual form of the displacement operator, since on the lattice the Baker-Hausdorff formula is not valid due to the commutator $[\hat{a}, [\hat{a}, \hat{a}^\dagger]] \neq 0$. Therefore we define here the displacement (or translation) operator for lattice and continuum as $\hat{D}(\alpha) = e^{-\mathrm{i}2\alpha\hat{P}}$, which generates *unnormalized* coherent states.

7.2.3. Angular momentum

A major inconvenience of lattice discretizations, if these are introduced artificially and not due to a true underlying crystal structure, is the absence of rotational symmetry. To be more concrete, we lack conservation of angular momentum or, more dramatically, we do not even have a definition of angular momentum on the lattice!

We propose here a rather simple lattice analog of the angular momentum. The requirements this operator has to satisfy are rather relaxed: (i) it should have a correct continuum limit, (ii) there should be a ground state of some relevant enough Hamiltonian with a well defined "angular momentum" on the lattice and, (iii) the lattice angular momentum cannot commute with the lattice Hamiltonian. Requirement (iii) is easy to satisfy: take *any* Hamiltonian which respects the symmetries of the lattice. We discuss now how (i) and (ii) can be met. Consider first a two-dimensional (2D) oscillator with Hamiltonian $H^{(2\mathrm{D})} = \hbar\omega[\hat{N}_1 + \hat{N}_2 + 1]$, with $\hat{N}_i = \hat{a}_i^\dagger\hat{a}_i$. We define the lattice angular momentum in 2D, in analogy with the continuum, as

$$\hat{L} \equiv \hat{x}_1\hat{p}_2 - \hat{x}_2\hat{p}_1 = \mathrm{i}(\hat{a}_1\hat{a}_2^\dagger - \hat{a}_1^\dagger\hat{a}_2), \tag{7.18}$$

and we see that condition (i) is fulfilled. As promised, requirement (ii) is automatically satisfied by the ground state of $H^{(2\mathrm{D})}$, $\psi_0^{(2\mathrm{D})}(k_1, k_2) = \psi_0(k_1)\psi_0(k_2)$, with $\psi_0(k_i)$ defined in Eq. (7.13), and by the ground state of the 2D free particle Hamiltonian $H_F = -2J\sum_{k_1,k_2}(\cos(k_1 d) + \cos(k_2 d))|k_1, k_2\rangle\langle k_1, k_2|$, $\psi(k_1, k_2) = \delta(k_1)\delta(k_2)$, both having angular momentum $L = 0$ as a good quantum number. It must be noted that lattice angular momentum operators have been defined in the context of rotating gases in an optical lattice in [BPS+06], but with such definition requirement (ii) is no longer satisfied for the ground state of the lattice oscillator. We now show by explicit calculation

that the angular momentum on the lattice is in general not a conserved quantity

$$[\hat{L}, \hat{N}_1 + \hat{N}_2] = i\big[\cos(k_1 d)\hat{a}_1\hat{a}_2^\dagger + \hat{a}_2\hat{a}_1^\dagger\cos(k_1 d)$$
$$- \hat{a}_1\hat{a}_2^\dagger\cos(k_2 d) - \cos(k_2 d)\hat{a}_2\hat{a}_1^\dagger\big], \tag{7.19}$$

which, as expected, is non-zero, but vanishes in the continuum limit. It must be noted now that the lattice angular momentum operator, Eq. (7.18), can be used as a definition not only for the model discussed here, but for *any* tight-binding lattice model even without next-nearest-neighbor hopping.

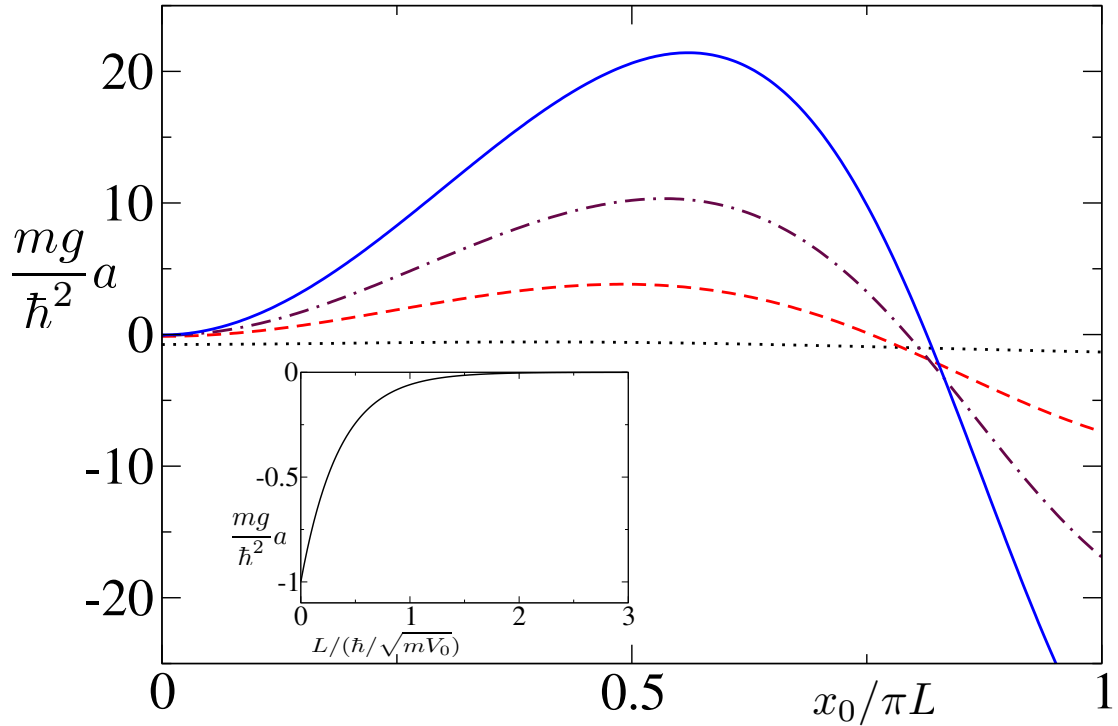## 7.3. Application to impurity scattering in a periodic potential

Figure 7.2.: Scattering lengths for $mV_0 L^2/\hbar^2 = 10^{-3}$, 1/2, 1 and 3/2 (at $x_0 = 0$ from bottom to top). Inset: $a(0)$ as a function of L.

The model presented here can be applied to construct completely different systems and obtain some of their properties exactly. As a first application, let us consider a single particle moving on the real line. It is readily verified that the Hamiltonian with the periodic potential,

$$V(x) = V_0 \sin^2(x/L) - \frac{\hbar}{L}\sqrt{\frac{V_0}{2m}}\cos(x/L) \tag{7.20}$$

has a ground state $\psi_0(x) = \exp[\lambda_L \cos(x/L)]$, with $\lambda_L = \sqrt{2mV_0}L/\hbar$, since the potential and kinetic energy operators are dual to those for the lattice Harmonic oscillator in

quasi-momentum space. We consider a single static impurity located at $x_0 \in (-\pi L, \pi L]$ (this is the central site, and by translation applies to an impurity at any site), with zero range interaction potential $V_g(x) = g\delta(x - x_0)$, and we show how to get the low-energy scattering properties of the system in a very simple manner. First we notice that, since V has a purely continuous spectrum and the impurity is immobile, upon collision the incident waves can only acquire a phase shift. Therefore, for low-energy scattering we only need the periodic (ψ_0) and aperiodic (which we call ψ_I) solutions for zero energy. The aperiodic solution centered at the first site is given by

$$\psi_I(x) = \psi_0(x) \int^x dx\, e^{-2\lambda_L \cos(x)} \equiv \psi_0(x)\Phi(x). \tag{7.21}$$

This aperiodic solution is clearly antisymmetric and it holds that $\Phi(x) = \beta x + \phi_p(x)$, where $\phi_p(x + 2\pi L) = \phi_p(x)$. Recall that *without* the periodic potential, this solution corresponds to setting $\phi_p \equiv 0$, and the scattering length a_0 of a static Dirac delta impurity is defined [LSSY05] by the zero-energy solution $f_0(x) = 1 - |x|/a_0$. Clearly, f_0 is the sum of the periodic (free) solution and the aperiodic (unnormalizable) solution, with the inverse scattering length as a coefficient. In analogy to the free space situation, we define a position dependent scattering length $a(x_0)$, $x_0 \in (-\pi L, \pi L]$, in terms of the zero-energy solution

$$f(x; x_0) = \psi_0(x) - \frac{|\psi_I(x) - \psi_I(x_0)|}{a(x_0)}, \tag{7.22}$$

which, written in this way, satisfies the boundary condition

$$f'(x_0^+) - f'(x_0^-) = 2mg f(x_0)/\hbar^2 \tag{7.23}$$

imposed by the Dirac delta, if

$$a(x_0) = -\frac{\hbar^2}{mg} \left[\frac{(\psi_0 \Phi)'}{\psi_0} \right]_{x=x_0} \tag{7.24}$$

for $x_0 \in (-\pi L, \pi L]$, and $a(x_0 + n2\pi L) = a(x_0)$, with $n \in \mathbb{Z}$. In the simplest case of $x_0 = 0$, the scattering length is shown to have the form $a(0) = -\hbar^2 e^{-2\lambda_L}/(mg)$. If $x_0 \neq 0$ it has to be calculated numerically. In Fig. 7.2 we plot the scattering length $a(x_0)$, showing how strongly it depends on the position of the impurity. The scattering length never diverges (there is no resonance), but $mga(x_0)/\hbar^2$ can actually become positive and indeed very large with increasing V_0 at $x_0 \neq 0$, even though the corresponding free-space scattering length (we assume $g > 0$) is negative. This means that interactions in a periodic potential can effectively change both quantitative and qualitatively, depending on where the scattering takes place.

7.4. A many-body system

As a second application, we construct a many-body Hamiltonian of interacting particles on a finite ring whose ground state can be obtained in closed form. We consider N particles on a ring of length $2\pi L$. The position of particle $i \in \{1, \ldots, N\}$ is denoted
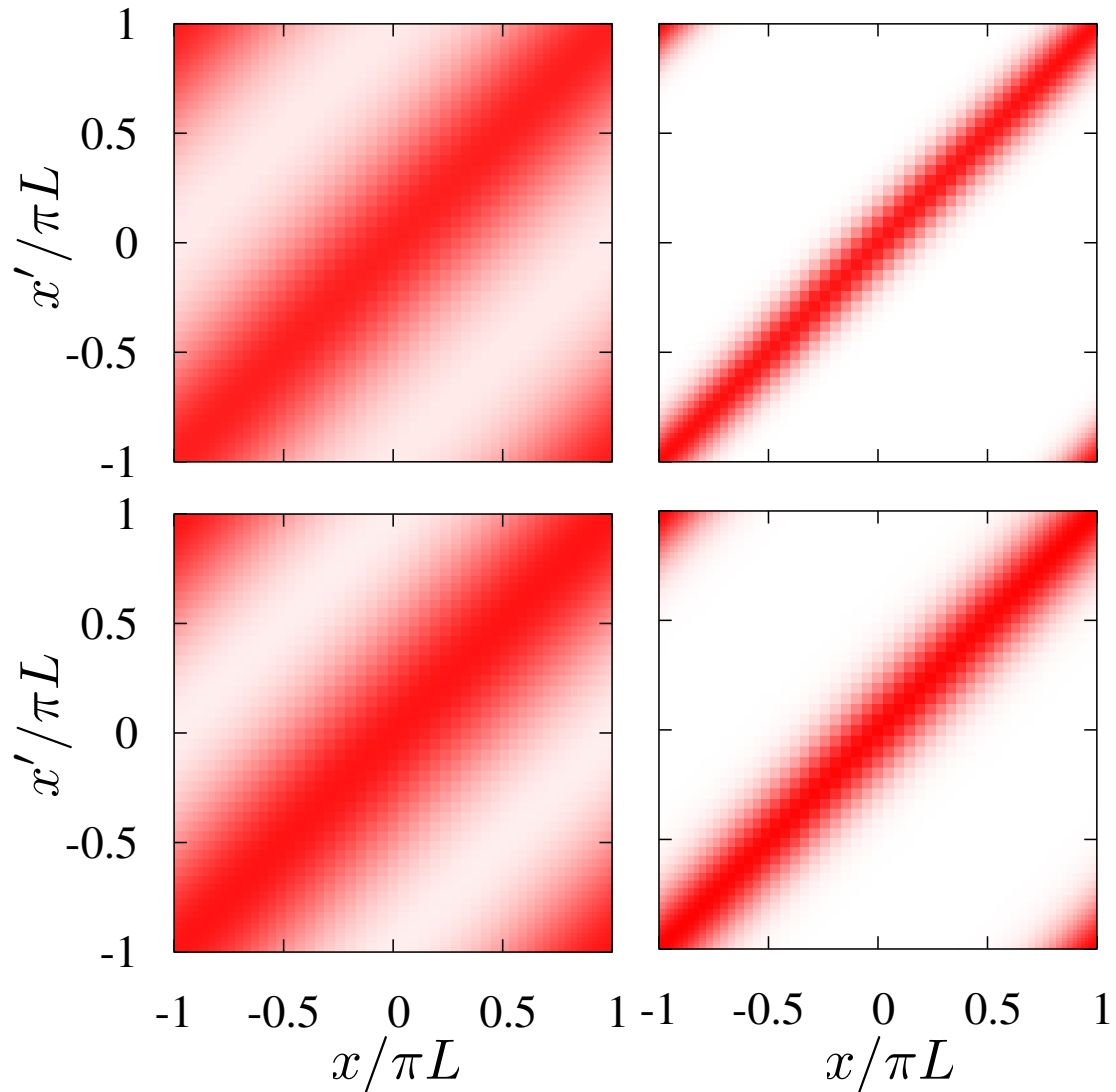
Figure 7.3.: Pair correlation functions $\rho(x, x')$; the clearer the color the lower its value. Top $N = 4$ particles, bottom $N = 2$ particles. Left $\lambda L^2 = 0.1$, right $\lambda L^2 = 1$. All values are normalized to the peak.

by $x_i \in (-\pi/L, \pi L]$ and its momentum by $p_i = -i\hbar\partial/\partial x_i$, and for all the functions involved we use PBC. We consider the following Hamiltonian

$$H = \frac{\hbar^2}{2m} \sum_{i=1}^{N} \hat{A}_i^\dagger \hat{A}_i, \tag{7.25}$$

$$\hat{A}_i = \frac{\partial}{\partial x_i} + \lambda L \sum_{\substack{j=1 \\ j \neq i}}^{N} \sin(x_{i,j}/L), \tag{7.26}$$

where $x_{i,j} = x_i - x_j$. With these definitions, the many-body Hamiltonian (7.25) is 2π-periodic. In the limit of an infinitely long ring, $L \to \infty$, we are left with N particles interacting via pairwise harmonic potentials. However, for any finite-size ring the interactions are anharmonic and contain three-body terms.

Since the Hamiltonian H, Eq. (7.25), is the sum of semi-positive operators, it follows that $H \geq 0$. Hence, if there exists a non-singular periodic function ψ_0 which is annihilated by all A_i, $i = 1, \ldots, N$, then it is the ground state of H and its eigenenergy is zero. The set of N equations $\hat{A}_i \psi_0 = 0$ is easily shown to be satisfied by the wave function

$$\psi_0(x_1, \ldots, x_N) = \mathcal{N} \prod_{i<j=1}^{N} \exp\left[2\lambda L^2 \cos(x_{i,j}/L)\right], \qquad (7.27)$$

with $\mathcal{N}$ the normalization constant. It is remarkable that for any $L < \infty$, the ground state (7.27) is square integrable, even if $\lambda < 0$, but in taking the limit of $L \to \infty$ this will no longer be true.

In Fig. 7.3 we plot some ground state pair correlation functions, defined as

$$\rho(x, x') \propto \int_\Omega dx_3 \ldots dx_N |\psi_0(x, x', \ldots, x_N)|^2, \qquad (7.28)$$

where $\Omega \equiv (-\pi/L, \pi/L]^{N-2}$. We note that as $\lambda L^2 (> 0)$ becomes larger, the particles tend to be tighter co-localized, which also happens for increasing number of particles.

7.5. Conclusions

We have constructed a lattice model of the harmonic oscillator with a correct continuum limit whose properties, especially in the ground state, are the perfect analogous of those in continuous space. We have also defined lattice coherent states and a lattice "angular momentum" in terms of the creation and annihilation operators of the model. By establishing connections with other systems, we were able to describe low-energy scattering in a periodic potential and an anharmonically interacting many-body system. These results are relevant for lattice simulations as well as cold collisions and many-body theory.

A. Effective strongly coupled theories

We describe here how to obtain effective Hamiltonians, to second order in $J/|U|$ (in general, to second order in a certain "small" parameter of the Hamiltonian), following [CTDRG92, LSA$^+$07].

Let H be the Hamiltonian

$$H = H_0 + \xi V, \tag{A.1}$$

and let us assume that we know the eigenstates (and eigenvalues) of H_0, which can be grouped in different subspaces labeled by the index α. If we define P_α to be the projection operator on the subspace denoted by the index α, it holds that $P_\alpha H_0 P_\beta = 0$ for $\alpha \neq \beta$. Consider now the transformation of the original Hamiltonian H,

$$H_{\text{eff}} \equiv GHG^{-1}, \tag{A.2}$$

where $G \equiv e^{iS}$ is unitary, $GG^\dagger = G^\dagger G = 1$, and S is hermitian, $S^\dagger \subset S$. We have to choose G, or for that matter, S, so that the effective Hamiltonian does not couple states which lie in different subspaces,

$$P_\alpha H_{\text{eff}} P_\beta = 0 \tag{A.3}$$

if $\alpha \neq \beta$. We take now the specific choice of S in which $P_\alpha S P_\alpha = 0$. Assuming that ξ is a small parameter (in the usual sense of perturbation theory, $|\xi|$ must be much smaller than a certain parameter which quantifies H_0), we assume the operator S to be a holomorphic function of ξ.[1] We can then expand it in Taylor series as

$$S = \sum_{i=1}^\infty \xi^i S_i. \tag{A.4}$$

We make use of the Baker-Hausdorff formula [LP07] to second order,

$$H_{\text{eff}} \approx H + [\mathrm{i}S, H] + \frac{1}{2}[\mathrm{i}S, [\mathrm{i}S, H]], \tag{A.5}$$

obtaining, if we only keep terms up to ξ^2,

$$H_{\text{eff}} \approx H_0 + \xi H_{\text{eff}}^{(1)} + \xi^2 H_{\text{eff}}^{(2)}, \tag{A.6}$$

where we have defined the first and second order corrections to the unperturbed Hamil-

---

[1]This is the case for many lattice models; see [Kat95] for details.

A. Effective strongly coupled theories

tonian H_0 as

$$H_{\text{eff}}^{(1)} = [\text{i}S_1, H_0] + \xi V, \tag{A.7}$$

$$H_{\text{eff}}^{(2)} = [\text{i}S_2, H_0] + [\text{i}S_1, \xi V] + \frac{1}{2}[\text{i}S_1, [\text{i}S_1, H_0]]. \tag{A.8}$$

If $|\alpha, i\rangle$ and $|\beta, j\rangle$ are two states in the subspaces α and β, respectively, and using the condition $P_\alpha H_0 P_\beta = 0$, we find

$$\langle \alpha, i| \,\text{i}S_1 \,|\beta, j\rangle = \xi \frac{\langle \alpha, i| V |\beta, j\rangle}{E_{\alpha,i} - E_{\beta,j}}(1 - \delta_{\alpha,\beta}), \tag{A.9}$$

where we have defined the energies $E_{\alpha,i}$ as the eigenvalues of the unperturbed Hamiltonian H_0, $H_0 |\alpha_i\rangle = E_{\alpha,i} |\alpha_i\rangle$. We then get for the first order effective Hamiltonian within the α subspace

$$H_{\text{eff}}^{(1)} = \xi V. \tag{A.10}$$

After some algebraic manipulations we arrive at the second order correction in the desired subspace

$$H_{\text{eff}}^{(2)} = -\frac{\xi^2}{2} \sum_i V Q_{\alpha,i} V, \tag{A.11}$$

where the operators Q are defined as

$$Q_{\alpha,i} \equiv \sum_{l,\gamma \neq \alpha} \frac{|\gamma, l\rangle\langle\gamma, l|}{E_{\gamma,l} - E_{\alpha,i}}. \tag{A.12}$$

We finally obtain the effective Hamiltonian to second order in matrix form

$$\langle \alpha, i| H_{\text{eff}} |\alpha, j\rangle = E_{\alpha,i}\delta_{i,j} + \xi\langle \alpha, i| V |\alpha, j\rangle - \frac{\xi^2}{2}\langle \alpha, i| V[Q_{\alpha,i} + Q_{\alpha,j}]V |\alpha, j\rangle. \tag{A.13}$$

Abbreviations

Abbreviation	Explanation
BFMT	Bose-Fermi mapping theorem
CAR	Canonic anticommutation relation
CCR	Canonic commutation relation
DFT	Discrete Fourier transform
GUP	Generalized uncertainty principle
HM	Heisenberg model
LGF	Lattice Green's function
nBZ	n-th Brillouin zone
nBsZ	n-th Brillouin subzone
nD	n dimensions
OL	Optical lattice
PBC	Periodic boundary conditions
SMT	Spectral mapping theorem
SUSY	Supersymmetric

Acknowledgments

First, I thank my advisors Drs. David Petrosyan and Alejandro Saenz for their continuous scientific support and for their hospitality at IESL-FORTH and Humboldt-Universität zu Berlin, respectively.

I am thankful to Dr. Petrosyan for introducing the subject of this thesis to me. I thank him for his patience during the first stages of my PhD, for many useful scientific discussions and, especially, for his indeed close collaboration with me in the topics covered from chapter 3 to chapter 5. I also thank him for carefully proofreading this thesis.

I thank Dr. Saenz for his collaboration and advice concerning the contents described in chapters 5 and 6, and for a careful reading of this thesis and many useful suggestions.

I am glad to thank Prof. Gerald Teschl (Universität Wien) and Mr. Luis Rico (Technische Universität Kaiserslautern) for helpful feedback regarding subtle mathematical aspects presented in this thesis.

Illuminating correspondence with Prof. Daniel Mattis (University of Utah) on the three-body problem is gratefully acknowledged. I also thank him for introducing to me the many-body version of SUSY quantum mechanics, from which I constructed most of chapter 7.

I am indebted to Mr. Matthias Küster (Humboldt-Universität) for pointing out many mistakes and typos in an earlier draft of chapter 6 and for translating the abstract to German.

Last but not least, I wish to thank Mr. Francisco Cordobés-Aguilar (Royal Holloway, University of London) for the very exhausting task of proofreading all different versions of this thesis and correcting numerous typos, misprints and mistakes.

Bibliography

[AB59]   Aharonov, Y.; Bohm, D.: Significance of electromagnetic potentials in quantum theory. In: *Phys. Rev.*, volume 115:p. 485, 1959.

[ADL07]   Albeverio, S.; Dell'Antonio, G.F.; Lakaev, S.N.: The number of eigenvalues of three-particle Schrödinger operators on lattices. In: *J. Phys. A*, volume 40:p. 14819, 2007.

[AEM$^+$95] Anderson, M.H.; Ensher, J.R.; Matthews, M.R.; Wieman, C.E.; Cornell, E.A.: Observation of Bose-Einstein condensation in a dilute atomic vapor. In: *Science*, volume 269:p. 198, 1995.

[ALM04]   Albeverio, S.; Lakaev, S.N.; Muminov, Z.I.: Schrödinger operators on lattices. the Efimov effect and discrete spectrum asymptotics. In: *Ann. Henri Poincare*, volume 5:p. 743, 2004.

[AM76]   Ashcroft, N.J.; Mermin, N.D.: *Solid State Physics*. International Thomson Publishing, 1976.

[AS64]   Abramowitz, M.; Stegun, I.A.: *Handbook of Mathematical Functions with Formulas, Graphs, and Mathematical Tables*. Dover, 1964.

[BCS57]   Bardeen, J.; Cooper, L.N.; Schrieffer, J.R.: Theory of superconductivity. In: *Phys. Rev.*, volume 108:p. 1175, 1957.

[BDZ08]   Bloch, I.; Dalibard, J.; Zwerger, W.: Many-body physics with ultracold gases. In: *Rev. Mod. Phys.*, volume 80:p. 885, 2008.

[Bet31]   Bethe, H.A.: Zur theorie der metalle. In: *Z. Physik A*, volume 71:p. 205, 1931.

[Blo05]   Bloch, I.: Exploring quantum matter with ultracold atoms in optical lattices. In: *J. Phys. B*, volume 38:p. S629, 2005.

[BLV$^+$09] Bauer, D.M.; Lettner, M.; Vo, C.; Rempe, G.; Dürr, S.: Control of a magnetic feshbach resonance with laser light. In: *Nature Physics*, volume 5:p. 339, 2009.

[BPH$^+$07] Bouadim, K.; Paris, N.; Hebert, F.; Batrouni, G.G.; Scalettar, R.T.: Metallic phase in the two-dimensional ionic Hubbard model. In: *Phys. Rev. B*, volume 76:p. 085112, 2007.

[BPS$^+$06] Bhat, R.; Peden, B.M.; Seaman, B.T.; Kraemer, M.; Carr, L.D.; Holland, M.J.: Quantized vortex states of strongly interacting bosons in a rotating optical lattice. In: *Phys. Rev. A*, volume 74:p. 063606, 2006.

[Bri88]   Brigham, E.O.: *The fast Fourier transform and its applications*. Prentice Hall, 1988.

[Büc10]   Büchler, H.-P.: Microscopic derivation of Hubbard parameters for cold atomic gases. In: *Phys. Rev. Lett.*, volume 104:p. 090402, 2010.

[CGM86]   Chalbaud, E.; Gallinar, J.-P.; Mata, G.: The quantum harmonic oscillator on a lattice. In: *J. Phys. A*, volume 19:p. L385, 1986.

[CKS95]   Cooper, F.; Khare, A.; Sukhatme, U.: Supersymmetry and quantum mechanics. In: *Phys. Rep.*, volume 251:p. 267, 1995.

[CLH+08] Craco, L.; Lombardo, P.; Hayn, R.; Japaridze, G.I.; Mueller-Hartmann, E.: Electronic phase transitions in the half-filled ionic Hubbard model. In: *Phys. Rev. B*, volume 78:p. 075121, 2008.

[Con94]   Conway, J.B.: *A Course in Functional Analysis*. Springer, 1994.

[CST85]   Cafolla, A.; Schatterly, S.; Tarrio, C.: Translational mass of an exciton. In: *Phys. Rev. Lett.*, volume 55:p. 2818, 1985.

[CTDRG92] Cohen-Tannoudji, C.; Dupont-Roc, J.; Grynberg, G.: *Atom–Photon Interactions: Basic Processes and Applications*. Wiley-Interscience, 1992.

[Cwi77]   Cwikel, M.: Weak type estimates for singular values and the number of bound states of Schrödinger operators. In: *Ann. of Math.*, volume 106:p. 93, 1977.

[DGE09]   D'Incao, J.P.; Greene, C.H.; Esry, B.D.: The short-range three-body phase and other issues impacting the observation of Efimov physics in ultracold quantum gases. In: *J. Phys. B*, volume 42:p. 044016, 2009.

[DHKS03] Damanik, D.; Hundertmark, D.; Killip, R.; Simon, B.: Variational estimates for discrete Schrödinger operators with potentials of indefinite sign. In: *Commun. Math. Phys.*, volume 238:p. 545, 2003.

[Eco90]   Economou, E.N.: *Green's Functions in Quantum Physics*. Springer-Verlag, 1990.

[EFG+05] Essler, F.H.L.; Frahm, H.; Goehmann, F.; Kluemper, A.; Korepin, V.E.: *The One-Dimensional Hubbard Model*. Cambridge University press, 2005.

[Efi70]   Efimov, V.: Weakly-bound states of three resonantly-interacting particles. In: *Sov. J. Nucl. Phys.*, volume 12:p. 589, 1970.

[ET70]   Esaki, L.; Tsu, R.: Superlattice and negative differential conductivity in semiconductors. In: *IBM J. Res. Dev.*, volume 14:p. 61, 1970.

[FBZ04]   Fedichev, P.O.; Bijlsma, M.J.; Zoller, P.: Extended molecules and geometric scattering resonances in optical lattices. In: *Phys. Rev. Lett.*, volume 92:p. 080401, 2004.

[Fes58]   Feshbach, H.: Unified theory of nuclear reactions. In: *Ann. Phys. (NY)*, volume 5:p. 357, 1958.

[FKB⁺09]   Ferlaino, F.; Knoop, S.; Berninger, M.; Harm, W.; D'Incao, J.P.; Nägerl, H.-C.; Grimm, R.: Evidence for universal four-body states tied to an Efimov trimer. In: *Phys. Rev. Lett.*, volume 102:p. 140401, 2009.

[FVCPR09]   Fischer, A.M.; V.L. Campo, Jr.; Portnoi, M.E.; Römer, R.A.: Exciton storage in a nanoscale Aharonov-Bohm ring with electric field tuning. In: *Phys. Rev. Lett.*, volume 102:p. 096405, 2009.

[Gir60]   Girardeau, M.D.: Relationship between systems of impenetrable bosons and fermions in one dimension. In: *J. Math. Phys*, volume 1:p. 516, 1960.

[GME⁺02]   Greiner, M.; Mandel, O.; Esslinger, T.; Haensch, T.W.; Bloch, I.: Quantum phase transition from a superfluid to a Mott insulator in a gas of ultracold atoms. In: *Nature*, volume 415:p. 39, 2002.

[GP91]   Galindo, A.; Pascual, P.: *Quantum Mechanics I.* Springer, 1991.

[GWH⁺05]   Griesmaier, A.; Werner, J.; Hensler, S.; Stuhler, J.; Pfau, T.: Bose-Einstein condensation of chromium. In: *Phys. Rev. Lett.*, volume 94:p. 160401, 2005.

[Hof76]   Hofstadter, D.R.: Energy levels and wave functions of Bloch electrons in rational and irrational magnetic fields. In: *Phys. Rev. B*, volume 14:p. 2239, 1976.

[Hos06]   Hossenfelder, S.: A note on theories with a minimal length. In: *Class. Quantum Grav.*, volume 23:p. 1815, 2006.

[HR09]   Hen, I.; Rigol, M.: Superfluid to Mott insulator transition of hardcore bosons in a superlattice. In: *Phys. Rev. B*, volume 80:p. 134508, 2009.

[HS02]   Hundertmark, D.; Simon, B.: Lieb-Thirring inequalities for Jacobi matrices. In: *J. Approx. Theory*, volume 118:p. 106, 2002.

[JBC⁺98]   Jaksch, D.; Bruder, C.; Cirac, J.I.; Gardiner, C.W.; Zoller, P.: Cold bosonic atoms in optical lattices. In: *Phys. Rev. Lett.*, volume 81:p. 3108, 1998.

[JCS09]   Jin, L.; Chen, B.; Song, Z.: Coherent shift of localized bound pairs in the Bose-Hubbard model. In: *Phys. Rev. A*, volume 79:p. 032108, 2009.

[Joa75]   Joachain, C.J.: *Quantum Collision Theory.* North Holland, 1975.

[Kat95]   Kato, T.: *Perturbation Theory for Linear Operators.* Springer, 1995.

[KFM⁺09]   Knoop, S.; Ferlaino, F.; Mark, M.; Berninger, M.; Schöbel, H.; Nägerl, H.-C.; Grimm, R.: Observation of an Efimov-like trimer resonance in ultracold atom-dimer scattering. In: *Nature Phys.*, volume 5:p. 227, 2009.

Bibliography

[KL87] Kennedy, T.; Lieb, E.H.: Proof of the Peierls instability in one dimension. In: *Phys. Rev. Lett.*, volume 59:p. 1309, 1987.

[Kla77] Klaus, M.: On the bound state of Schrödinger operators in one dimension. In: *Ann. Phys.*, volume 108:p. 288, 1977.

[KM97] Karbach, M.; Müller, G.: Introduction to the Bethe ansatz I. In: *Comp. in Phys.*, volume 11:p. 36, 1997.

[KMW⁺06] Krämer, T.; Mark, M.; Waldburger, P.; Danzl, J.G.; Chin, C.; Engeser, B.; Lange, A.D.; Pilch, K.; Jaakkola, A.; Nägerl, H.-C.; Grimm, R.: Evidence for Efimov quantum states in an ultracold gas of caesium atoms. In: *Nature*, volume 440:p. 315, 2006.

[KS98] Kuhl, U.; Stöckmann, H.-J.: Microwave realization of the Hofstadter butterfly. In: *Phys. Rev. Lett.*, volume 80:p. 3232, 1998.

[Lie76] Lieb, E.H.: Bounds on the eigenvalues of the Laplace and Schrödinger operators. In: *Bull. Amer. Math. Soc.*, volume 82:p. 751, 1976.

[LL58] Landau, L.D.; Lifshitz, E.M.: *Quantum Mechanics: Non-relativistic Theory. Course of Theoretical Physics, Vol. 3.* Addison-Wesley, 1958.

[LL63] Lieb, E.H.; Liniger, W.: Exact analysis of an interacting Bose gas I. the general solution and the ground state. In: *Phys. Rev.*, volume 130:p. 1605, 1963.

[LM03] Lakaev, S.N.; Muminov, Z.I.: The asymptotics of the number of eigenvalues of a three-particle lattice Schrödinger operator. In: *Funct. Anal. Appl.*, volume 37:p. 228, 2003.

[LP07] Lambropoulos, P.; Petrosyan, D.: *Fundamentals of Quantum Optics and Quantum Information.* Springer, 2007.

[LSA⁺07] Lewenstein, M.; Sanpera, A.; Ahufinger, V.; Damski, B.; De, A. Sen; Sen, U.: Ultracold atomic gases in optical lattices: mimicking condensed matter physics and beyond. In: *Adv. Phys.*, volume 56(1-2):p. 243, 2007.

[LSSY05] Lieb, E.H.; Seiringer, R.; Solovej, J.P.; Yngvason, J.: *The Mathematics of the Bose Gas and its Condensation.* Birkhaeuser, 2005.

[LW68] Lieb, E.H.; Wu, F.Y.: Absence of Mott transition in an exact solution of the short-range, one-band model in one dimension. In: *Phys. Rev. Lett.*, volume 20:p. 1445, 1968.

[Mat86] Mattis, D.C.: The few-body problem on a lattice. In: *Rev. Mod. Phys.*, volume 58(2):p. 361, 1986.

[Mat93] Mattis, D.C.: *The Many-Body Problem: An Encyclopedia of Exactly Solved Models in One Dimension.* World Scientific, 1993.

[Mes99] Messiah, A.: *Quantum Mechanics.* Dover, 1999.

[MG84]   Mattis, D.; Gallinar, J.-P.: What is the mass of an exciton? In: *Phys. Rev. Lett.*, volume 53:p. 1391, 1984.

[MM05]   Morton, K.W.; Mayers, D.F.: *Numerical Solution of Partial Differential Equations, An Introduction.* Cambridge University Press, 2005.

[MO06]   Morsch, O.; Oberthaler, M.: Dynamics of Bose-Einstein condensates in optical lattices. In: *Rev. Mod. Phys.*, volume 78:p. 179, 2006.

[MRDG08]   Mehta, N.P.; Rittenhouse, S.T.; D'Incao, J.P.; Greene, C.H.: Efimov states embedded in the three-body continuum. In: *Phys. Rev. A*, volume 78:p. 020701(R), 2008.

[MRR90]   Micnas, R.; Ranninger, J.; Robaszkiewicz, S.: Superconductivity in narrow-band systems with local nonretarded attractive interactions. In: *Rev. Mod. Phys.*, volume 62:p. 113, 1990.

[NFJG01]   Nielsen, E.; Fedorov, D.V.; Jensen, A.S.; Garrido, E.: The three-body problem with short-range interactions. In: *Phys. Rep.*, volume 347:p. 373, 2001.

[NOdM+08] Ni, K.-K.; Olpelkaus, S.; de Miranda, M.H.G.; Peer, A.; Neyenhuis, B.; Zirbel, J.J.; Kotochigova, S.; Julienne, P.S.; Jin, D.S.; Ye, J.: A high phase-space-density gas of polar molecules. In: *Science*, volume 322:p. 231, 2008.

[Nys30]   Nystrom, E.J.: Über die praktische Auflösung von Integralgleichungen mit Anwendungen auf Randwertaufgaben. In: *Acta Mathematica*, volume 54:p. 185, 1930.

[Ols98]   Olshanii, M.: Atomic scattering in the presence of an external confinement and a gas of impenetrable bosons. In: *Phys. Rev. Lett.*, volume 81:p. 938, 1998.

[OOH+06]   Ospelkaus, C.; Ospelkaus, S.; Humbert, L.; Ernst, P.; Sengstock, K.; Bongs, K.: Ultracold heteronuclear molecules in a 3d optical lattice. In: *Phys. Rev. Lett.*, volume 97:p. 120402, 2006.

[Pei33]   Peierls, R.E.: Zur Theorie des Diamagnetismus von Leitungselektronen. In: *Z. Phys.*, volume 80:p. 763, 1933.

[Pei55]   Peierls, R.E.: *Quantum Theory of Solids.* Oxford University Press, 1955.

[PM07]   Piil, R.; Mølmer, K.: Tunneling couplings in discrete lattices, single-particle band structure, and eigenstates of interacting atom pairs. In: *Phys. Rev. A*, volume 76:p. 023607, 2007.

[PNM08]   Piil, R.T.; Nygaard, N.; Mølmer, K.: Scattering and binding of different atomic species in a one-dimensional optical lattice. In: *Phys. Rev. A*, volume 78:p. 033611, 2008.

[PPT+03] Peil, S.; Porto, J.V.; Tolra, B. Laburthe; Obrecht, J.M.; King, B.E..;
          Subbotin, M.; Rolston, S.L.; Phillips, W.D.: Patterned loading of a Bose-
          Einstein condensate into an optical lattice. In: *Phys. Rev. A*, volume 67:p.
          051603, 2003.

[PS08]   Pethick, C.J.; Smith, H.: *Bose-Einstein Condensation in Dilute Gases.*
          Cambridge University Press, 2008.

[PSAF07] Petrosyan, D.; Schmidt, B.; Anglin, J.R.; Fleischhauer, M.: Quantum
          liquid of repulsively bound pairs of particles in a lattice. In: *Phys. Rev.
          A*, volume 76:p. 033606, 2007.

[PSAF08] Petrosyan, D.; Schmidt, B.; Anglin, J.R.; Fleischhauer, M.: Erratum. In:
          Phys. Rev. A, volume 77:p. 039908(E), 2008.

[RAR+06] Rousseau, V.G.; Arovas, D.P.; Rigol, M.; Hebert, F.; Batrouni, G.G.;
          Scalettar, R.T.: Exact study of the one-dimensional boson Hubbard
          model with a superlattice potential. In: *Phys. Rev. B*, volume 73:p.
          174516, 2006.

[RGB+07] Rey, A.M.; Gritsev, V.; Bloch, I.; Demler, E.; Lukin, M.D.: Preparation
          and detection of magnetic quantum phases in optical superlattices. In:
          Phys. Rev. Lett., volume 99:p. 140601, 2007.

[RM84]   Rudin, S.; Mattis, D.: Three-body bound states on a lattice. In: *Phys.
          Rev. Lett.*, volume 52:p. 755, 1984.

[RMO06]   Rigol, M.; Muramatsu, A.; Olshanii, M.: Hard-core bosons on optical
          superlattices: Dynamics and relaxation in the superfluid and insulating
          regimes. In: *Phys. Rev. A*, volume 74:p. 053616, 2006.

[Rot05]   Rothe, H.J.: *Lattice Gauge Theories, An Introduction.* Cambridge Uni-
          versity Press, 2005.

[RRBV08] Rosch, A.; Rasch, D.; Binz, B.; Vojta, M.: Metastable superfluidity of
          repulsive fermionic atoms in optical lattices. In: *Phys. Rev. Lett.*, volume
          101:p. 265301, 2008.

[RSF+09] Rey, A.M.; Sensarma, R.; Fölling, S.; Greiner, M.; Demler, E.; Lukin,
          M.D.: Controlled preparation and detection of d-wave superfluidity in
          two-dimensional optical superlattices. In: *Europhys. Lett.*, volume 87:p.
          60001, 2009.

[SBE+09] Schmidt, B.; Bortz, M.; Eggert, S.; Fleischhauer, M.; Petrosyan, D.:
          Attractively bound pairs of atoms in the Bose-Hubbard model and anti-
          ferromagnetism. In: *Phys. Rev. A*, volume 79:p. 063634, 2009.

[SEG94]   Scott, A.; Eilbeck, J.C.; Gilhøj, H.: Quantum lattice solitons. In: *Physica
          D*, volume 78:p. 194, 1994.

[SGD09]   Stoof, H.T.C.; Gubbels, K.B.; Dickerscheid, D.B.M.: *Ultracold Quantum
          Fields.* Springer, 2009.

[SGJ+08] Strohmaier, N.; Greif, D.; Joerdens, R.; Tarruell, L.; Moritz, H.; Esslinger, T.; Sensarma, R.; Pekker, D.; Altman, E.; Demler, E.: Observation of elastic doublon decay in the Fermi-Hubbard model. In: *Phys. Rev. Lett.*, volume 104:p. 080401, 2008.

[SGS09] Schneider, P.-I.; Grishkevich, S.; Saenz, A.: Ab initio determination of Bose-Hubbard parameters for two ultracold atoms in an optical lattice using a three-well potential. In: *Phys. Rev. A*, volume 80:p. 013404, 2009.

[Sim76] Simon, B.: The bound state of weakly coupled Schrödinger operators in one and two dimensions. In: *Ann. Phys.*, volume 97:p. 279, 1976.

[SJ09] Shi-Jie, Y.: Superfluidity of paired bosons from correlated tunneling. In: *Commun. Theor. Phys.*, volume 52:p. 611, 2009.

[SJS10] Shi-Jie, Y.; Shiping, F.: Fermionic superfluidity and spontaneous superflows in optical lattices. In: *New. J. Phys.*, volume 12:p. 023032, 2010.

[SLS+08] Sias, C.; Lignier, H.; Singh, Y.P.; Zenesini, A.; Ciampini, D.; Morsch, O.; Arimondo, E.: Observation of photon-assisted tunneling in optical lattices. In: *Phys. Rev. Lett.*, volume 100:p. 040404, 2008.

[SSBD05] Stock, R.; Silberfarb, A.; Bolda, E.L.; Deutsch, I.H.: Generalized pseudopotentials for higher partial wave scattering. In: *Phys. Rev. Lett.*, volume 94:p. 023202, 2005.

[Sut71] Sutherland, B.: Quantum many-body problem in one dimension: Ground state. In: *J. Math. Phys.*, volume 12:p. 246, 1971.

[Tay06] Taylor, J.R.: *Scattering Theory.* Dover, 2006.

[Tes00] Teschl, G.: *Jacobi Operators and Completely Integrable Nonlinear Lattices.* American Mathematical Society, 2000.

[TFJ+09] Thogersen, M.; Fedorov, D.V.; Jensen, A.S.; Esry, B.D.; Wang, Y.: Conditions for Efimov physics for finite range potentials. In: *Phys. Rev. A*, volume 80:p. 013608, 2009.

[TNB09] Tincani, L.; Noack, R.M.; Baeriswyl, D.: Critical properties of the band-insulator-to-Mott-insulator transition in the strong-coupling limit of the ionic Hubbard model. In: *Phys. Rev. B*, volume 79:p. 165109, 2009.

[TVCLR+10] Teodoro, M.D.; V.L. Campo, Jr.; Lopez-Richard, V.; E. Marega, Jr.; Marques, G.E.; Gobato, Y. Galvao; Iikawa, F.; Brasil, M.J.S.P.; AbuWaar, Z.Y.; Dorogan, V.G.; Mazur, Yu.I.; Benamara, M.; Salamo, G.J.: Aharonov-Bohm interference in neutral excitons: effects of built-in electric fields. In: *Phys. Rev. Lett.*, volume 104:p. 086401, 2010.

[Val10] Valiente, M.: Lattice two-body problem with arbitrary finite range interactions. In: *Phys. Rev. A (in press). E-print arXiv:1001.3805*, 2010.

[VP08a] Valiente, M.; Petrosyan, D.: Quantum dynamics of one and two bosonic atoms in a combined tight-binding periodic and weak parabolic potential. In: *Europhys. Lett.*, volume 83:p. 30007, 2008.

[VP08b] Valiente, M.; Petrosyan, D.: Two-particle states in the Hubbard model. In: *J. Phys. B*, volume 41:p. 161002, 2008.

[VP09] Valiente, M.; Petrosyan, D.: Scattering resonances and two-particle bound states of the extended Hubbard model. In: *J. Phys. B*, volume 42:p. 121001, 2009.

[VPS10] Valiente, M.; Petrosyan, D.; Saenz, A.: Three-body bound states in a lattice. In: *Phys. Rev. A*, volume 81:p. 011601(R), 2010.

[vSDG09] von Stecher, J.; D'Incao, J.P.; Greene, C.H.: Signatures of universal four-body phenomena and their relation to the Efimov effect. In: *Nature Phys.*, volume 417:p. 5, 2009.

[Wan60] Wannier, G.H.: Wave functions and effective Hamiltonian for Bloch electrons in an electric field. In: *Phys. Rev.*, volume 117:p. 432, 1960.

[Wat39] Watson, G.N.: Three triple integrals. In: *Q.J. Math. Oxford*, volume 10:p. 266, 1939.

[WB09] Weiss, C.; Breuer, H.-P.: Photon-assisted tunneling in optical lattices: Ballistic transport of interacting boson pairs. In: *Phys. Rev. A*, volume 79:p. 023608, 2009.

[WE09] Wang, Y.; Esry, B.D.: Efimov trimer formation via ultracold four-body recombination. In: *Phys. Rev. Lett.*, volume 102:p. 133201, 2009.

[Wei10] Weiss, C.: Scattering tightly bound dimers off a scattering potential. In: *Laser Phys.*, 2010.

[WHC08] Wang, L.; Hao, Y.; Chen, S.: Quantum dynamics of repulsively bound atom pairs in the Bose-Hubbard model. In: *Eur. Phys. J. D*, volume 48:p. 229, 2008.

[WLG+09] Würtz, P.; Langen, T.; Gericke, T.; Koglbauer, A.; Ott, H.: Experimental demonstration of single-site addressability in a two-dimensional optical lattice. In: *Phys. Rev. Lett.*, volume 103:p. 080404, 2009.

[WO06] Wouters, M.; Orso, G.: Two-body problem in periodic potentials. In: *Phys. Rev. A*, volume 73:p. 012707, 2006.

[WTL+06] Winkler, K.; Thalhammer, G.; Lang, F.; Grimm, R.; Denschlag, J. Hecker; Daley, A. J.; Kantian, A.; Büchler, H. P.; Zoller, P.: Repulsively bound atom pairs in an optical lattice. In: *Nature*, volume 441:p. 853, 2006.

[ZWB+07] Zvyagin, S.A.; Wosnitza, J.; Batista, C.D.; Tsukamoto, M.; Kawashima, N.; Krzystek, J.; Zapf, V.S.; Jaime, M.; N.F. Oliveira, Jr.; Paduan-Filho, A.: Magnetic excitations in the spin-1 anisotropic Heisenberg antiferromagnetic chain system NiCl$_2$-4SC(NH$_2$)$_2$. In: *Phys. Rev. Lett.*, volume 98:p. 047205, 2007.

[ZZH+06] Zapf, V.S.; Zocco, D.; Hansen, B.R.; Jaime, M.; Harrison, N.; Batista, C. D.; Kenzelmann, M.; Niedermayer, C.; Lacerda, A.; Paduan-Filho, A.: Bose-Einstein condensation of $S = 1$ nickel spin degrees of freedom in NiCl$_2$-4SC(NH$_2$)$_2$. In: *Phys. Rev. Lett.*, volume 96:p. 077204, 2006.

List of Figures

Selbständigkeitserklärung

Ich erkläre, dass ich die vorliegende Arbeit selbständig und nur unter Verwendung der angegebenen Literatur und Hilfsmittel angefertigt habe.

Berlin   Manuel Valiente Cifuentes